SINGLE FAULT LOCATION METHODS APPLIED TO BRAKE PIPE MODELS

Venkateshwer Aula

A Thesis

in the

Faculty of Engineering

Presented in Partial Fulfilment of the Requirements for
the Degree of Master of Engineering at
Concordia University
Montreal, Quebec

March 1980

SINGLE FAULT LOCATION METHODS APPLIED TO BRAKE PIPE MODELS

VENKATESHWER AULA

ABSTRACT

Whereas there exists a procedure for detecting excessive leakage in a brakepipe, the methods employed in actually locating the leaks are still very crude. Such methods are invariably labour intensive and time consuming, requiring railway personnel to walk alongside the train to hear for audible leaks either by unaided ear, or sometimes with a sonic meter.

This thesis proposes, analyzes and tests some methods of locating single faults, all based on a limited number of pressure measurements (possibly localized at the front-end or the rear end of the train). The methods are called the Difference method, the Ratio method and the Transformation method. They are developed by treating a brakepipe with leakage as linear electrical ladder network and nonlinear pneumatic network consisting of in-line and shunt fluid resistances. The validity of the analytical methods are confirmed by experiment on a scaled model of the brakepipe.

ACKNOWLEDGEMENT

The author is very grateful to his thesis supervisors Dr. S. Katz and Dr. R. M. H. Cheng for their excellent guidance, encouragement and moral support throughout this research.

He thanks his colleagues in the Fluid Control Centre for providing a conducive environment for his research, giving moral support, and also making his stay here memorable.

He would like to acknowledge the help of Mr. Albert Carbone for providing him with efficient plotting routines and Mr. Bernard Trudel for his assistance during the summer of 1978.

He also wishes to acknowledge Concordia University for the facilities provided through the Fluid Control Centre, where this work was conducted and Mr. John Elliot for his assistance during the experimentation.

This study has been supported by a research grant from the National Research Council of Canada.

TABLE OF CONTENTS

LIST OF FIGURES

NOMENCLATURE

P_0	source
P_n	last node pressure
R	linear series resistor
R_s	linear shunt resistor
R_m	faulty resistor
e_0	driving potential
i_k	in-line current i at node k
k	arbitrary node
i_n	current in last node n
e_{n+1}	potential at node n+1
e_n	potential at node n
e_k	potential at any arbitrary node k
K	a constant evaluated from boundary conditions
b	a function of R and R_s and is equal to $\cosh^{-1}[1+R/2R_s]$
i_s	current at source s
e_m	is the potential at the faulty resistor located at m
m	is the location of the faulty resistor
K_R	constant refers to the rear part, portion after the fault

n	the last node
x	is a relation which is equal to $bn+b/2$
K_F	constant for the forward part i.e., portion before the fault
i_{m-1}	current at $(m-1)^{th}$ node
i_m	current at m^{th} (fault) node
e_{m-1}	potential at $(m-1)^{th}$ node
e_{m+1}	potential at $(m+1)^{th}$ node
A	is a variable equal to $1+R/R_m - \frac{\cosh[x-bm+b]}{\cosh[x-bm]}$
e_1/e_0	ratio of potential at node 1, to that of the source i.e., 0
e_{10}/e_0	ratio of potential at node 10 to that of the source i.e., 0
R_m/R_s	ratio of resistance of faulty shunt resistor to unfaulted shunt resistor
E_1	is normalized quantity equal to e_1/e_0
E_n	is normalized quantity equal to e_n/e_0
E_k	is normalized quantity equal to e_k/e_0
m_p	predicted fault position
S	sensitivity function = $dm/dE_k E_k$
dm/dE_k	change in fault position m for a small change in normalized potential E_k
Δm	$= m_p - m$, is the fault position error
$\Delta m E_k/E_k$	is the measuring error

R/R_s	ratio of the resistance of linear series resistor to linear shunt resistor
$e_0, e_1, \ldots e_n$	is the unfaulted potential distribution
$e_0^1, e_1^1, \ldots e_n^1$	is the faulted potential distribution
e_{k-1}	potential at k-1th node
i_{k-1}	current at k-1th
$R_{s,k}$	linear shunt resistor at node k
$\Delta E/E$	measurement error
p_n	absolute pressure at nth node
p_i	absolute pressure at ith node
p_0	absolute pressure at 0th node, source
p_{i+1}	absolute pressure at the i+1th node
m_i	is the flow at the ith node
KF	constant characterizing flow resistance
m_{L_i}	leakage mass flow in the ith car
j	summing index
m_{L_j}	leakage mass flow in the jth car
p_{i-1}	absolute pressure at i-1th node
R_i	linear shunt resistance at node i
p_j	absolute pressure node j
R_j	linear shunt resistance at node j
B_i	ratio of adjoining car pressures (= p_{i-1}/p_i)
R_R	linear reference resistance, kPa.sec/kg.m^2
R_F	faulty shunt resistor in transformed section
R_F/R_R	ratio of the resistance of the fault to the resistance of the reference resistor in transformed section

P_I	absolute pressure at the car I in transformed section
N	total number of cars in the transformed network
I	position of the fault in transformation method
K/R^2_R	a dimensionless ratio
M_F	fault position in the transformed section
f	fault in the brakepipe model
F	fault in the transformed section

CHAPTER 1

INTRODUCTION

1.1 HISTORICAL BACKGROUND OF AIR BRAKES IN FREIGHT TRAINS

Leakage and leakage detection in pneumatic brakepipes of long trains are a major concern in the railroad industry. Excessive leakage affects the safety of the train by transmitting false signals to the brake cylinder as well as overloading the compressor units in the locomotives. Thus excessive brakepipe leakage is one of the major contributors to poor train handling, high cost of operating and maintaining air compressors on locomotives and production of shocks due to slack action during the ordinary service braking of long trains..

Since the inception of compressed air brakes of the automatic air brake type in 1870's, numerous changes have taken place in valve equipment, auxiliary systems and pipe fittings in the air brake although essentially the system has remained the same.

Tracing back the air brake history briefly, automatic air brakes were first introduced in freight cars in 1870's. At that time, the air brake consisted of a compressor unit, braking cylinders and brake shoes. In 1886 the automatic air brake was provided with an emergency feature, the H-triple valve equipment. Improvements in the air brake equipment were made along with the introduction of the K-type triple valve. The

brakepipe, an important feature of the airbrake also underwent many changes. Because of the leakage resulting from broken pipes which had developed fractures in the threaded area, threadless fitting employing a rubber compression grip and seal were developed. Although this virtually eliminated pipe breakage, it created leakage problems. This problem was more acute in cold weather due to insufficient tightening of gland nuts. This has lead to the use of welded brakepipe and welded flanged fittings which has reduced leakage to some extent.

As the need for bigger and heavier cars and longer trains increased, a more efficient and dependable brake was required. This culminated in the development of "AB" type brake. An improved "ABD" type brake was introduced in 1965. Since then a number of modifications have been made to enhance the dependability and efficiency of air brakes.

1.2 DESCRIPTION OF THE BRAKEPIPE

Each car of the train is equipped with a $3.175*10^{-4}$ m diameter brakepipe and separate braking equipment. The pipe is not always straight through its entire length and generally has at least one cross-over in each car.

The brakepipe (also called the train line) plays a vital dual role of being the alimentary canal and the nerve-line of the air brake system. As the alimentary canal, it supplies the necessary fluid power in the form of pressurized air, to the control valves and brake cylinders at each and every car and as the nerve-line, it transmits the braking signal from the

locomotive to the individual cars in correct magnitudes and proper timing.

The brakepipe is made up of sections running underneath each car, with adjacent sections connected by flexible hoses and couplings. At some point or points along each section of the brakepipe, control valves (the AB-the ABD valves, etc.), reduction relay valves and quick service valves are installed by using tee-branch pipes. As a result brakepipe leakage is unavoidable and primarily occurs at these locations. Also, it has been estimated [1] that, for a typical freight car, there exist some 100 joints and seals in the various control valves and braking cylinder arrangement. As a result of this quantity and complex of "plumbing", leakage becomes an unavoidable feature in train operation and train handling, something which in practice cannot be totally estimated but which has to be controlled so that it can be kept within established limits.

1.3 BRIEF DESCRIPTION OF AIR BRAKE OPERATION

A schematic illustration of a train air brake system is shown in figure (1).

For service application, the compressor provided in the locomotive units charges the air brake system with compressed air when the locomotive brake valve is in release position. Compressed air is stored in reservoirs on each car as directed by the control valve in each car. The car reservoir has two separate sections. One section is called the auxiliary reservoir volume, and the other is called the emergency reservoir

volume. To activate the brakes, the brakepipe pressure is reduced at a service rate, when the control valve on each car responds by directing air to flow from the auxiliary reservoir to the brake cylinder. The pressure thus acting on the brake cylinder piston creates a force which acts through a system of levers and rods to press the brake shoe against the wheels and thus creates the retarding force for braking. The amount of brakepipe reduction determines the relative amount of brake cylinder pressure (ranging from a minimum of approximately 68 kPa to full service i.e., 552 kPa to 758 kPa) which equalizes the pressure between cylinder and auxiliary reservoir.

To release the brakes, the brakepipe pressure is increased by placing the locomotive brakepipe valve in "release" position. This will cause the control valve on each vehicle to again assume release position, exhausting the brake cylinder pressure and recharging the reservoir.

1.4 EFFECTS OF BRAKEPIPE LEAKAGE

The effects of brakepipe leakage are well documented in [1], [2], [3].

The brakepipe leakage tends to accentuate the difference in pressure between the front and rear end of the train which is called "pressure gradient". The brakepipe leakage also makes it longer to fully charge or recharge the system thereby shortening the brakepipe exhaust time. When excess leakage has developed within a certain section of the brakepipe, faulty signals may be created thereby causing undesirable braking action.

In view of these and other effects of leakage in brakepipe, a

leakage test is mandatory at the train yards to ascertain that the leakage stays below the maximum established by regulations. However, whereas such a procedure or test may from time to time establish that leakage of the given train is excessive (that is, above the established limits), there is no systematic method available to help locate where such excessive leakage actually exists along the brakepipe. The present practice of engaging railroad workers to walk along the entire length of the train looking for (or rather listening) for the excessive leak(s) can at best be described as tedious and time consuming. Even the occasional use of a sonic meter does not alter the fact that there is a need for a quick and efficient method to locate excessive leakage when it exists. This should be based on a good analytical understanding of the interplay between pressure gradient in a brakepipe and the leakage in question (in magnitude, location and distribution).

Based on this understanding a method should evolve which relies on a small number of measurements preferably localized to eliminate necessity of travelling up and down the train, sometimes for hours and even days on end in severe climatic and environmental conditions.

Before proceeding any further, it is necessary to define some terminology that will be used in the rest of the thesis. A no fault brakepipe is one which has an acceptable amount of leakage, evenly distributed through every section of the brakepipe (on every car). This is represented by each section having a leakage hole of an identical nominal area. A single fault is said to exist in the brakepipe when one of these holes assumes an area which is significantly different from the

nominal value. For practical reasons this is taken to be significantly larger.

1.5 REVIEW OF PREVIOUS WORK

Although there exist two different methods, namely "leakage flow" and "leakage drop" to measure the brakepipe leakage on a single small car, no definite methods are available to locate the excessive leaks in a multicar train.

In the former method the flow supplied from the locomotive is measured by the pressure drop across an orifice plate between the locomotive and brakepipe. This measures the "leakage flow" directly. In the latter method the time rate of pressure change in the brakepipe is measured with all valves closed. The pressure drop that occurs in one minute is the actual measurement. This is a dynamic measurement and is termed "leakage drop". [1]

However, substantial work has been done in fault detection and analysis in electrical networks. Many of the advances are summarized in the proceedings of the state-of-the-art symposium edited by Saeks and Liberty [4]. In this volume, Rault, Garzia and Bedrosian [5] provide a bibliography of 193 papers that deal with fault detection and location in analog circuits. Also Berkowitz [6], Shekel [7], Gefferth [8] and Trick and Chien [9] have made significant contributions towards fault diagnosis.

Berkowitz [6] has derived conditions for single-element-kind network solvability. If those conditions were applied to ladder networks,

the network could be specified with potential measurements on each node. This presumes that there is one accessible node and other nodes are partially accessible.

For a single fault in a network Shekel [7] and Gefferth [8] have shown that it may be located by formulating two network functions. For a ladder network this means that the fault may be isolated with one accessible node and two partially accessible nodes.

Trick and Chien [9] have proved that the potential at the fault node of any positive resistor network has the maximum deviation from the potential at the same node when the circuit has no fault. When this fact is used to locate the fault in the ladder network, several measurements may be required to isolate the fault. However it is a potentially valuable approach when dealing with non-linear resistors.

Katz and Cheng [1] have suggested a network approach to study the effects of leakages in brakepipe models and developed mathematical equations for generating pressure distribution for the model. This offers the possibility of using network theory to detect leaks in brakepipes.

Katz, Cheng and Aula [10] have derived an analytically exact formula for a single shunt fault location in a recurrent ladder network. The approach suggested by Shekel [7] and Gefferth [9] was followed to obtain two functions from which the formula was derived.

Katz, Aula and Cheng [11] have investigated and developed several methods for locating a single fault in the brakepipe model proposed in [1]. The applicability of these methods was demonstrated through computer simulation.

Aula, Cheng and Katz [12] have discussed the methods proposed in the light of the experimental results. They have confirmed the validity of the analytical methods by experiments on a small scale model of the brakepipe.

Chun-Tat Kwan [13] proposed network models for brakepipe leakage and classified them according to their treatment of leakage flow. He demonstrated that the effects of leakage on pressure gradient and brakepipe taper depended on the position of the fault and that leakage at the rear had larger effect on the pressure gradient than leakage at front.

1.6 SCOPE OF THE THESIS

As stated earlier, no definite methods exist to locate the position of the fault in the brakepipe of a train. This research concerns with developing methods to locate a single fault in the brakepipe.

The problem may be stated as follows:
Definite methods have to be formulated to locate fault position in the brakepipe from a number of pressure measurements. The measurements would be preferably localized to eliminate the tedious and time consuming features that are present in the existing methods. The methods so developed should be based on a sound theory and backed up by experimentation on brakepipe models. Subsequently, the proposed methods would have to be tested extensively on actual brakepipes. This thesis is confined only to developing and verifying the proposed methods on a small scale model of the brakepipe.

This thesis is divided into four chapters. The first chapter briefly introduces the air brake of the freight train, its operation and reviews the previous work that has been done in the area of fault detection and location in electrical and pneumatic circuits.

The second chapter begins with the linear model (ladder network) of the brakepipe. Three methods of fault location, the Direct method, the Difference method and the Ratio method are developed.

In the Direct method an analytically exact equation is developed for fault location requiring only two nodal measurements. They are verified by performing experiments on the computer and the electrical rig shown in figure (24).

The difference method is based on the idea proposed by Trick and Chien wherein they show that maximum difference between no fault and single fault voltage distribution occurs where the fault exist. This has been demonstrated to be applicable to the linear model of the brakepipe both by computer simulation and experiments.

For the Ratio method, the fault is replaced by a voltage source. The no fault and fault voltage distributions are measured and the ratio of any nodal potential to last nodal potential is calculated. The fault is located by calculating the difference of ratios from the rear. Zero difference indicates that the fault is either at or precedes the measurement node.

The third chapter deals with formulation of the nonlinear model of the brakepipe, developing a formula for pressure distribution and the three fault location methods. The Difference and Ratio methods were

demonstrated to be applicable to the nonlinear brakepipe model both by simulation and experiments on small scale brakepipe model.

The Transformation method is developed by linearizing the nonlinear ladder network using the pressure squared as potential variable and flow squared as current variable. The network is transformed to compensate for violating Kirchoff's current law. The equation developed for Direct method is used here with modifications to locate the fault.

The last chapter briefly summarizes the previous chapters, concludes the discussion and presents some suggestions for further work.

CHAPTER 2

SINGLE FAULT LOCATION IN LINEAR MODEL

2.1 LINEAR MODEL

It has been shown by Katz and Cheng [1] that the brakepipe may be modelled as a ladder network with linear shunt resistors and nonlinear series resistors as shown in figure (2). Since it is very difficult to obtain an analytically exact relationship between the source p_0 and the last node pressure p_n, the ladder network with linear resistors only are considered first. The voltage source models the compressor unit in the locomotive, the linear series resistors "R" represent the resistance of the brakepipe to air flow and the linear shunt resistor R_s models the leakage in brakepipe at each section of the network. Thus we have a ladder network with all series resistors equal and all but one shunt resistor equal. The objective is to locate the faulty shunt resistor (i.e., excessive leak in brakepipe) with the minimum number of nodal potential measurements.

2.2 ANALYSIS OF THE LINEAR MODEL

Since the objective of this analysis is to develop a method that would identify the fault with minimum measurements, the approach suggested by Shekel [7] and Gefferth [8] is followed. The procedure would be to

derive two functions for the recurrent ladder network with a single fault. From these the fault can be located.

The ladder network under consideration figure (2a), consists of in-line resistors and shunt resistors. All of the in-line resistors are equal and have a resistance R. The shunt resistors are all equal except for one resistor which has a resistance, R_m which is referred to as the fault. The driving potential is located at the input to the ladder network and is designated as e_0. All the subsequent nodes are numbered consecutively from 1 to n. The in-line current i_k is the current leaving node k and the current i_n leaves node n and a node at the potential e_{n+1}. These variables are included to provide a boundary condition on the equation developed. For the network considered here the boundary conditions are i_n equals zero and therefore $e_{n+1} = e_n$.

Cheng [14] shows that when there is a recurrence of structure i.e., when all in-line resistor equals R and all shunt resistors equals R_s, the "Z" transform may be used to obtain a relationship between the nodal potentials and the source potential of the form:

$$e_k = e_0 \cosh bk - K \sinh bk \quad \ldots (1)$$

where e_k is the potential at node k, e_0 is the source potential, K is a constant that must be evaluated from the boundary conditions, k refers to the nodal position and $b = \cosh^{-1}[1+R/2R_s]$.

The complete derivation of the relationship between the nodal and source potential is shown in Appendix I.1

Since equation (1) applies only to a recurrent structure, the faulty

shunt, R_m is replaced by a parallel combination as shown in figure (2a). One of the resistors in the combination is R_s and the other is R_sR_m/R_s-R_m. The ladder network is now separated into two parts which have recurrent structure. The part from the fault rearward is shown in figure (3a) and the portion from the fault forward is shown in figure (3b). In the forward part, figure (3b), we use the substitution theorem to replace the resistance R_sR_m/R_s-R_m by a flow source i_s, Scott [15]. In this way the recurrent structure of the forward part is maintained justifying the application of the relationship developed by Cheng [14].

Equation (1) is first applied to the rear part figure (3a) with the result that

$$e_k = e_m\cosh(bk - bm) - K_R\sinh(bk - bm),\ k \geq m \qquad \ldots(2)$$

where the constant K_R refers to the rear part. This constant may be evaluated from equation (2) by using the no current boundary $e_n = e_{n+1}$ i.e.,

$$K_R = \frac{e_m\left[\cosh(bn - bm + b) - \cosh(bn - bm)\right]}{\left[\sinh(bn - bm + b) - \sinh(bn - bm)\right]} \qquad \ldots(3)$$

(please refer to Appendix I.2)

If equation (3) is substituted in equation (2) the resulting expression simplifies

$$\frac{e_k}{e_m} = \frac{\cosh(x - bk)}{\cosh(x - bm)},\ k \geq m \text{ and } x = bn + b/2 \qquad \ldots(4)$$

(refer to Appendix I.2)

Now applying equation (1) to the forward part figure (3b), we obtain

$$e_k = e_0 \cosh bk - K_F \sinh bk, \quad k \leq m \qquad \ldots(5)$$

where K_F, refers to the forward part.

To evaluate K_F, the condition provided by Kirchoff's current law is used at node m, which yields

$$i_{m-1} = i_m + e_m / R_m \qquad \ldots(6a)$$

or

$$(e_{m-1} - e_m) = (e_m - e_{m+1}) + \frac{R}{R_m} e_m \qquad \ldots(6b)$$

If equation (5) is used to evaluate the left side of equation (6b) and equation (4) is used to evaluate the right hand side, the result is:

$$K_F = \frac{Ae_m + \left[\cosh bm - \cosh(bm - b)\right]}{\left[\sinh bm - \sinh(bm - b)\right]} \qquad \ldots(7)$$

where

$$A = 1 + \frac{R}{R_m} - \frac{\cosh[x - bm + b]}{\cosh[x - bm]}$$

(refer to Appendix I.2)

The substitution of equation (7) in equation (5) yields

$$\frac{e_k}{e_0} = \frac{(1 + A)\sinh(bm - bk) - \sinh(bm - bk - b)}{(1 + A)\sinh bm - \sinh(bm - b)}, \quad k \leq m \qquad \ldots(8)$$

Equation (8) relates the potential at the nodes (upto and including the fault node) to the driving potential. To relate the nodes after the fault to the driving potential we specify k = m in equation (8) and

substitute the result in equation (4). The result is:

$$\frac{e_k}{e_0} = \frac{\cosh(x - bk)\ \sinh bk}{\cosh(x - bm)\left[(1 + A)\ \sinh bm - \sinh(bm - b)\right]}, \quad k \geq m \qquad \ldots(9)$$

(for equations (8) and (9) please refer to Appendix I.2).

Since equations (8) and (9) are valid on opposite sides of the fault, one potential measurement made on each side of the fault would yield two equations in the two unknowns m and A. Thus to make certain that the two measurements come from opposite sides of the fault would require measurements at nodes 1 and n. As an example for a 10 section ladder network, figure (4) shows the results of plotting e_1/e_0 from equation (8) against e_{10}/e_0 from equation (9). The relation is plotted with fault location and magnitude as parameters. For any particular fault location the relation between e_1/e_0 and e_{10}/e_0 are straight lines. This is in accordance with the findings of Gefferth [8]. The slope of the lines are different for each fault position but all the lines intersect at a common point. The point of intersection represents the values of the variables when there is no fault ($R_m/R_s = 1$). The loci for various values of the fault to shunt resistance ratio R_m/R_s, are also shown on figure (4). As the difference between the fault and shunt resistances increases, the circuit operating point (E_1, E_n) moves further away from the point of intersection. Thus the tolerance for the measurement errors in E_1 and E_n increases as the fault becomes significantly different than other shunts. In addition, the potential measurement at node 1 must be extremely accurate

when the fault is in the rear of ladder. This may be observed by selecting a value of E_{10} and noticing that the distance between fault lines decreases as the fault position moves toward the rear.

Since node 1 requires very precise measurements and the accuracy requirements reduces if the measurements are made nearer the fault, a slightly different approach is adopted. Node n is still used in conjunction with equation (9) to ensure a measurement after the fault. However, an arbitrary node, k, (presumably before the fault) is used in equation (8). For the case when k is not before the fault (i.e., when k>m) will be considered later in the analysis.

Now by eliminating A from equations (8) and (9) yields:

$$\frac{E_n}{\cosh b/2} = \frac{E_k \sinh bm - \sinh(bm - bk)}{\cosh(x - bm)\sinh bk}, \quad k \leq m \qquad \ldots(10)$$

where the measurements e_n and e_k are given in normalized form

$$E_n = e_n/e_0 \text{ and } E_k = e_k/e_0 \qquad \text{(refer Appendix I.2).}$$

Thus equation (10) has been obtained which has only one unknown, m, the fault location. The equation (10) is solved for m by expanding the multiple arguments of the hyperbolic functions, so that

$$\tanh bm = \frac{\sinh bk \cosh b/2 - E_n \cosh x \sinh bk}{\cosh bk \cosh b/2 - E_k \cosh b/2 - E_n \sinh x \sinh bk}, \quad k \leq m \qquad \ldots(11)$$

Trigonometric manipulation yields

$$m = \frac{1}{2b} \ln \frac{\left[E_k - \sinh bk - \cosh bk\right] \cosh b/2 + E_n \sinh bk \left[\sinh x + \cosh x\right]}{\left[E_k + \sinh bk - \cosh bk\right] \cosh b/2 + E_n \sinh bk \left[\sinh x - \cosh x\right]} \quad \ldots(12)$$

where $k \leq m$

Equation (12) gives the fault location as a function of two potential measurements. One measurement is at node n and the other at a node k which must be before or at the fault node. Since the fault node is unknown, m would be calculated from equation (12) when the measuring node selected is actually after the fault. That is, how is it to be recognized whether the arbitrarily selected position, k, violates the condition that $k \leq m$? To determine this we substitute into equation (11) values of E_k and E_n that are obtained from equation (9) alone. The result is:

$$\tanh bm = \tanh bk \quad \ldots(13)$$

or

$$m = k \quad , \; k \geq m$$

(refer to Appendix II).

This means that whenever the selected measuring node is behind the fault, equation (12) will predict the measuring node location and not the fault location.

It is interesting to note that equation (13) is not a function of potential measurements. This is due to an exact cancellation of terms in

equation (12). This fact is illustrated in figure (5) and (6) where E_2 (e_2/e_0) and E_7 (e_7/e_0) are plotted against E_n (e_n/e_0). The graphs are similar to figure (4) except for the difference that for k>m (i.e., when the selected measuring node is after the fault), the lines for m = 1 in former case and m = 1, 2, 3, ... 6 do not appear at all thereby illustrating the above fact. In actual case an exact cancellation may not be achieved. The results suggest, however, that the measurements made after the fault will be less sensitive to measuring errors.

Figure 7 shows in normalized form the effect of measuring position on the predicted fault location. The true fault location is a parameter on the graph. This in an idealized representation under the assumption of exact potential measurements and exact components values. The figure shows that when the measurement position is anywhere in front of the fault position is predicted accurately. But if the measurement position is after the fault, then the position of measurement is predicted. This fact is made use of in identifying and locating the fault.

2.2.1 SENSITIVITY ANALYSIS

In theory {equation (12)}, potential measurements at nodes 1 and n are all that is required to locate a fault in any position. This presumes the source voltage is known. However, inaccuracy in measuring potentials may produce a large discrepancy between the predicted (m_p) and the actual (m) fault position. Since it is also possible to calculate the fault location from measurement made at other nodes, it is essential to determine the nodes which will produce the minimum fault error. To

obtain this information a modified sensitivity function, S is defined, as:

$$S \equiv \frac{dm}{dE_k} E_k = \Delta m/(\Delta E_k/E_k) \qquad \ldots(14)$$

where $\Delta m = m_p - m$, is the fault position error. This function is chosen rather than the conventional sensitivity function because the fault position error is important no matter where the fault is located.

The sensitivity of the nodes before the fault ($k \leq m$) is first considered. The derivative in equation (14) is obtained by differentiating equation (8). The reason equation (8), is chosen rather than equation (12) is that in equation (8), the fault location is a function of one normalized potential (E_k) and the fault magnitude. If the fault magnitude is held constant figure (4) shows that the sensitivity obtained is larger than the sensitivity at constant E_n. Thus, the sensitivity calculated from equation (8) produces conservative results.

Intuitively, the largest errors should occur when the measuring position is further from the fault. To place an upper bound on the error, the fault is placed in the last section (node n). Figure (8) shows the sensitivity plotted against measuring position for ladder networks with 10, 20, 50 and 100 sections. As expected, the sensitivity is largest when the measurement is made at node 1. The sensitivity decreases monotonically as the measuring position approaches the fault location. It is also noted that as the number of nodes increases the sensitivity increases at the forward nodes but decreases at the rear nodes. A sensitivity value of 10^4 produces a position error of one node if the measuring error

$(\Delta e_k/E_k)$ is 10^{-4}.

The sensitivity of nodes after the fault ($k \geq m$) is obtained through the use of equation (9). The sensitivity function for these nodes is independent of measurement position. It is also much less than the sensitivity measured before the fault. For example when the fault is at node 1, the sensitivity is less than $0.12*10^3$ for any number of sections. From this it appears that the error magnitude will depend on the accuracy of the measurements before the fault.

Another important factor in fault detection is the magnitude of the fault. It is expected that (figure 3) as the ratio of fault resistance to shunt resistance (R_m/R_s) approaches unity, the fault will become more difficult to locate. Figure 9 shows the sensitivity of measurements made at the last node, for various values of R_m/R_s. These sensitivities represent the smallest values that are possible since the measurements are made at the fault. If the measuring accuracy of $\Delta E_n/E_n$ is 10^{-4}, the fault of $R_m/R_s = 0.1$ can be located within one node. Faults with $R_m/R_s = 0.3$ could be replaced within one node if the number of nodes exceeded 14. The nearer R_m/R_s approaches unity, the more accuracy for the measurements are required.

The parameter R/R_s in the ladder network is also a factor in the fault position error. Figure (10) shows the sensitivity plotted against R/R_s for various values of R_m/R_s. Here the sensitivity is based on measurements at the fault location and the location is at the last node of a 100 node ladder. As the ratio R/R_s increases, the sensitivity decreases for a given value of R_m/R_s. Thus fault discrimination improves

with an increase in R/R_s. However it must be recognized that when R_s becomes small, the end of ladder networks with a large number of nodes may have vanishingly small potentials. This could make fault detection very difficult, if not impossible. As a practical matter such networks are rare since they do not perform useful functions.

2.3 OTHER SINGLE FAULT DETECTION METHODS

2.3.1 DIFFERENCE METHOD

In any positive resistor circuit with a single fault, Trick and Chien [9] have proved that maximum difference in the absolute value of the potential with and without fault occurs at the node with the faulty resistor. For example consider figure (2a) wherein there is no fault in the network. All the voltages $e_0, e_1, \ldots\ldots e_n$ are noted. This is the no fault distribution. Now consider one of the resistors to have changed from the rest. The circuit now contains a fault. Again the voltages $e_0^1, e_1^1, \ldots\ldots e_n^1$ are noted. This is the fault distribution of voltages. The corresponding difference in voltages are calculated i.e., $e_0 - e_0^1, e_1 - e_1^1$ and so on. The fault occurs where the maximum difference in voltages takes place. This fact is made use of in identifying the fault in the linear ladder resistor network under consideration.

This procedure is verified by simulating it on the computer. The voltages are generated by using the basic matrix element relating two adjacent nodes of the ladder network which is:

$$\begin{bmatrix} e_{k-1} \\ i_{k-1} \end{bmatrix} = \begin{bmatrix} (1+R/R_k) & R \\ 1/R_k & 1 \end{bmatrix} \begin{bmatrix} e_k \\ i_k \end{bmatrix} \quad \ldots(15)$$

(refer Appendix III)

where R_k is the shunt resistance at node k. The nodal potentials for any number of nodes are calculated by multiplying the individual matrix elements together and applying the appropriate boundary conditions (e_0 and i_n). Figures (11), (12), and (13) illustrate this method. The values are n = 10, 20, 50, e_0 = 10 volts, R = 1 ohm, R_s = 1000 ohms and R_m = 100 ohms. It is observed that the relationship is almost linear through zero for nodes in front of the fault position and almost horizontal for nodes after the fault position for n = 10 and 20. For n = 50, the relationship droops down considerably after the fault position indicating a considerable decrease in flow of current after the fault. The point at which it starts dropping indicates the position of the fault. That is, at this position the difference in no fault and fault voltages is maximum. Figures (14), (15) and (16) illustrate the same method but with R_m = 333 ohms. It is noted that the difference in voltages reduce considerably (i.e., 10^{-2} to 10^{-3}) necessitating accurate nodal measurements to identify the fault.

2.3.2 RATIO METHOD

The resistor ladder network may be interpreted in a different manner

by applying the theorem of substitution in network theory [15]. It may be considered to have two "sources" a voltage source at the head end (i.e., node 0), and a current or flow source which replaces the fault (see figure 17). In this method, the ratio of voltage at the k^{th} node, e_k to that of the last node n (e_n) is evaluated for the single fault situation and the so-called no-fault situation. The difference between the two ratios is then plotted as shown in figures (18), (19) and (20) for different locations of the fault and when n = 10, 20, 50 respectively. The value of the fault is R_m = 100 ohms and that of other parameters, R_s = 1000 ohms, R = 1 ohm and e_0 = 10 volts. It is observed that the point at which the graph cuts the abscissa is the location at which the fault lies. This is because the difference of the pressure ratios at and after the fault is zero. It is noted that the graphs are inclined at an angle approximately 30° with respect to the abscissa. This fact may be made use of in locating the fault with few measurements and extrapolating.

Figures (21), (22) and (23) illustrate the above method but with R_m = 333 ohms. As in the case of the difference method, it is noted that the value of the difference of ratios become small and hence requiring accurate measurements to locate the fault. Thus as the value of R_m increases i.e., as the size of fault decreases, it becomes increasingly difficult to identify the fault.

2.4 EXPERIMENTS ON THE LINEAR MODEL

To test the validity of the theory derived (section 2.2.1 and

2.2.2) and the methods formulated (section 2.3.1 and 2.3.2) for the fault location, two types of experiment are performed. In one, the ladder network is simulated on the computer. In the other, an electric ladder network model shown figure (24) is used.

2.4.1 SIMULATION ON THE COMPUTER FOR THE DIRECT METHOD

The basic matrix element relating two adjacent nodes of the ladder network is as shown in equation (15). (Refer to Appendix II.3) for derivation), where R_k is the shunt resistance at node k. The nodal potentials for any number of nodes may be calculated by multiplying the individual matrix elements together and applying the appropriate boundary conditions (e_0 and i_n). If required for a particular ladder network, each matrix element may contain different values of shunt and series resistance. For the case under consideration only one matrix element is very different. However, it is possible with the computer simulation to vary each series and shunt resistance within its tolerance range. Nevertheless, the effect of the component tolerance is left to the electrical model tests. Instead, the computer is used to demonstrate the effect of measurement errors.

The procedure for computer testing is to calculate the nodal potentials with one matrix element different from all others. These calculated values which are accurate to seven decimal places are then multiplied by a fixed percentage error. The resulting error potentials are then used in conjunction with equation (12) to predict the fault location.

Figure (25) shows some typical results of the computer testing.

The predicted fault node is plotted against the measuring node position for the situation where the fault is actually at 50^{th} node of a 100 node ladder network. The in-line resistances are one ohm and the normal unfaulted shunt resistances are 100 ohms. The faulted shunt resistances is varied and has a value of either 10, 50 or 90 ohms. The assumed measurement error is ±0.1 percent ($\Delta E = \pm 10^{-3}$) and is applied to both potential measurements E_k and E_n. The results show that the sign of the error, the fault magnitude and the measuring node are all significant factors in detecting the fault. When the error is positive, there is a region of nodes extending from the source for which no solution is obtained. For $R_m/R_s = 0.1$, the region where the measuring node is from 1 to 21 produces no result. As R_m/R_s increases, the number of unproductive nodes increases. The reason for this is that the error potential cause negative arguments for the natural logarithm in equation (12). When the error is negative, each node yields a finite prediction. The predictions improve as the fault is approached. As expected the utilization of measuring nodes after the fault gave almost exact predictions of measuring node rather than the fault node.

2.4.2 TESTS ON THE EXPERIMENTAL MODEL

In the experimental ladder network the in-line resistances were 1.±0.01 ohms and the unfaulted resistances were 1000.±10 ohms. The in-line resistors were soldered to the measuring nodes but the shunt resistors were mounted on removable plugs. This facilitated the moving

of the fault from one position to another or vary the size of the fault. The set up was fabricated so that it could accomodate up to 100 nodes.

2.4.2.1 DIRECT METHOD

While conducting a test, the potential at the source was maintained at 10 volts by a regulated power supply. The faulted shunt resistances was either 100 or 333 ohms and its location was varied. For each fault location potential measurements were made at all the nodes. A predicted fault location was calculated from equation (12) by using the potential at the last node and the potential at one other node. Some of the typical test results are shown in figures (26), (27) and (28).

For a ladder network of twenty sections, figures (26) and (27) show the results when the fault is located at nodes 4, 6, 8, 12, 16 and 20. The faulted shunt resistor is 100 ohms in figure (26) and 333 ohms in figure (27). In both the cases the discrepancy between the predicted and the actual fault location is generally largest when the first node is used in the calculations. The discrepancy is least when the measuring node coincides with the fault location. In addition the results show that the discrepancy increases, when the faulted shunt resistor approaches the magnitude of the unfaulted shunt resistors. Thus, there are larger errors for a 333 ohm fault than for a 100 ohm fault.

Figure (28) shows the relation between the predicted fault node and the measurement node when there are 50 sections. Here again the prediction generally improves as the measurement node approaches the fault

location. Of course once the measurement node exceeds the fault location, the prediction corresponds to the measurement location and not the fault location. Again as the magnitude of the fault decreases i.e., as the resistance increases, larger errors in prediction occurs.

It is also noted that the faults located nearer the source are more difficult to locate.

2.4.2.2. DIFFERENCE METHOD

Figures (29), (30) and (31) show the graphs obtained by plotting the difference in normalized ratios between no fault and fault potential distribution against the measurement position, k with the fault position as the parameter. The values of n are 10, 20, and 50 and that of R_m and R_s, 100 ohms and 1000 ohms respectively. By comparing these to the figures obtained by theory {figures (11), (12) and (13)} it is observed that they verify the theoretical predictions both qualitatively and quantitatively.

For the case when R_m = 333 ohms i.e., when the size of the fault is smaller, the resulting plots are shown in figures (32), (33) and (34). For n = 10 and 20 it is observed that they correspond very well with theory {figures (14), (15)} both qualitatively and quantitatively. But when n = 50, quantitative discrepancies are observed although qualitatively they are satisfactory. This leads us to conclude that as the size of the fault decreases and the number of sections increases accurate measurements are necessary to identify the fault.

2.4.2.3 RATIO METHOD

Figures (35), (36) and (37) show the graphs obtained when the ratio method is applied to the data obtained from the electrical model. The ratio of the first to the last node for both fault and no fault conditions are calculated and their difference is plotted against the measurement position, k with the fault position as the parameter. The values of n are 10, 20 and 50 that of R_m and R_s, 100 ohms and 1000 ohms respectively.

These graphs correspond very well with those of the theory for similar values {figures (18), (19) and (20)} both qualitatively and quantitatively.

The same reasons may be given for the correspondence between figures (38), (39), (40) and figures (21), (22), (23) when R_s = 333 ohms.

CHAPTER 3

SINGLE FAULT LOCATION IN NONLINEAR MODEL

3.1. NONLINEAR BRAKEPIPE MODEL

In an assembled train, the physical configuration of the brakepipe is a combination of a series of lengths of pipes and other accessories. For the purpose of modelling, the brakepipe is simplified into a form consisting of a series of pipes with leakage holes.

A constant supply of air is provided by an air compressor in the locomotive at the head end of the train. Because of leaks and friction of brakepipe to air flow, the pressure decreases monotonically from the head end pressure (p_0, which is constant) toward the rear of the train.

To model this condition, each car is assumed to be represented by a single pressure (p) and a lumped restriction is chosen to represent the pipe flow resistance KF. This restriction is assumed to follow the standard forms [13] and [14] for isothermal pipe flow:

$$p_i^2 - p_{i+1}^2 = KF_i m_i^2 \qquad \ldots(16)$$

where p is the absolute pressure, m is the flow and KF is a constant that characterizes the flow resistance. For a train with cars of equal length, the value of KF will be approximately equal for each car. The subscripts

refer to the car position with n as the total number of cars in train. A leakage is flow that passes from the brakepipe to the atmosphere. Thus leakage is modelled as a shunt component from the pipe to the atmosphere. The shunt elements are linear resistances R, which are used to model a choked orifice leak. The brakepipe pressures are always sufficient to ensure choked flow conditions through leakage apertures.

The circuit representation of the model is shown in figure (41).

3.2 ANALYSIS OF THE MODEL

The objective of this analysis is to obtain a relationship between the source p_0 and the pressure in the last car p_n with intermediate pressure terms not appearing. If this was possible an analytically exact formula could be developed for the location of the fault. But since the circuit is nonlinear, it is very difficult to obtain such a direct and exact relationship.

Hence a recursive formula is developed from which normalized pressures at each of the nodes (i.e., the pressure distribution) may be obtained.

The constant pressure p_0 at the head end monotonically decreases as we proceed towards the last car due to leakage and resistance of the brakepipe. The shunt carries the leakage mass flow m_{L_i}. Thus the in-line flow in the i^{th} car (m_i) is equal to the sum of the leakage flows in all the cars that come after:

$$m_i = \sum_{j=i+1}^{n} m_{L_j} \qquad \ldots(17)$$

where j is the summation index.

The shunt resistances R may be assumed to be linear, because of the sonic condition of leakage flow. Thus leakage flows may be expressed as:

$$m_{L_i} = p_i/R_i \qquad 1 \leq i \leq n \qquad \ldots(18)$$

From equations (16), (17) and (18) a pressure relation between the $(i-1)^{th}$ car and i^{th} car is given as

$$p_{i-1}^2 - p_i^2 = KF \left[\sum_{j=1}^{n} p_j/R_j \right]^2 \qquad \ldots(19)$$

The pressure dependency of the leakage flows suggests the use of ratios to calculate the pressure distribution. If a variable, B_i, is defined as the ratio of pressures of adjacent cars equation (19) becomes:

$$B_i^2 = \frac{p_{i-1}^2}{p_i^2} = 1 + \frac{KF}{R_R^2} \left[\sum_{j=1}^{n} \left(\frac{p_j}{p_i}\right)\left(\frac{R_R}{R_j}\right) \right]^2 \qquad \ldots(20)$$

where R_R is a reference resistance that may be arbitrarily selected to normalize the equations.

The variable B_i, can only be calculated from the rear of the train moving forward because it depends on all values of B that come after the i^{th} car.

For example

$$B_n^2 = 1 + \frac{KF}{R_R^2} \left[\frac{R_R}{R_n} \right]^2 \qquad \ldots(21a)$$

$$B_{n-1}^2 = 1 + \frac{KF}{R_R^2} \left[\frac{R_R}{R_{n-i}} + \frac{1}{B_n} \frac{R_R}{R_n} \right]^2 \qquad \ldots(21b)$$

Thus generalizing, B_i is given by the recursive formula:

$$B_i^2 = 1 + \frac{KF}{R_R^2} \left[\frac{R_R}{R_i} + \sum_{j=1}^{n-i} \left(\prod_{k=1}^{j} \frac{1}{B_{k+i}} \right) \frac{R_R}{R_{j+1}} \right]^2 \qquad \ldots(22)$$

and the ratio of the pressures between the i^{th} car and that of the locomotive is given by:

$$\frac{p_i}{p_0} = \frac{1}{\prod_{j=1}^{i} B_j} \qquad \ldots(23)$$

(refer to Appendix IV).

3.3 SINGLE FAULT LOCATION METHODS FOR THE NONLINEAR BRAKEPIPE MODEL

3.3.1 DIFFERENCE METHOD

Trick and Chien [9] have proved that in case of a single fault in a positive resistor circuit the absolute potential change across the faulty resistor is greater than or equal to the potential change across any resistor in the circuit.

That this phenomenon also exists in the nonlinear model of the brakepipe is demonstrated by calculating the pressure differences for a few particular cases of single shunt fault, R_f. In this case the pressures are obtained using equations (22) and (23). Figures (42) and (43) shows the difference between the no fault pressure and single fault pressure at each section of the brakepipe, for various locations and two sizes (R_f/R_R = 0.465 and 0.3) of the fault. Similar to the linear case, the maximum pressure difference is seen to occur at the single fault of the brakepipe. Proceeding from the head end, the pressure difference increases monotonically and reaches a maximum at the fault after that the pressure difference decreases slowly. As the size of the fault increases, the curve droops more steeply after the fault thereby clearly identifying the fault position. Thus to locate a fault, one needs to measure the pressures at several positions and calculate the pressure difference between the no fault and single fault situation. The fault occurs at the position where this difference is the maximum.

3.3.2 RATIO METHOD

As in the case of the linear model, the nonlinear ladder resistor network can be considered to have two sources one being the applied source at the head end (i.e., at node 0), and the other one being the flow source replacing the fault. The flow source is in parallel with other shunt elements {figure (44)}. This means that the network model contains no sources from the fault position rearward.

Consequently the ratio of any nodal potential measurements made at or to the rear of the fault is not a function of the fault. Simulation with equations (22) and (23) confirm this conclusion. The difference in the ratio of potentials will therefore be zero where there is no fault between the nodes. To demonstrate this, the ratio of pressures at node i to node n is selected because this permits elimination from the rear.

Figures (45) and (46) shows the difference in the pressure ratio as a function of measurement position for various fault positions and also when R_f/R_R = 0.465 and 0.3 respectively. The other parameters have the same values as in the Difference method. When the difference in pressures ratios is used, the fault occurs where each curve intersects the abscissa. Thus in locating a single fault by this method, a zero difference indicates that the fault is either at or precedes the measurement node. This eliminates locations to the rear of the measurement node and offers the possibility of fault location with fewer nodal measurements.

3.3.3 TRANSFORMATION METHOD

In this novel method, the nonlinear model is transformed in to a linear one by linearizing figure (40) using the square of the pressure (p^2) as the potential variable and square of the flow as the current variable. Except at the last node, the linearization violates Kirchoff's current law at each node. To compensate for the violation the model is transformed (or stretched) by inserting additional sections which are

added between nodes. These are calculated by matching the nonlinear no-fault pressure distribution {equations (22),(23)} with linear no-fault distribution developed in (section 2.2).

In terms of the square of the potentials the linear distribution is given by

$$\frac{p_I^2}{p_0^2} = \frac{\cosh b(N - I + \frac{1}{2})}{\cosh b(N + \frac{1}{2})} \qquad \ldots(24)$$

where N and I are transformed values corresponding to n and i in the nonlinear model and $b = \cosh^{-1}[1 + KF/(2R_R^2)]$. The equivalent values for i and I are shown in table I below for $KF/R_R^2 = 0.00077$ and n = 10. The transformation is obtained by inserting the nonlinear network calculation equation (22) and (23) in to equation (24) beginning at the last section and working backwards towards the source.

Since Kirchoff's law is not violated in the last section, the transformed difference between the last two nodes is only 1 (i.e., 27.07 - 26.07). The transformation of the nonlinear model to a linear model permits the application of the linear fault location formula {equation (12) developed in {section 2.2}.

TABLE I

Correspondence between the Number of Nonlinear Sections and the Number of Linear Sections

Nonlinear i	Linear I
1	3.8
2	7.44
3	10.88
4	14.1
5	17.09
6	19.82
7	22.26
8	24.37
9	26.09
10	27.07

In terms of transformed values the fault location I_f is:

$$I_f = \frac{1}{2b} \ln \frac{(P_I^2 - \sinh bI - \cosh bI)\cosh b/2 + P_N^2 \sinh bI(\sinh x + \cosh x)}{(P_I^2 + \sinh bI - \cosh bI)\cosh b/2 + P_N^2 \sinh bI(\sinh x - \cosh x)} \quad \ldots(25)$$

where $I \leq I_f$

where $P_I = \frac{P_I}{P_0}$, $P_N = \frac{P_N}{P_0}$, $b = \cosh^{-1}(1 + KF/(2R_R^2))$ and $x = b_N + b/2$

Equation (25) gives the transformed fault location as a function of two pressure measurements. One required measurement is always at node n (transformed to N in equation (10)) and the other at a node i which must be at or before the fault node i_f (transformed to $I \leq I_f$ in equation (10) where the arbitrarily selected measurement node (P_I) is after the fault, equation (25) will predict the measurement node (i.e., $I_f = I$). This occurs for the same reason as in the ratio method. That is, the pressure measurement made at or to the rear of the fault does not depend on the fault.

Figures (47) and (48) show the predicted location of the fault may vary with position at which measurements are made according to equation (25). All the positions in the figure have been transformed back to their true positions in the nonlinear ladder network. For example, when the fault is in the last node ($i_f = 10$) and the measurement is made in the first node ($i = 1$), equation (25) will predict a fault at $i_f = 6.8$. As the measurement node gets closer to fault, the prediction improves. Also when the size of the fault increases (i.e., as R_f decreases) we observe improved fault predictions.

3.4 EXPERIMENTS

3.4.1 DESCRIPTION OF THE TEST SET UP

Figure (49) is a picture of the scaled-down brakepipe model along

with some measuring equipment. The brakepipe essentially consists of ten galvanized pipes of internal diameter $6.35*10^{-3}$m and each 3.05 m long. This arrangement gives an approximate scale down ratio of 5:1. The pipes are connected to each other by lengths of flexible plastic tubing each $2.54*10^{-1}$ m in length. The value of KF as defined in equation (16), characterizing the pipe resistance, is taken to be approximately $2.21*10^{13}$ $(kPa)^2.s^2/kg^2.m^4$, as suggested by Kwan [10], although it was pointed out in the same reference that KF is not constant for every pipe and tends to vary over a range of values. The leak in each pipe is simulated by an orifice. A cross is fitted at the end of each pipe so that a toggle valve and an orifice may be located. The purpose of the toggle is to permit the measurement of static pressure at each node.

A regulated supply of air (600 kPag) is provided at the head end of the brakepipe. A surge tank is used to reduce pressure fluctuation at the supply. A differential transducer (0-150 kPa) is used to provide the pressure reading. Another transducer (0-600 kPa) is used to monitor the supply pressure. The tranducers have an accuracy of 0.5% and a digital multimeter of 0.04% accuracy is employed to provide easy read out. The transducers are calibrated against a Bourdon gage (accuracy 0.1%) and the digital multimeter is set to provide 0-10 volt reading to cover the working range of the transducer in both cases.

3.4.2 TEST PROCEDURE AND TEST DATA

First, the no-fault situation is simulated by using ten orifices of each diameter $5.72*10^{-4}$m, at cross fittings located between pipes as described in section 3.4.1. An orifice of this size is equivalent to a fluid resistance value R_R of $1.687*10^{8}$ kPa.s/kg.m^2. The differential pressure transducer is connected across the air supply line and each cross in turn, so as to establish the pressure distribution for the no-fault situation.

Next to simulate a single fault situation, a larger orifice is used to replace one of the ten identical orifices. The resistance value R_f of this fault is chosen arbitrarily (e.g., R_f/R_R = 0.465 and 0.3). For each case, the corresponding single fault pressure distribution is established, one for each size, and for different positions of the fault. The results are shown in figure (50) (for R_f/R_R = 0.465) and figure (51) (for R_f/R_R = 0.3). It is noted that in both graphs, the no-fault, corresponding to minimum leakage, is above the other curves, indicating least pressure drop at each node. As the fault is located towards the rear end of the brakepipe, the corresponding pressure drop becomes more serious. This coincides at least qualitatively with the observations made for real-sized brakepipes as contained in reference [1]. Because of the small amount of pressure drops occuring at the front end of the brakepipe in every case, it becomes somewhat difficult to distinguish between the curves for one fault location from the other, even though precautions have been taken to use a differential transducer

to obtain the data.

The data on figures (50) and (51) have been processed according to each of these fault location methods described in section 3.5 (refer to the data given in the table (I).

3.5 EXPERIMENTAL RESULTS OBTAINED BY APPLYING THE SINGLE FAULT DETECTION METHODS

3.5.1 DIFFERENCE METHOD

Figure (52) shows the normalized difference between the no-fault pressure and the corresponding single fault pressure for each position along the brakepipe. By comparing it with corresponding theoretical curve in figure (42) two observations can be made. First, because of extremely small pressure differences resulting from leakage, it has been difficult to obtain with the necessary number of significant figures to produce better curves.

It is for this reason there is a discrepancy between figure (52) and figure (42) of about 30% - 40% quantitatively at practically every point.

The second but more important observation is that in spite of the difficulty in measurement and somewhat dubious value of the brakepipe parameter KF/R_R^2 (since KF is not constant throughout the pipe as assumed), it is very evident that the maximum difference occurs at the location of the fault itself. This is more obvious in figure (53) where $R_f/R_R = 0.3$, due to a larger orifice diameter representing the fault.

Hence it can be established that the difference method, based on pressure measurements is a viable method for locating a single fault.

3.5.2 RATIO METHOD

By comparing the experimental curves in figure (53) for difference of ratios as defined in section 3.3.2, with the theoretical curves of figure (45), observations similar to Difference method may also be made for the Ratio method. It is observed that each line meets the abscissa at the location of the fault. However, the method seems to work less well when the fault is located at the front. This is because of limitations in measuring accurately small differences in pressures. The situation is much improved when the fault consists of a larger orifice as is demonstrated in figure (55). Hence the validity of the Ratio method is established.

As in the linear case, a practical approach may also be developed requiring a small number of pressure measurements at the front end of the brakepipe only, provided one can establish the curvilinear line segment sufficiently accurately.

3.5.3 TRANSFORMATION METHOD

By applying the test data in figure (50) to equation (25), figure (51) is obtained. It is observed that if the points are taken individually, the prediction is somewhat unsatisfactory, unless the measurement position happens to be close to the position of the fault itself. If the

measurements are taken to the rear of the fault, the predicted value i_f is likely to lie on the straight line $i_f = i$. As an illustration and referring to figure (56), if the fault is located at i = 6, then the predicted i_f is 4.5 (say 5) when the measurement is at i = 1 the predicted i_f is, however, 6 if the measurement is carried out at i = 6. However if the measurement is carried out at i = 8, the predicted i_f turns out to be 7.8 (or 8) lying on the line $i_f = i$.

Consequently the transformation method can be utilized to advantage in the following manner:

a) if the predicted i_f is found to be the same as the position of the measurement i, it may be concluded that the fault has to lie either at or before i

b) when the measurement position i is before i_f, a reiterative approach may be pursued by taking a second measurement at the position predicted by the previous method and so on. This carries on until convergence, i.e., predicted $i_f = i$.

CHAPTER 4

CONCLUSION

4.1 SUMMARY AND DISCUSSION

Single fault location methods for linear and nonlinear ladder resistor networks have been investigated. The objective of this study was to locate the fault with minimum number of nodal potential elements.

The linear network consisted of in-line series and shunt resistors. The in-line resistors were all equal. The unfaulted shunt resistors were also equal but in general had larger resistance values than the in-line resistors. The faulty shunt resistor differed from other shunts and could be positioned at any node.

Circuit analysis showed that the network with a single fault could be separated into two networks with recurrent structure. One network was before the fault and the other after the fault. From the theory of recurrent structure networks, two relations were developed between nodal potentials, fault location and fault magnitude. One of these relations were valid on each side of the fault. Thus a nodal potential measurement before and after the fault yield two equations in the two unknowns, the fault position and the fault magnitude. The equations were then solved for fault position. To ensure that there

was one measuring node before and after the fault, the first and the last nodes were initially selected. Although theoretically these two potentials were sufficient the first node was very sensitive to measurement error. Analysis showed that the measuring node before the fault became much less sensitive as it neared the fault. Thus for practical reasons the first node was not the most appropriate node with which to begin the search for the fault. It then became necessary to determine the effect of using another measuring node that might occur after the fault. It has been proved that if the equation valid before the fault, was used incorrectly with measurements after the fault, the resulting prediction yielded the measurement position instead of the fault location. This was significant because it provided the basis for recognizing possible erroneous fault predictions when less sensitive measuring nodes were used.

A sensitivity analysis indicated that the sensitivity was largest when the front measuring node was furthest from the fault. The rear measuring node (the last node) was an order of magnitude less sensitive than the forward nodes. In general, fault identification improves for smaller R_m/R_s and larger R/R_s.

Experiments were made with a computer simulation and with an electrical network model. The experiments confirm the equations developed for the fault location. A study of the experimental results suggested that the search procedure for the fault should begin with a measurement at the last node and a measurement at about 0.3 n. If the predicted fault value calculated from these measurements is larger than

0.3 n, another measurement node is selected rearward but slightly before the first prediction. Then the second prediction is calculated using a new measuring node and the last node (n). Comparison of the two faults should uncover the fault or indicate the appropriate position for another measurement node. If however, the first predicted fault location occurs at the measuring node (0.3 n), the fault is either as predicted or before 0.3 n. In this case another measurement node is chosen at about 0.09 n. The second prediction is calculated from the node at 0.09 n and the last node (n). The second prediction is then examined in a similar manner and should suggest whether it is correct or where to make another measurement. Thus, although in theory only two potential measurements are needed, the measurement errors and component tolerances may require additional measurements.

The Difference method was based on the theory developed by Trick and Chien [9]. They proved that for a single fault in a positive resistor circuit, the maximum difference in no-fault and fault potentials indicated the location of the fault. This was verified by computer simulation and experiments on the electrical model. In this method a number of measurements are required to identify the fault. But for practical purposes a location procedure may be developed along the following lines. Referring to figure (11) each curve may be considered to consist of two line segments meeting at the position where the fault exists. Hence by taking a small number of voltage readings at the front end of the network, the first line segment may be established assuming it to be a straight line. Similarly by taking a small number of readings at

rear end, the second segment of the curve may be constructed. The point where they meet is a very good indication of the neighbourhood of the fault. It should be pointed out here that as the number of sections increase, the second segment becomes more curvilinear and this should be taken into consideration when locating the fault by the practical method suggested.

The Ratio method was based on the theory that the fault could be substituted for by the current source in parallel with the unfaulted resistors. As a result the ratio of any nodal potential measurements made at or to the rear of the fault is not a function of the fault. This was demonstrated both by computer simulation and experiments. In both cases the no-fault and fault distributions were obtained and the ratio of potentials at node i to node n were calculated. The differences in the ratio of potentials identified the fault by a process of eliminating from the rear.

A practical location procedure can also be suggested for this method. Referring to figures (18) and (21) we observe that the curves are parallel to each other and are inclined at an angle of approximately 60°. Thus a few potential measurements at the front end of the section are plotted and extended to cut the abscissa at approximately 60°. This should give a very good indication of the fault position.

For the nonlinear resistor ladder network model of the brakepipe, it was demonstrated without any doubt that the Difference and Ratio methods developed for the linear model were equally applicable here. They were done so both by computer simulation and experiments on the scaled

down model of the brakepipe. But it has to be pointed out that the experimental results were not in good agreement because of difficulties in measuring small differences in potentials. These errors were magnified when plotted, thereby making fault identification a difficult task. The same practical fault location procedure suggested earlier may be applied here, although with some modifications. It is important to take into consideration the curvilinear or nonlinear aspect of the curve when trying to identify the fault.

The Transformation method was a novel one because it is thought that an entirely new concept was applied in locating a fault in the non-linear model of the brakepipe. The nonlinear network was transformed into a linear one by inserting the required number of linear recurrent sections. This number was calculated by matching the nonlinear unfaulted distribution {equations (22) and (23)} with the linear unfaulted distribution {equation (15)}.

These numbers were then made use of in the equation (25) along with the squared potentials to calculate the fault location. The practical fault location procedure as stated for the Direct method (linear case) may also be applied here although more number of trials would have to be undertaken to identify the fault.

It is to be remembered that the final goal of all this work is to able to identify the fault in the brakepipe of the freight train consisting of 100 to 150 freight car of unequal tonnage and unequal distribution of leaks and faults. This work is felt to be a first step forward in achieving the final goal. When that goal is achieved it is

hoped that the difficulties of the railworker may considerably be alleviated and save significant time and money for the rail companies in North America and elsewhere.

4.2 SUGGESTIONS FOR FURTHER WORK

Three analytical approaches were developed for locating a single fault in both linear and nonlinear model of the brakepipe.

Test results were satisfactory for the linear case. But the results obtained by applying the 3 methods developed for the nonlinear model indicated that further work was warranted. The following suggestions may be given serious consideration:

(i) extensive testing for more number of sections (ranging from 50 to 100) on the scaled model of the brakepipe and a greater range of those physical parameters representing pipe resistance, nominal leakage and fault leakage.

(ii) extension of single fault location methods to multiple fault location.

(iii) finally, test should be carried out in brakepipe test racks and utlimately on typical train consists.

REFERENCES

1. Katz, S., and Cheng, R. M. H., "A Network Approach to Brakepipe Leakage", ASME paper 77-WA/FLCS-12, December 1977.

2. "Management of Train Operation and Train Handling", The Air Brake Association Handbook 1972.

3. Blaine, D. G., and Hengel, M. F., "Brake-System Operation and Testing Procedures and their effects on Train Performance", ASME paper 71-WA/rt-9, 1971.

4. Saeks, R., and Liberty, S. R., (editors), "Rational Fault Analysis", Proceedings of Symposium on Rational Fault Analysis held at Texas Technical University, August 1974. Published by Marcel Dekker Inc., 1977.

5. Rault, J. C., Garzia, R., and Bedrosian, S. D., "Fault Detection and Location in Analog Circuits - A Bibliography", Rational Fault Analysis, Marcel Dekker, 1977, pp. 165-175.

6. Berkowitz, R. S., "Conditions for Network-Element Value Solvability", IRE Transactions on Circuit Theory, Vol.CT-9, March 1962, pp. 24-29.

7. Shekel, J., "Some Properties of Networks with One Variable Element", IEEE Transactions on Circuit Theory, Vol. CT-14, 1967, pp. 89-92.

8. Gefferth, H. L., "Fault Identification in Resistive and Reactive Networks", International Journal of Circuit Theory and Applications, Vol. 2, 1974, pp. 273-277.

9. Trick, T. N., and Chien, R. T., "A Note on Single Fault Detection in Positive Resistor Circuits", IEEE Transactions on Circuits and Systems, Vol. CAS-25, No. 1, January 1978, pp. 46-48.

10. Katz, S., Cheng, R. M. H., and Aula, V., "Locating a Single Shunt Fault in Resistor Ladder Networks", International Journal of Circuit Theory and Applications in October 1979, vol. 7, no. 4, pp. 399-412.

11. Katz, S., Aula, V., And Cheng, R. H. M., "Some Single Fault Detection Methods in Nonlinear Resistor Ladder Network". Fourth International Symposium on Network Theory held in Bled, Yugoslavia, September 5-8, 1979.

12. Aula, V., Cheng, R. M. H., Katz, S., "Single Fault Location Methods Applied to Brakepipe Models", Winter Annual Meeting, N.Y. of A.S.M.E. 79-WA/RT-11, held in December 1979

13. Kwan, Chun-tat, "Network models for Brakepipe Leakage", A Master's Thesis in the Faculty of Engineering, Concordia University, Montreal, Quebec, CANADA, June 1977.

14. Cheng, D. K., "Analysis of Linear Systems", Addison-Wesley publishing Company, Inc., 1959, pp. 316-320.

15. Scott, R. E., "Elements of Linear Circuits", Addison-Wesley Series in Electrical Engineering, 1965.

16. Streeter, V. L., and Wylie, E. B., "Fluid Mechanics", Sixth Edtition, McGraw-Hill, 1975.

17. Binder, R. C., "Fluid Mechanics", Third Edition, Prentice-Hall, 1955.

APPENDIXES

APPENDIX I

Appendix I.1

Derivation of the relationship between the nodal and source potential

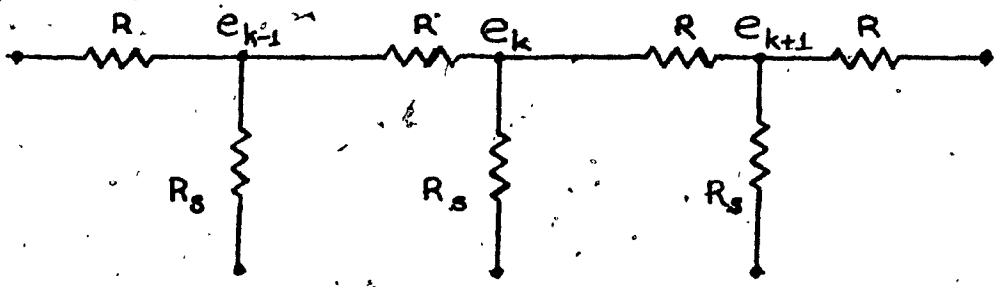

At node k

$$\frac{e_{k-1} - e_k}{R} = \frac{e_k}{R_s} + \frac{(e_k - e_{k+1})}{R}$$

$$- e_{k-1} + (2 + R/R_s)e_k - e_{k+1} = 0$$

$$e(i) - ye(i+1) + e(i+2) = 0$$

where $y = 2 + R/R_s$

Z transforms of the above yields

$$e(Z) - yZ(e(Z) - e(0)) + Z^2(e(Z) - e(0)) - Ze(1) = 0$$

$$e(Z) = \frac{e(0)\,Z(Z - y) + Ze(1)}{Z^2 - yZ + 1}$$

e(0) is known but e(1) is not.

$$e(Z) = \frac{e(0).\,Z(Z - y/2)}{Z^2 - yZ + 1} + \frac{(e(1) - e(0)\,y/2)Z}{Z^2 - yZ + 1}$$

$$e(i) = e(0)\cosh bi - \frac{1}{\sqrt{\cosh^2 b - 1}}\,(e(0)y/2 - e(1))\,\sinh bi$$

where $b = \cosh^{-1} y/2$ or $y = 2\cosh b$

$$\therefore\ e(i) = e(0)\cosh bi - \frac{2}{\sqrt{y^2 - 4}}\left[\frac{e(0)y}{2} - e(1)\right]\sinh bi$$

To determine e(1), let it be recognized that e(n) = e(n+1) i.e., there is no flow from the rear car.

$$e(n) = e(0)\cosh bn + K \sinh bn$$

where

$$k = \frac{2}{\sqrt{y^2 - 4}}\left[\frac{e(0)y}{2} - e(1)\right]$$

$$e(n+1) = e(0)\,\text{coshb}(n+1) - K\,\text{sinh}(n+1)$$

$$K = e_0 \frac{(\text{coshb}(n+1) - \text{coshbn})}{(\text{sinhb}(n+1) - \text{sinhbn})}$$

$$\frac{e(1)}{e(0)} = \text{coshbi} - \frac{\text{coshb}(n+1) - \text{coshbn}}{\text{sinhb}(n+1) - \text{sinhbn}}\,\text{sinhbi}$$

where $b = \cosh^{-1} y/2$

$$\frac{e_1}{e_0} = \frac{\text{coshb}(n - 1 + \frac{1}{2})}{\text{coshb}(n + \frac{1}{2})}$$

Appendix I.2

Derivation of an analytically exact equation for locating a single shunt fault in a linear model

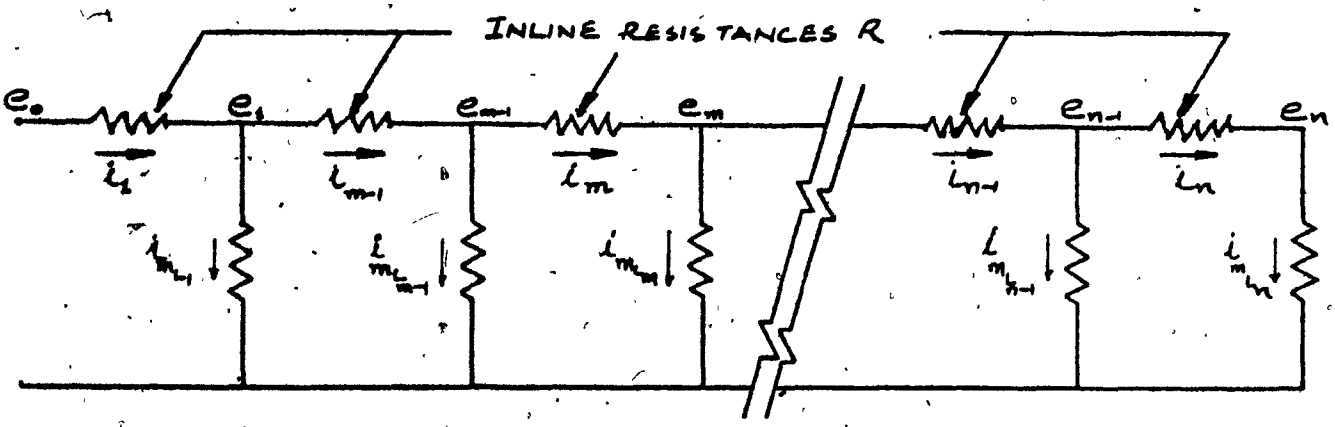

From m rearward it is known:

$$\frac{e_1}{e_m} = \frac{\cosh b(n - 1 + \tfrac{1}{2})}{\cosh b(n - m + \tfrac{1}{2})}$$, where $1 \geq m$ and $b = \cosh^{-1}\left(\frac{2 + R/R_s}{2}\right)$

Now the current $i_m = \dfrac{e_m - e_{m+1}}{R}$

$$\frac{e_{m+1}}{e_m} = \frac{\cosh b(n - m - \tfrac{1}{2})}{\cosh b(n - m + \tfrac{1}{2})}$$

$$i_m = \left[1 - \frac{\cosh b(n - m - \tfrac{1}{2})}{\cosh b(n - m + \tfrac{1}{2})}\right] \frac{e_m}{R}$$

Let $A = \left[1 - \dfrac{\cosh b(n - m - \tfrac{1}{2})}{\cosh b(n - m + \tfrac{1}{2})}\right]$

$$\therefore \quad i_m = \frac{Ae_m}{R}$$

when $i \leq m$ the relation between e_i and e_0 is

$$e_i = e_0 \cosh bi - K \sinh bi, \quad i \leq m$$

K may be evaluated using the boundary condition that

$$i_{m-1} = i_m + i_{m_L}$$

$$e_{m-1} = e_0 \cosh b(m-1) - K \sinh b(m-1)$$

$$e_m = e_0 \cosh bm - K \sinh bm$$

$$i_{m-1} = \frac{e_{m-1} - e_m}{R} = e_0 [\cosh b(m-1) - \cosh bm] \ldots$$

$$\ldots + K [\sinh bm - \sinh b(m-1)]$$

$i_{m_L} = e_m/R_m$ Thus from $i_{m-1} = e_m + i_{m_L}$ we obtain

$$\frac{e_0\,[\cosh b(m-1) - \cosh bm] + K\,[\sinh bm - \sinh b(m-1)}{R} = \left(\frac{A}{R} + \frac{1}{R_m}\right)e_m$$

Let $y_m = R/R_m$ then K equals

$$K = \frac{(A + y_m)e_m + e_0\left[\cosh bm - \cosh b(m-1)\right]}{\left[\sinh bm - \sinh b(m-1)\right]}$$

Let $A_1 = A + y_m$; $s = \sinh bm - \sinh b(m-1)$

and $c = \cosh bm - \cosh b(m-1)$

$$\therefore\ K = \frac{A_1 e_m + ce_0}{s}$$

Thus

$$e_i = e_0 \cosh bi - \frac{A_1 e_m + ce_0}{s}\sinh bi \qquad i \le m$$

Solving for e_m for the case when $i = 1$

$$se_m = se_0\cosh bm - A_1 e_m \sinh bm - ce_0 \sinh bm$$

$$e_m = \frac{e_0(s\cosh bm - c\sinh bm)}{s + A_1 \sinh bm}$$

$$\frac{e_i}{e_m} = \cosh bi - \left[\frac{A_1\,\dfrac{s\cosh bm - c\sinh bm}{S + A_1\sinh bm} + c}{s}\right]\sinh bi \quad \text{for } i \le m$$

$$\frac{e_i}{e_0} = \frac{\cosh b(n - i + \tfrac{1}{2})}{\cosh b(n - m + \tfrac{1}{2})} \left[\frac{\text{scohbm} - \text{csinhbm}}{s + A_1 \sinh bm} \right] \quad \text{for } e \geq m$$

$$s = \sinh bm - \sinh b(m-1)$$

$$c = \cosh bm - \cosh b(m-1)$$

$$A_1 = y_{m+1} - \frac{\cosh b(n - m - \tfrac{1}{2})}{\cosh b(n - m + \tfrac{1}{2})}$$

Substituting

$$\text{scoshbm} - \text{csinhbm} = \sinh bm \cosh bm - \sinh b(m-1)\cosh bm - \sinh bm \cosh bm \ldots + \cosh b(m-1)\sinh bm$$

$$\therefore \quad \text{scoshbm} - \text{csinhbm} = \cosh b(m-1)\sinh bm - \sinh b(m-1)\cosh m$$

or

$$\text{scoshbm} - \text{csinhbm} = \sinh(bm - bm + b)$$

i.e., $$\text{scoshbm} - \text{csinhbm} = \sinh b$$

$$S + A_1 \sinh bm = \sinh bm - \sinh b(m-1) + \left(y_m + 1 - \frac{\cosh b(n - m - \tfrac{1}{2})}{\cosh b(n - m + \tfrac{1}{2})}\right)\sinh bm$$

For $i \leq m$

$$\frac{e_i}{e_0} \cosh bi - \left[\frac{A_1 \text{scoshbm} - A_1 \text{csinhbm} + cs + A_1 \text{csinhbm}}{s(s + A_1 \sinh bm)} \right] \sinh bi$$

$$\frac{e_i}{e_0} = \cosh bi - \left[\frac{A_1 \cosh bm + c}{A_1 \sinh bm + s} \right] \sinh bi$$

$$\frac{e_1}{e_0} = \frac{(A_1 + 1)(\sinh b(m - i)) - \sinh b(m - i - 1)}{(A_1 + 1)\sinh bm - \sinh b(m-1)}, \quad i \leq m \qquad \ldots(A)$$

$$\frac{e_n}{e_0} = \frac{\cosh b(n - i + \tfrac{1}{2})\sinh b}{\cosh b(n - m + \tfrac{1}{2})\left[(A_1 + 1)\sinh bm - \sinh b(m-1)\right]}, \quad i \geq m \qquad \ldots(B)$$

Both these equations are used to solve the unknowns y_m and m

To ensure that the equations hold true for all locations of the fault, i = 1 and i = n are chosen respectively in equations (A) and (B). Thus

$$\frac{e_1}{e_0} = R_1 = \frac{(A_1 + 1)\sinh b(m-1) - \sinh b(m-2)}{(A_1 + 1)\sinh bm - \sinh b(m-1)} \qquad \ldots(C)$$

$$\frac{e_n}{e_0} = R_n = \frac{\cosh b/2 \sinh b}{\cosh b(n - m + \tfrac{1}{2})\left[(A_1 + 1)\sinh bm - \sinh b(m-1)\right]} \qquad \ldots(D)$$

Considering (C), and solving for $(A_1 + 1)$

$$A_1 + 1 = \frac{R_1 \sinh b(m-1) - \sinh b(m-2)}{R_1 \sinh bm - \sinh b(m-1)}$$

Considering (D)

$$\frac{R_n}{\cosh b/2 \sinh b} = \frac{1}{\cosh b(n - m + \tfrac{1}{2})\left[(A_1 + 1)\sinh bm - \sinh b(m-1)\right]} \qquad \ldots(E)$$

Subtituting for $(A_1 + 1)$

$$\frac{R_n}{\text{coshb/2sinhb}} = \frac{R_1\sinh(bm) - \sinh(bm - b)}{\cosh(bn - bm + b/2)\left[\sinh^2(bm - b) - \sinh(bm)\sinh(bm - 2b)\right]} \quad \ldots(F)$$

Let $x = bm$; $R_1 = R$; $Q = R - \text{coshb}$; $K = \text{sinhy}$

$$W = \frac{R_n}{\text{coshb/2sinhb}} \; ; \; y = bn + b/2; M = \text{sinhb}; \; L \; \text{coshy}$$

Combining (E) and (F)

$$W = \frac{(R - \text{coshb})\sinh x + \cosh x \sinh b}{\left[\cosh x \cosh y - \sinh x \sinh y\right]\left[\cosh^2 x \sinh^2 b - \sinh^2 x \sinh^2 b\right]}$$

$$= \frac{(R - \text{coshb})\sinh x + \cosh x \sinh b}{(\cosh x \cosh y - \sinh x \sinh y)\left[(\cosh^2 x - \sinh^2 x)\sinh^2 b\right]}$$

$$= \frac{Q \sinh x + M \cosh x}{M^2 L \cosh x - M^2 K \sinh x}$$

$$(WM^2L - M)\cosh x = (Q - WM^2K)\sinh x$$

$$\tanh x = \frac{WM^2L - M}{Q + M^2KW}$$

$$x = \tan^{-1}\left(\frac{WM^2L - M}{Q + WM^2k}\right)$$

$$x = \tfrac{1}{2}\ln\left[\frac{Q + WM^2k + WM^2L - M}{Q + WM^2k - WM^2L - M}\right]$$

$$m = \frac{1}{2b}\ln\frac{(R_i - \sinh bi - \cosh bi)\cosh b/2 + R_n \sinh bi(\sinh y + \cosh y)}{(R_i + \sinh bi - \cosh bi)\cosh b/2 + R_n \sinh bi(\sinh y - \cosh y)}$$

APPENDIX II

Analytical proof to show that the selected measuring node if behind the fault, predicts the measuring node location.

i.e., for $i \leq m$, $m_{predicted} = m_{actual}$

and for $i > m$, the measurement position i is predicted

Considering the following equation

$$R_i = \frac{e_i}{e_0} = \frac{LG\cosh(Z) - LF\sinh(Z)}{\left[(T - K)DEG - (T - K)D^2F + LE^2G - LDEF\right]}$$

where

$y = bn + b/2$, $A = bm_{actual}$

$L = \sinh b$, $Z = bi$, $T = A_1 + 1$

$K = \cosh b$, $D = \sinh A$, $E = \cosh A$

$F = \sinh y$, $G = \cosh y$, $H = \cosh b/2$

$$R_n = \frac{LH}{\left[(T - k)DEG - (T - k)D^2F + LE^2G - LDEF\right]}$$

Let

$$DENO = \left[(T - k)DEG - (T - k)D^2F + LE^2G - LDEF\right]$$

Considering the equation

$$\tanh(x) = \frac{WM^2L - M}{Q + M^2kW}$$

Substituting and simplyfing

$$\tanh(x) = \frac{\sinh(Z)[LHG - H.DENO]}{LGH\cosh(Z) - LHF\sinh Z - H.DENO\cosh(Z) + LHF\sinh(Z)}$$

$$\tanh(x) = \frac{\sinh(Z)[LGH - H.DENO]}{\cosh(Z)[LHG - H.DENO]}$$

$$\tanh(x) = \tanh(Z)$$

$$bm = bi$$

$$\therefore m = i$$

APPENDIX III

Generalized matrix representation of the ladder network

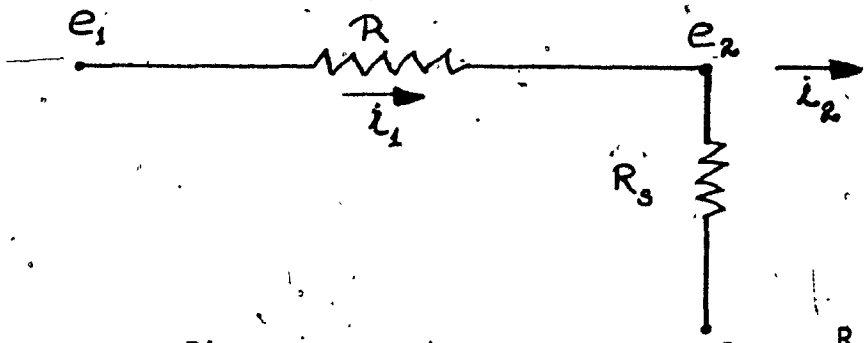

$$e_1 - e_2 = Ri_1 \qquad \text{and} \qquad e_1 - e_2 = Ri_2 + \frac{R}{R_s} e_2$$

$$i_1 = i_2 + e_2/R_s$$

Representing in a matrix form

$$\begin{bmatrix} e_1 \\ i_1 \end{bmatrix} = \begin{bmatrix} (1 + R/R_s) & R \\ 1/R_s & 1 \end{bmatrix} \begin{bmatrix} e_2 \\ i_2 \end{bmatrix}$$

Generalizing

$$\begin{bmatrix} e_{k-1} \\ i_{k-1} \end{bmatrix} \begin{bmatrix} (1 + R/R_R & R \\ (1/R_R) & 1 \end{bmatrix} \begin{bmatrix} e_k \\ i_k \end{bmatrix}$$

APPENDIX IV

Formulation of equations for generating pressure distribution in a nonlinear model

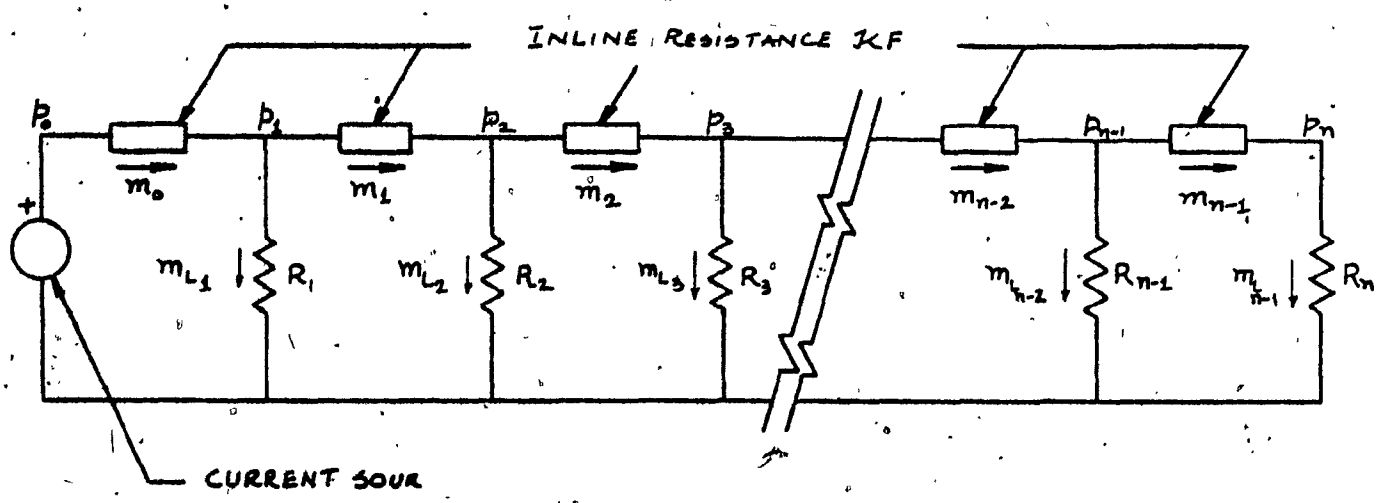

$$p_i^2 - p_{i+1}^2 = KFm_i^2 \qquad \ldots(1)$$

where p is the absolute pressure, m is the mass flow and KF is the constant that depends on the restriction between cars.

i = car position

n = number of cars

$$m_{L_i} = p_i/R_i \qquad \ldots(2)$$

$$m_i = \sum_{j=i+1}^{n} m_{L_j} \qquad \ldots(3)$$

From (1) and (3)

$$p_i^2 - p_{i+1}^2 = KF \left[\sum_{j=i+1}^{n} m_{L_j} \right]^2 \qquad \ldots(4)$$

$$p_i^2 - p_{i+1}^2 = KF \left[\sum_{j=i}^{n} p_j/R_j \right]^2 \qquad \ldots(5)$$

If a variable B_i is defined as the ratio of adjoining pressures equation (5) becomes

$$B_i^2 = \frac{p_{i-1}^2}{p_i^2} = 1 + \frac{KF}{R_R^2} \left[\sum_{j=1}^{n} \left(\frac{p_j}{p_i}\right)\left(\frac{R_R}{R_j}\right) \right]^2$$

where R_R is a reference resistance that is arbitrarily selected to normalize the equations.

The variable B_i can now be calculated from the rear since it depends on all B's that come after

$$B_n^2 = 1 + \frac{KF}{R_R^2} \left[\frac{R_R}{R_n} \right]^2$$

$$B_{n-1}^2 = \frac{p_{n-2}^2}{p_{n-1}^2} = 1 + \frac{KF}{R_R^2} \left[\frac{R_R}{R_{n-1}} + \frac{1}{B_n} \cdot \frac{R_R}{R_n} \right]^2$$

$$B_{n-2}^2 = \frac{p_{n-3}^2}{p_{n-2}^2} = 1 + \frac{KF}{R_R^2}\left[\frac{R_R}{R_{n-2}} + \frac{p_{n-1}}{p_{n-2}} \cdot \frac{R_R}{R_{n-1}} + \frac{p_n}{p_{n-2}} \cdot \frac{R_R}{R_n}\right]^2$$

$$= 1 + \frac{KF}{R_R^2}\left[\frac{R_R}{R_{n-2}} + \frac{p_{n-1}}{p_{n-2}} \cdot \frac{R_R}{R_{n-1}} + \left(\frac{p_{n-1}}{p_{n-2}}\right)\left(\frac{p_n}{p_{n-1}}\right) \frac{R_R}{R_n}\right]^2$$

because $$\frac{p_n}{p_{n-2}} = \frac{p_{n-1}}{p_{n-2}} \cdot \frac{p_n}{p_{n-1}}$$

$$B_{n-2}^2 = 1 + \frac{KF}{R_R^2}\left[\frac{R_R}{R_{n-2}} + \frac{1}{B_{n-1}} \cdot \frac{R_R}{R_{n-1}} + \frac{1}{B_{n-1}} \cdot \frac{1}{B_n} \cdot \frac{R_R}{R_n}\right]^2$$

Therefore by recursion

$$B_i^2 = 1 + \frac{KF}{R_R^2}\left[\frac{R_R}{R_i} + \sum_{j=1}^{n-i}\left(\prod_{k=1}^{j} \frac{1}{B_{k+1}}\right) \cdot \frac{R_R}{R_{j+1}}\right]^2$$

where the calculations must proceed form i = n toward i = 1 in consecutive integer steps.

After all B_i's are determined, the ratio of the pressure in any car to the locomotive pressure may be determined as

$$\frac{p_1}{p_0} = \frac{1}{\prod_{j=1}^{1} B_j}$$ (from reference 1)

APPENDIX V

A) Derivation of choke flow equation in metric units.

General flow through a converging nozzle

$$\dot{m} = \left[\frac{\rho_e}{\rho_0}\right]\left[\frac{T_e}{T_0}\right]^{\frac{1}{\gamma}} P_0 M_e A_e \left[\frac{\gamma}{R_g T_0}\right]^{\frac{1}{2}}$$

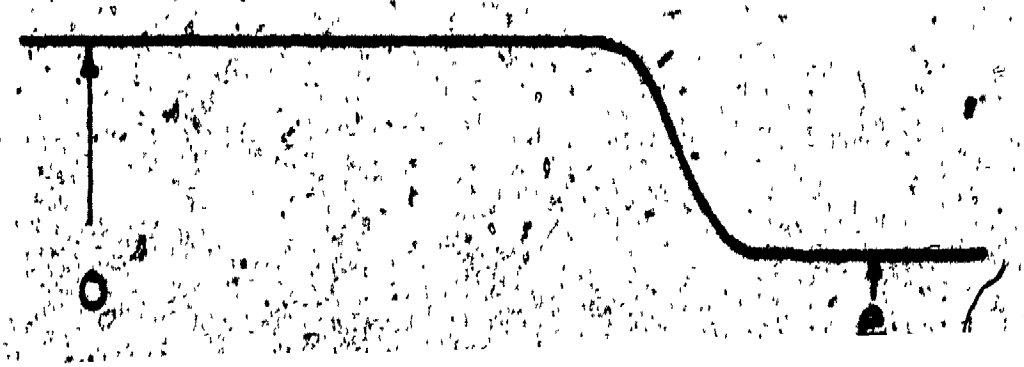

ρ_e = density at section e kg/m^3

ρ_0 = density at section 0

T_e = absolute temperature at section e in °K

T_0 = absolute temperature at section 0 in °k

M_e = Machnumber at section e and is equal to 1

A_e = Area at section e $\frac{\Pi}{4} d_e^2$, d_e in m and A_e in m^2

γ = 1.4

p_0 = absolute pressure kgf/m^2

R_g = gas constant

$T_0 = 293°k$

$R_g = 287 \frac{Nm}{kg°k}$

$$\frac{\rho_0}{\rho_e} = \left[1 + \frac{\gamma - 1}{2} M_e^2\right]^{\frac{1}{\gamma - 1}}$$

$$\frac{T_0}{T_e} = 1 + \frac{\gamma - 1}{2} M_e^2$$

when flow is choked $M_e = 1$

and $\gamma = 1.4$

and $\frac{\rho_0}{\rho_e} = 1.577$

and $\frac{T_0}{T_e} = 1.2$

Therefore $\dot{m} = 0.237 * 10^{-2} P_0 A_e$

$$\frac{P_0}{\dot{m}} = \frac{422}{A_e}$$

$$\therefore R_s = \frac{P_0}{\dot{m}} = \frac{537}{d_e^2}$$

Units for $R_s = \frac{Pa}{kg/s} = \frac{10^{-3} kPa.s}{kgg}$

B) Conversion and Estimation of value of KF in SI Units

KF is the in-line pipe resistance (nonlinear)

R is shunt resistance (linear) above 206.85 kPa

$$\Delta p = KF\dot{m}_1$$

Pressure drop is related to velocity

$$\Delta p = \frac{fl}{d} \frac{\rho v^2}{2}$$

For uniform flow distribution

$$\dot{m} = \rho A v \quad \text{or} \quad v = \frac{\dot{m}}{\rho A}$$

Estimating the value of KF for the experimental setup

$l = 3.429$ m; $d = 6.35*10^{-3}$ m; $f = 0.052$

$A = 3.167*10^{-7} m^2$; $\rho = 1.2$ kg/m^3

$$K_0 = 1.17*10^{7} \frac{kPa - s^2}{kg^2}$$

$K_n = K_0 \rho_{avg}$ to match the Units

$$= 6.05*10^{9} \frac{kPa^2 - s^2}{kg^2}$$

APPENDIX VI

Calculator program (for SR-52 Texas Instruments) for solving for fault location m (ladder network) given N (number of cars), i (measurement position) R_i (e_i / e_0), R_n (e_n / e_0) and B (= $\text{Cosh}^{-1}((2R_s + R)/2R_s)$.

Step	0	LRN	Step	1	2nd lbl
	2	Rcl 06		3	:
	4	2		5	+
	6	Rcl 06		7	*
	8	Rcl 01		9	=
	10	Sto 02		11	Rcl 06
	12	*		13	Rcl 03
	14	=		15	Sto 07
	16	Rcl 06		17	+
	18	2		19	=
	20	Sto 08		21	( )
	22	(		23	(
	24	Rcl 04		25	-
	26	(		27	Rcl 07
	28	SBR		29	2nd 1
	30	+		31	Rcl 07
	32	SBR		33	2nd 2
	34	)		35	Sto 09
	36	-		37	(
	38	Rcl 07		39	SBR
	40	2nd 1		41	-
	42	Rcl 07		43	SBR 2nd 2
	44	)		45	Sto 10
	46	)		47	*
	48	(		49	Rcl 08
	50	SBR		51	2nd 1
	52	+		53	Rcl 08
	54	SBR		55	2nd 2

Step	56	)	Step	57	Sto 11
	58	+		59	Rcl 05
	60	*		61	Rcl 10
	62	*		63	(
	64	(		65	Rcl 02
	66	SBR		67	2nd 1
	68	-		69	Rcl 02
	70	SBR		71	2nd 2
	72	)		73	Sto 12
	74	+		75	(
	76	Rcl 02		77	SBR
	78	2nd 1		79	+
	80	Rcl 02		81	SBR
	82	2nd 2		83	)
	84	Sto 13		85	)
	86	)		87	÷
	88	(		89	(
	90	Rcl 04		91	-
	92	Rcl 09		93	+
	94	Rcl 10		95	)
	96	*		97	Rcl 11
	98	+		99	Rcl 05
	100	*		101	Rcl 10
	102	*		103	(
	104	Rcl 12		105	-
	106	Rcl 13		107	)
	108	)		109	)
	110	Inx		111	*
	112	(		113	Rcl 06
	114	*		115	2
	116	)		117	2nd 1/x
	118	=		119	HLT

SBR 1	SBR 2
2nd lbl	2nd lbl
2nd 1	2nd 2
(	(
INV	+/-
LNX	INV
+	LNX
2	+
).	2
RTN	)
	RTN

With slight modification it may be used with TI-59

UNIFORM VOLTAGE DISTRIBUTION

N = 10 e_0 = 10 VDC

e1 = 9.901
e2 = 9.814
e3 = 9.737
e4 = 9.671
e5 = 9.615
e6 = 9.567
e7 = 9.528
e8 = 9.5
e9 = 9.481
e10 = 9.47

UNIFORM VOLTAGE DISTRIBUTION

N = 20 e_0 = 10 VDC

e1 = 9.819
e2 = 9.651
e3 = 9.496
e4 = 9.351
e5 = 9.216
e6 = 9.087
e7 = 8.967
e8 = 8.857
e9 = 8.758
e10 = 8.664
e11 = 8.58
e12 = 8.503
e13 = 8.436
e14 = 8.378
e15 = 8.327
e16 = 8.286
e17 = 8.252
e18 = 8.228
e19 = 8.211
e20 = 8.203

UNIFORM VOLTAGE DISTRIBUTION (Electrical)

N = 50 cars e_0 = 10 VDC

e1 = 9.692
e2 = 9.402
e3 = 9.127
e4 = 8.862
e5 = 8.607
e6 = 8.353
e7 = 8.109
e8 = 7.876
e9 = 7.655
e10 = 7.432
e11 = 7.220
e12 = 7.012
e13 = 6.812
e14 = 6.622
e15 = 6.436
e16 = 6.257
e17 = 6.085
e18 = 5.923
e19 = 5.763
e20 = 5.610
e21 = 5.46
e22 = 5.32
e23 = 5.18
e24 = 5.048
e25 = 4.917
e26 = 4.792
e27 = 4.673
e28 = 4.56
e29 = 4.452
e30 = 4.349

UNIFORM VOLTAGE DISTRIBUTION(electrical)

N = 50 e_0 = 10 VDC

e31	= 4.248	e41	= 3.477
e32	= 4.151	e42	= 3.419
e33	= 4.061	e43	= 3.368
e34	= 3.978	e44	= 3.319
e35	= 3.893	e45	= 3.271
e36	= 3.813	e46	= 3.228
e37	= 3.739	e47	= 3.187
e38	= 3.668	e48	= 3.152
e39	= 3.600	e49	= 3.119
e40	= 3.536	e50	= 3.088

DIRECT METHOD ON ELECTRICAL MODEL OF THE BRAKEPIPE

N = 10 cars e_0 = 10 VDC R_m = 332.9 ohms R_R = 1000.0 ohms

	e_i	Actual Fault m_A	Predicted Fault m_p	e_i	Actual Fault mA	Predicted Fault	e_i	Actual Fault	Predicted Fault	e_i	Actual Fault	Predicted Fault
1.	9.877	1	1.2200	9.875	2	1.8158	9.878	3	2.6935	9.877	4	3.2711
2.	9.789	1	2.2817	9.768	2	2.1096	9.770	3	2.9227	9.769	4	3.6083
3.	9.721	1	3.3464	9.691	2	3.1141	9.674	3	3.1060	9.673	4	3.8562
4.	9.645	1	4.4073	9.624	2	4.1116	9.608	3	4.1644	9.589	4	4.0993
5.	9.588	1	5.5081	9.568	2	5.2289	9.552	3	5.2659	9.531	4	5.0471
6.	9.539	1	6.2739	9.519	2	6.0714	9.503	3	6.1563	9.483	4	5.9979
7.	9.500	1	7.0639	9.481	2	7.0549	9.464	3	7.0513	9.445	4	6.9703
8.	9.471	1	7.9179	9.452	2	7.9574	9.436	3	8.0888	9.416	4	7.8957
9.	9.433	1	9.1574	9.433	2	8.9278	9.417	3	9.0771	9.398	4	8.9609
10.	9.44	1	10.0002	9.424	2	10.001	9.407	3	10.000	9.388	4	10.000

N = 10 e_0 = 10 VDC R_m = 332.9 ohms R_R = 1000.0 ohms

	e_i	m_a	m_p	e_i	m_a	m_p	e_i	m_a	m_p	e_i	m_a	m_p
1.	9.879	5	4.1702	9.874	6	4.2533	9.879	7	5.5959	9.88	8	6.4624
2.	9.773	5	4.6363	9.767	6	4.9978	9.774	7	6.3560	9.774	8	7.067
3.	9.677	5	4.832	9.772	6	5.4740	9.677	7	6.7494	9.679	8	7.4282
4.	9.592	5	5.0135	9.588	6	5.8333	9.594	7	6.8829	9.595	8	7.7450
5.	9.517	5	5.1489	9.512	6	5.9833	9.519	7	7.0376	9.520	8	7.9019
6.	9.469	5	6.123	9.445	6	6.033	9.451	7	6.9980	9.454	8	7.9749
7.	9.430	5	7.0476	9.406	6	6.9922	9.393	7	6.9967	9.395	8	7.8884
8.	9.401	5	7.9904	9.379	6	8.0585	9.366	7	8.0551	9.349	8	8.0014
9.	9.383	5	9.054	9.359	6	8.9768	9.347	7	9.0421	9.333	8	8.9820
10.	9.373	5	10.000	9.35	6	10.000	9.337	7	10.000	9.321	8	10.000

N = 10 e_0 = 10 VDC R_m = 333.9 ohms R_R = 1000.0 ohms

	e_i	m_a	m_p	e_i	m_a	m_p	e_i	m_a	m_p	e_i	m_a	m_p
1.	9.88	9	7.2051	9.88	10	7.9312						
2.	9.774	9	7.8627	9.774	10	8.6552						
3.	9.679	9	8.2645	9.679	10	9.0977						
4.	9.595	9	8.6176	9.595	10	9.4868						
5.	9.520	9	8.7918	9.520	10	9.7788						
6.	9.454	9	8.8729	9.453	10	9.6873						
7.	9.396	9	8.8391	9.396	10	9.7311						
8.	9.350	9	8.9585	9.350	10	9.8627						
9.	9.313	9	9.0354	9.313	10	9.9476						
10.	9.303	9	10.000	9.285	10	10.000						

SIZE OF THE FAULT IN THE BRAKEPIPE MODEL OF THE AIR BRAKE

0.5715 mm (diameter) R_R (Resistance$_{Reference}$)=1.687E+08 $\frac{kg_f.s}{kg_m.m^2}$

0.8128 mm;	R_F/R_R=0.5132;	R_F (Resistance$_{Fault}$) =8.568E+07
0.838	=0.465	=7.849E+07
1.067	=0.287	=4.846E+07
1.143	=0.25	=4.221E+07
1.778	=0.103	=1.744E+07

AVERAGE VALUES OF UNFAULTED
PRESSURE DISTRIBUTION IN BRAKE PIPE MODEL (experimental)

CALIBRATION : 0 kPa - 150 kPa — 0V - 10V
0 kPa - 600 kPa — 0V - 10V

N=10

R_R = 1.687 E+08 $kg_f.s/kg_m.m^2$

Pressure at	Trial 1		Trial 2		Trial 3		Trial 4	
Node i	Multimeter V Volts	Pressure Gage P kPa	Multimeter V Volts	Pressure Gage P kPa	Multimeter V Volts	Pressure Gage P kPa	Multimeter V Volts	Pressure Gage P kPa
P_0	10.00	600.00	10.00	600.00	10.00	600.00	10.00	600.00
P_1	1.375	579.375	1.364	579.54	1.374	579.39	1.371	579.435
P_2	2,397	564.065	2.421	563.85	2.422	563.67	2.1433	563.855
P_3	3.161	552.585	3.202	551.97	3.223	551.665	3.1953	552.07
P_4	3.722	544.17	3.767	543.495	3.778	543.33	3,756	543.665
P_5	4.136	537.96	4.108	538.38	4.123	538.155	4.1223	538.165
P_6	4.383	534.255	4.380	534.30	4.386	534.21	4.383	534.255
P_7	4.581	531.285	4.581	531.285	4.589	531.165	4.584	531.245
P_8	4.701	529.485	4.696	529.56	4.712	529.32	4.703	529.455
P_9	4.829	527.565	4.771	528.435	4.779	528.315	4.793	528.105
P_{10}	4.834	527.49	4.781	528.285	4.789	528.169	4.8013	527.98

DIFFERENCE METHOD (PNEUMATIC)

PRESSURE DISTRIBUTION FOR DIFFERENT FAULT POSITIONS IN THE MODEL

$\bar{P}_0$ = 600 kPa V_0=10V $DIAR_R$ = 0.5715mm $DIAR_m$ = 1.0414mm R_m/R_R = 0.3 N=10 cars m = fault pos.

	Fault Position 1		Fault Position 2		Fault Position 3		Fault Position 4		Fault Position 5	
	V Volts	P kPa	V Volts	P kPa	V Volts	P kPa	V Volts	P kPa	V Volts	P kPa
1.	2.014	569.79	1.949	570.77	1.895	571.58	1.890	571.65	1.905	571.43
2.	3.074	553.89	3.454	548.19	3.382	549.27	3.350	549.75	3.384	549.24
3.	3.833	542.51	4.215	536.78	4.567	531.495	4.530	532.05	4.576	531.36
4.	4.416	533.76	4.799	528.02	5.116	523.26	5.457	518.24	5.511	517.34
5.	4.798	528.03	5.179	722.32	5.489	517.67	5.788	513.18	6.163	507.56
6.	5.098	523.53	5.474	517.89	5.786	513.21	6.093	508.61	6.428	503.58
7.	5.309	520.37	5.677	514.85	5.985	510.23	6.280	505.80	6.630	500.55
8.	5.441	518.39	5.809	512.87	6.117	508.25	6.410	503.85	6.758	498.63
9.	5.515	517.28	5.882	511.77	6.194	507.09	6.484	502.74	6.835	497.48
10.	5.522	517.17	5.896	511.56	6.210	506.85	6.498	502.53	6.846	497.31

	Fault Position 6		Fault Position 7		Fault Position 8		Fault Position 9		Fault Position 10	
	V Volts	P kPa	V Volts	P Kpa	V Volts	P kPa	V Volts	P kPa	V Volts	P kPa
1.	1.890	571.65	1.826	572.61	1.776	573.36	1.773	573.41	1.812	572.82
2.	3.344	549.84	3.264	551.04	3.188	552.18	3.185	552.23	3.225	551.63
3.	4.521	532.19	4.438	533.43	4.328	535.05	4.309	535.37	4.379	534.42
4.	5.435	518.48	5.358	519.63	5.217	521.75	5.194	522.09	5.271	520.94
5.	6.094	508.59	6.007	509.875	5.839	512.42	5.806	512.91	5.894	511.59
6.	6.620	500.70	6.565	501.53	6.374	504.39	6.331	505.04	6.424	503.64
7.	6.816	497.76	7.009	494.87	6.848	497.28	6.744	498.84	6.856	497.16
8.	6.943	495.86	7.124	493.14	7.165	492.53	7.158	492.63	7.185	492.23
9.	6.996	495.12	7.198	492.03	7.232	491.52	7.302	490.47	7.448	488.28
10.	7.016	494.76	7.213	491.81	7.238	481.43	7.442	488.37	7.558	486.63

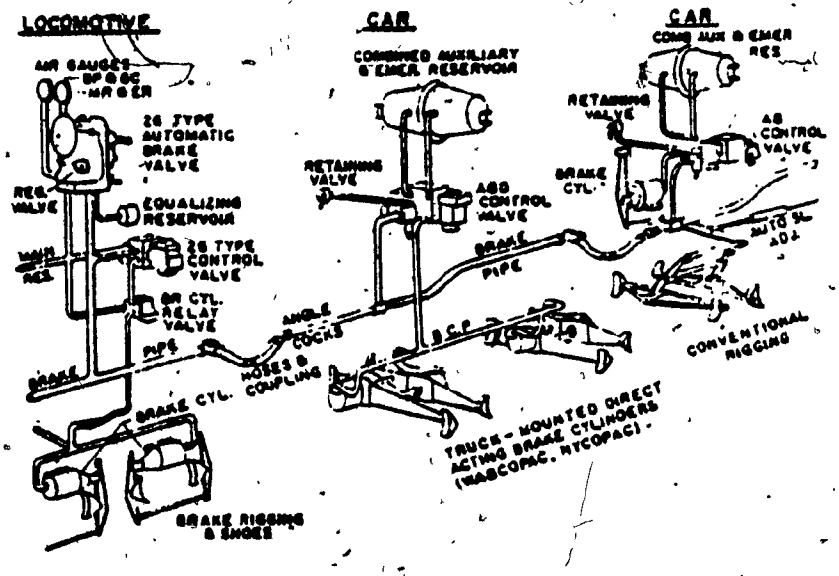

Figure 1: Schematic of the Air brakepipe system

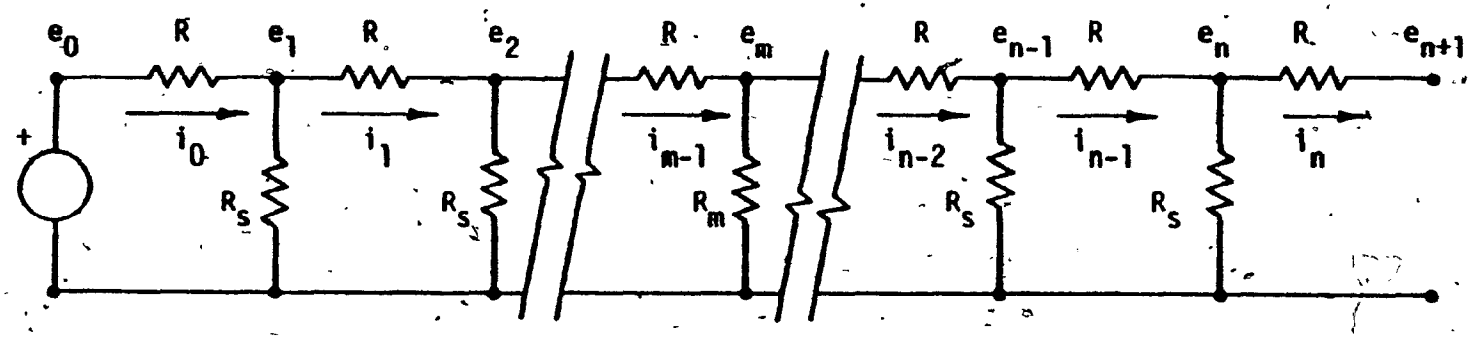

a) Complete network with one shunt fault

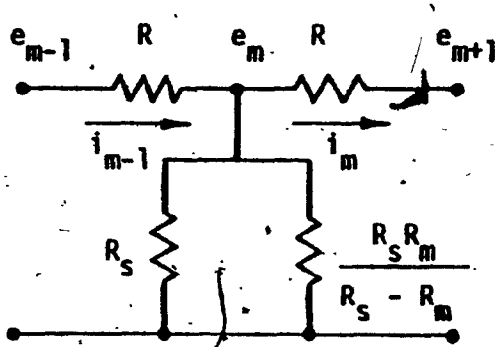

b) Network at fault node

Figure 2. Ladder Network

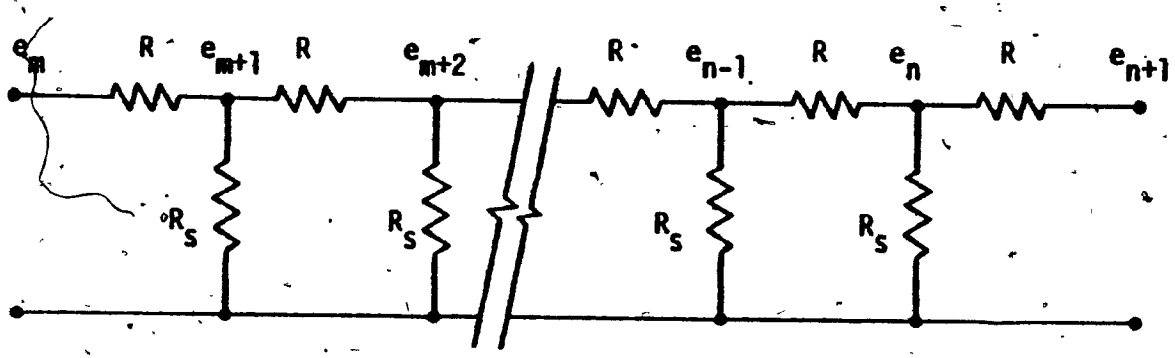

a) Circuit to the rear of the fault

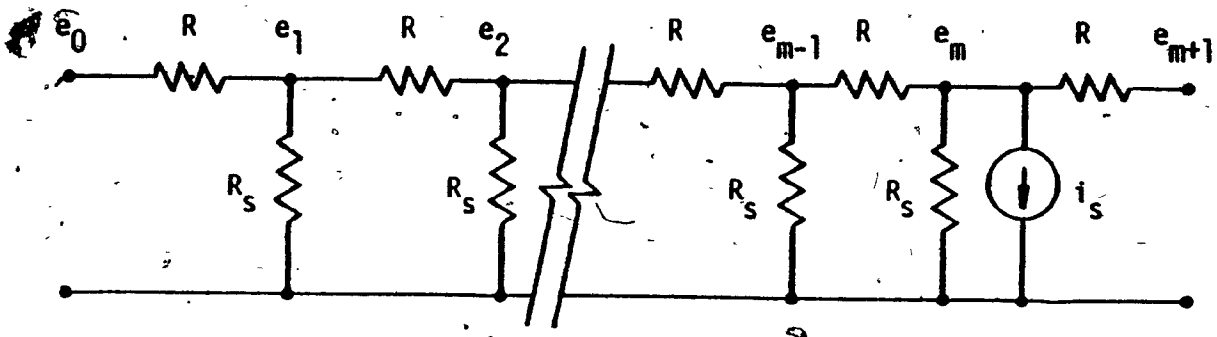

b) Circuit in front of the fault

Figure 3. Separating the ladder network into two sections

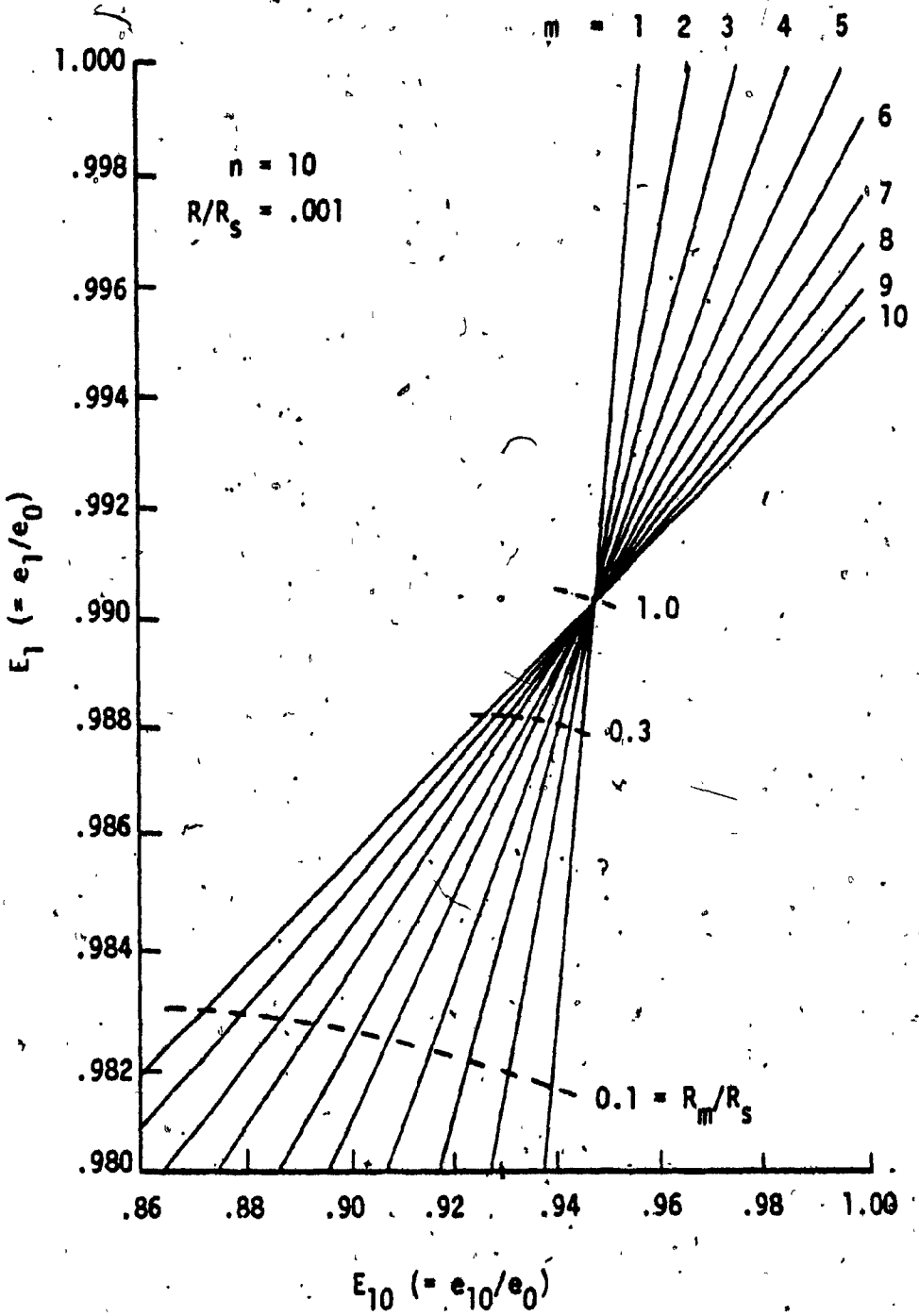

Figure 4. Relation between first and last nodal potentials as a function of fault location

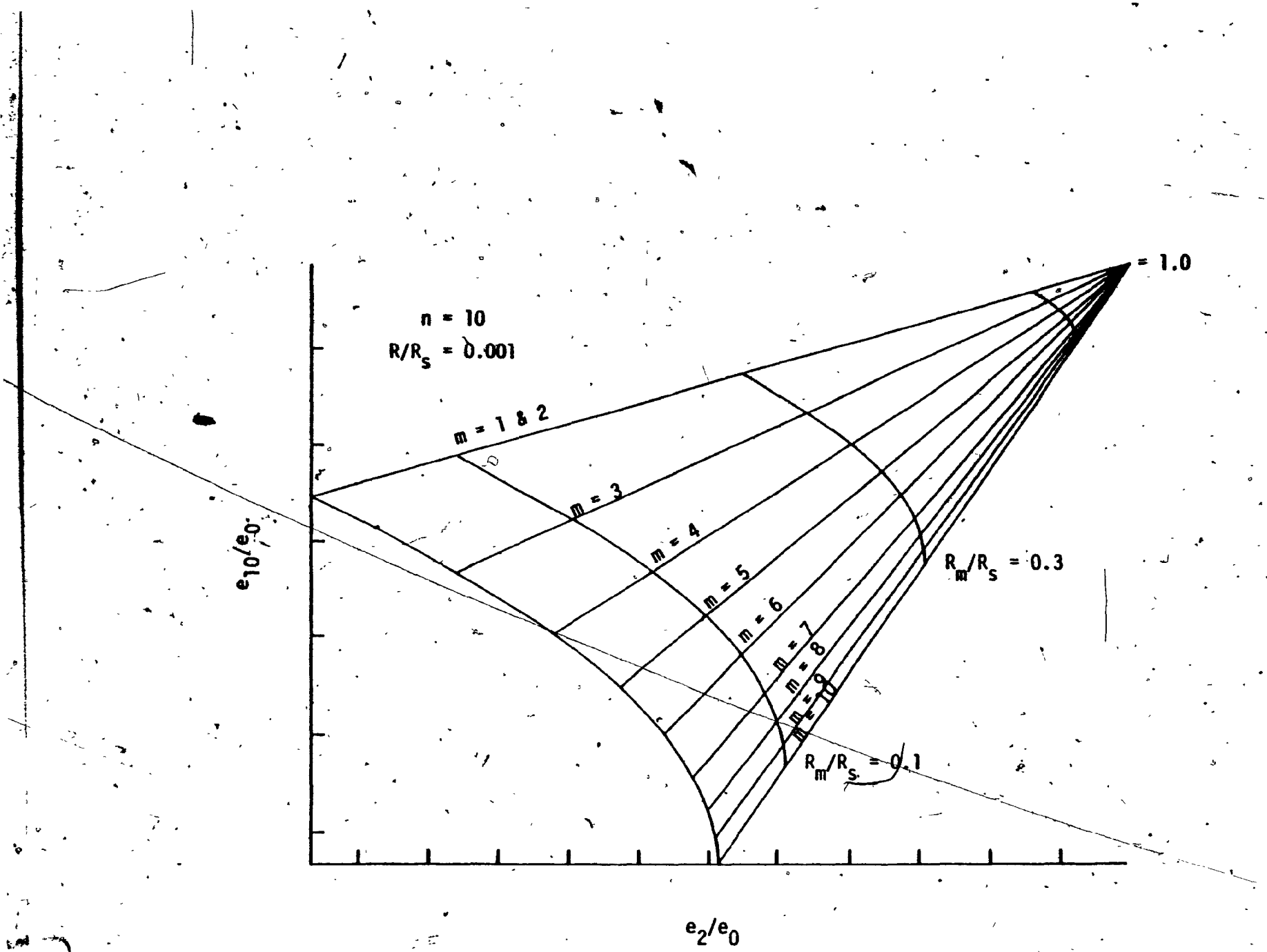

Figure 5. Illustration of the fact that equation 12 is not function of potential measurements after the fault (e_{10}/e_0 (vs) e_2/e_0)

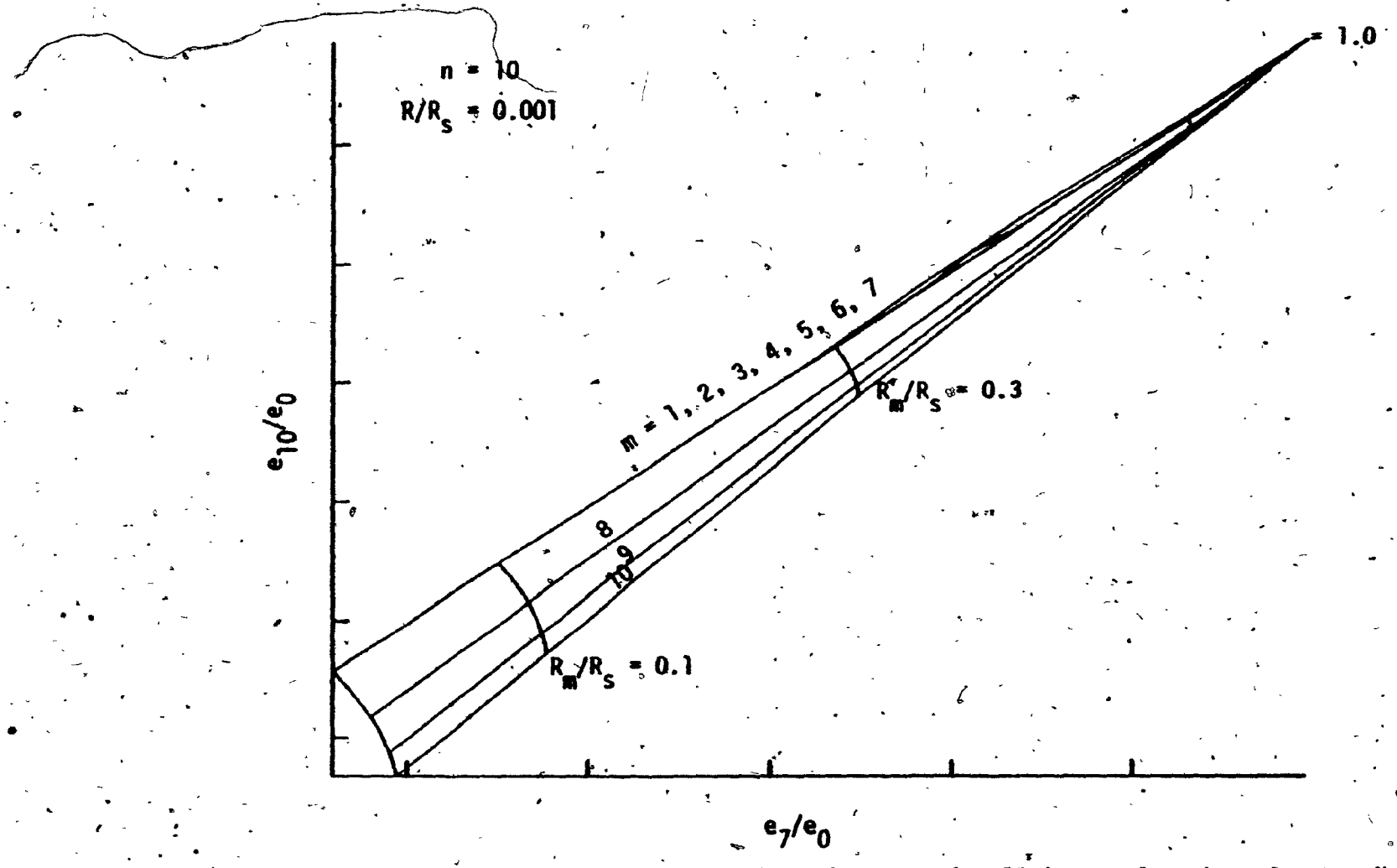

Figure 6. Illustration of the fact that equation 12 is not function of potential measurements after the fault (e_{10}/e_0 (vs) e_7/e_0)

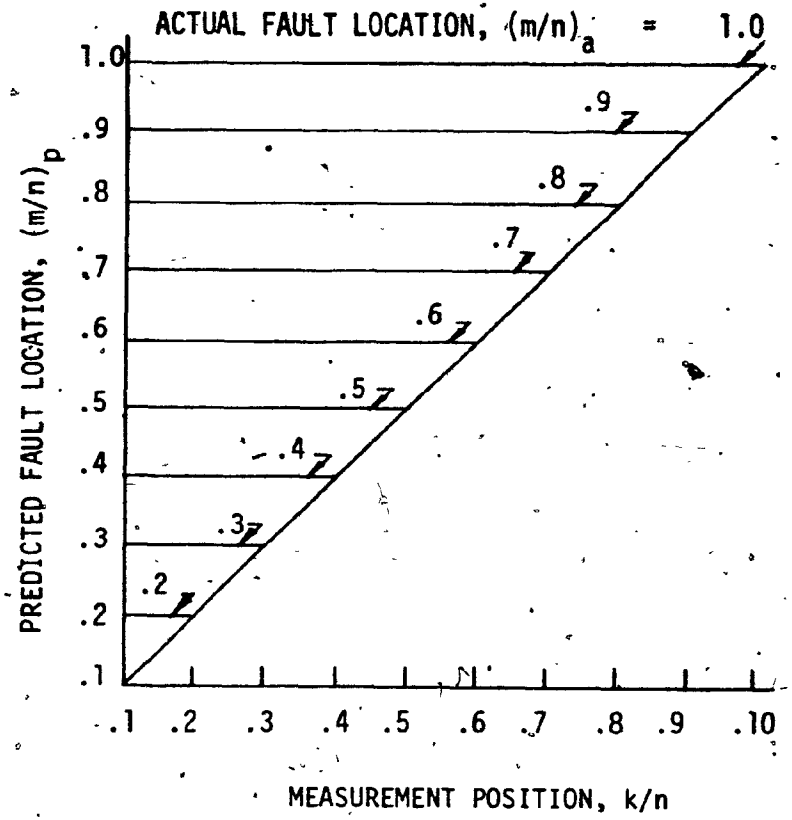

Figure 7. Effect of measurement position on predicted fault location

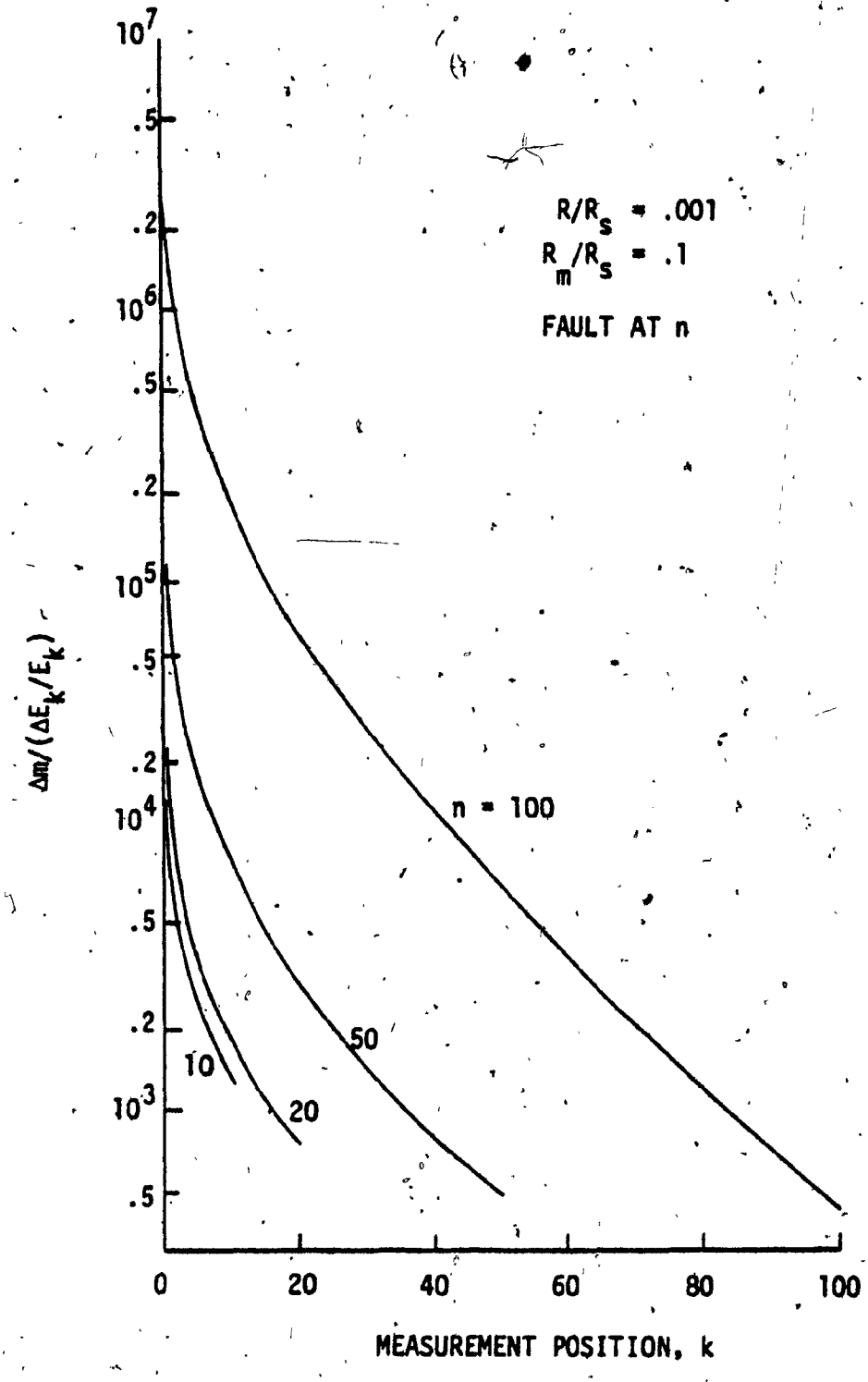

Figure 8. Sensitivity of fault prediction as a function of measurement position

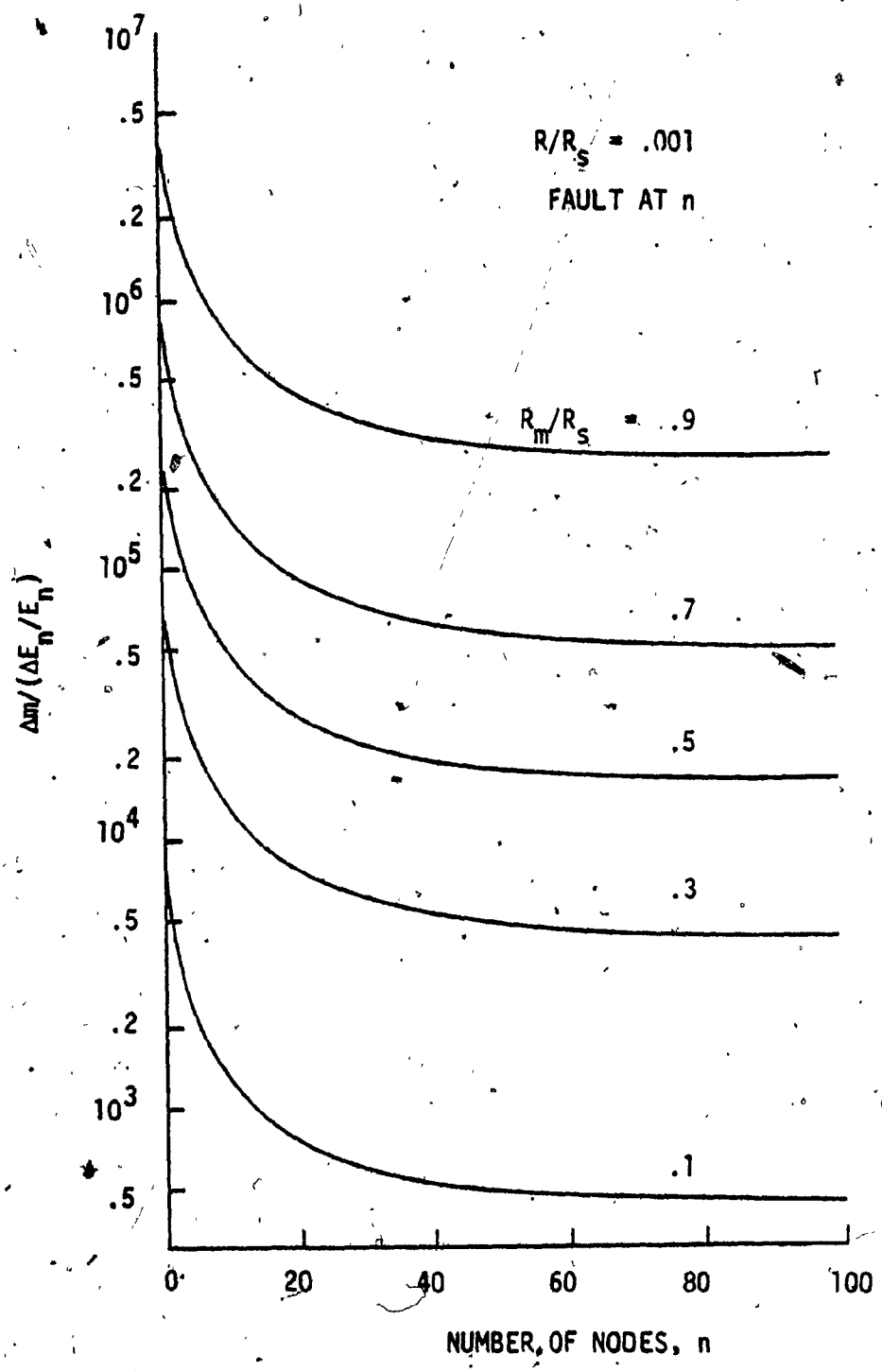

Figure 9. Sensitivity of fault prediction as a function of the number of nodes with fault magnitude as a parameter

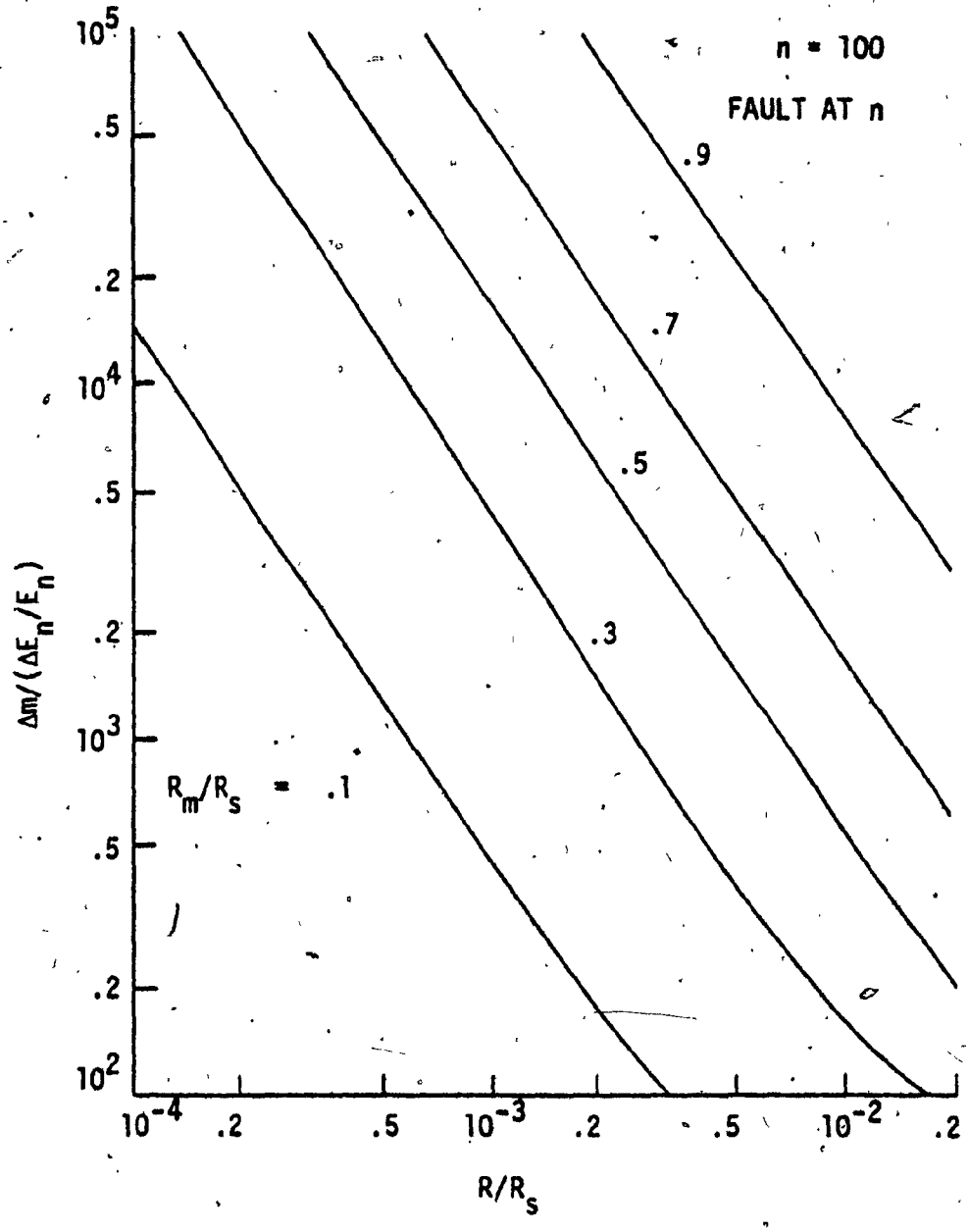

Figure 10. Sensitivity of fault prediction as a function of resistance ratio with fault magnitude as a parameter

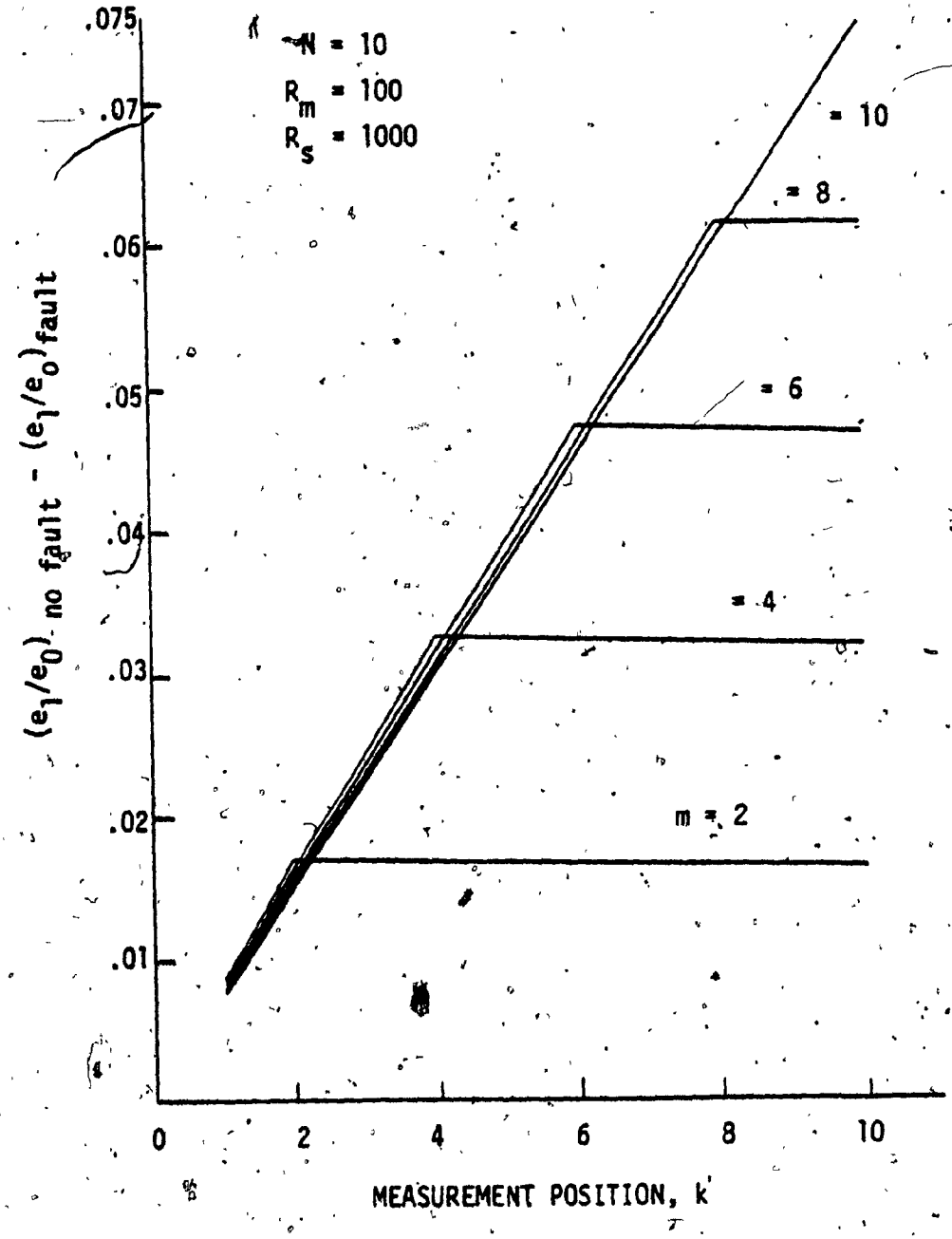

Figure 11. Simulated results of the difference method when applied to linear ladder network for N = 10 and R_m = 100 ohms.

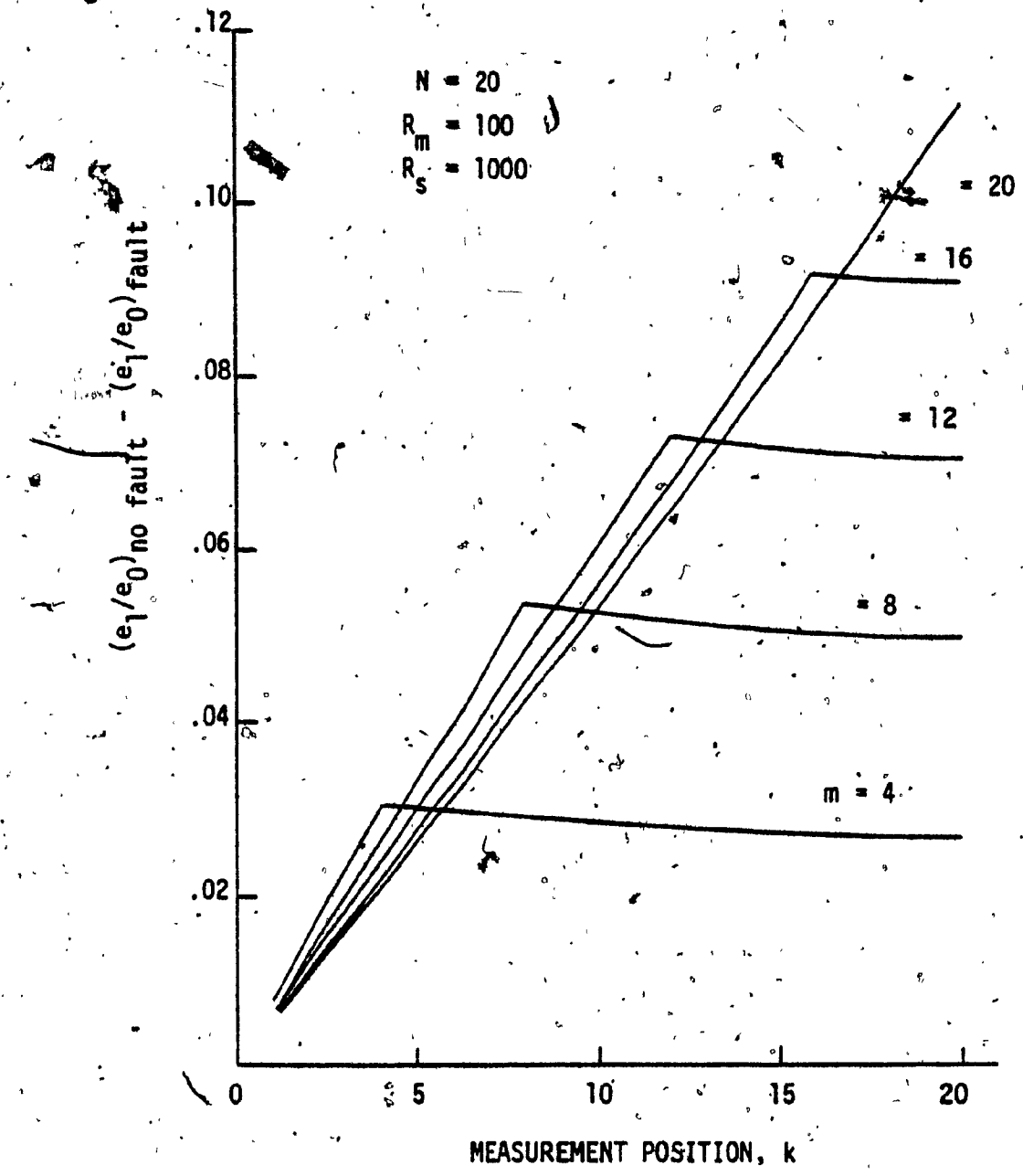

Figure 12. Simulated results of the difference method when applied to linear ladder network for N = 20 and R_m = 100 ohms

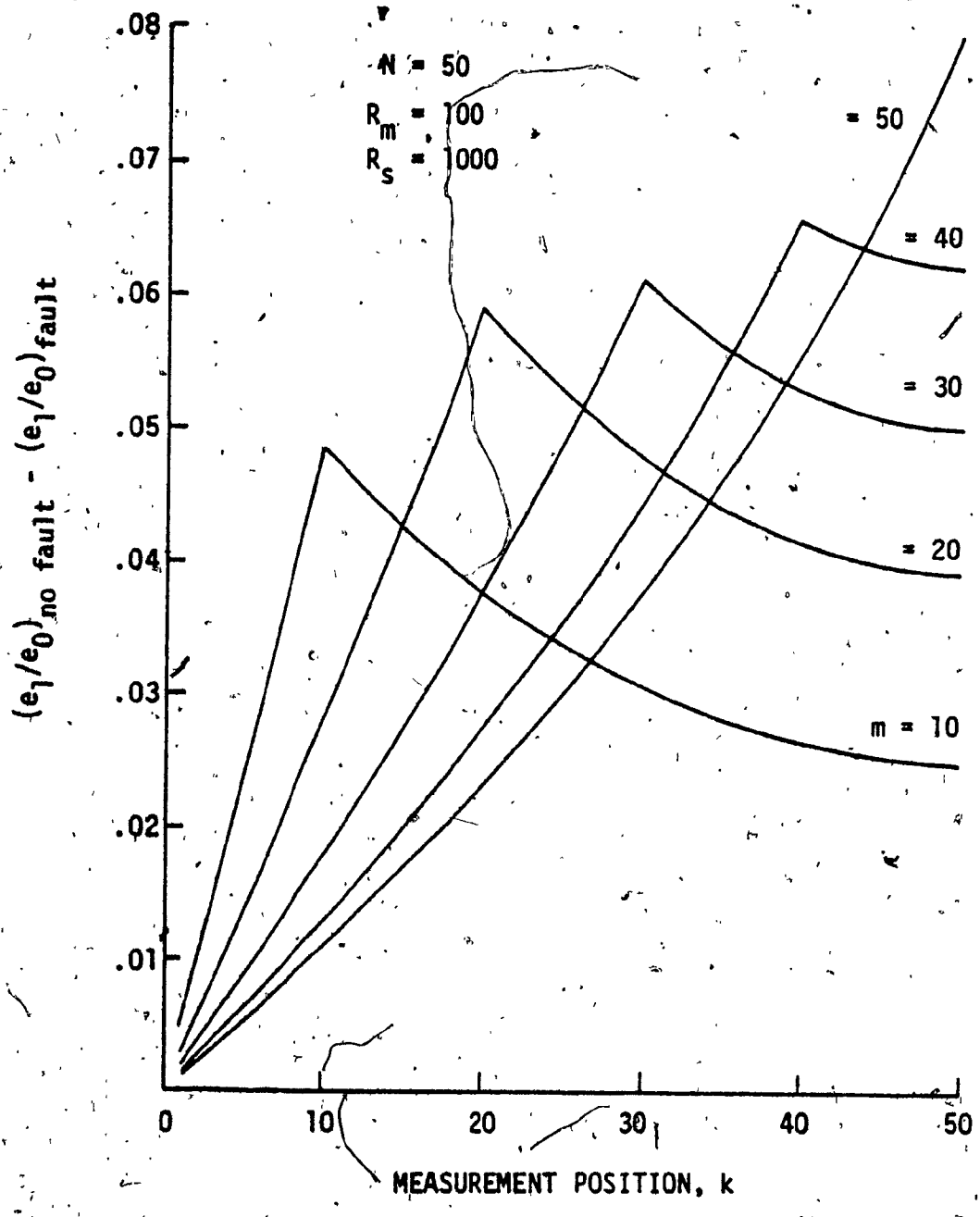

Figure 13. Simulated results of the difference method when applied to linear ladder network for N = 50 and R_m = 100 ohms

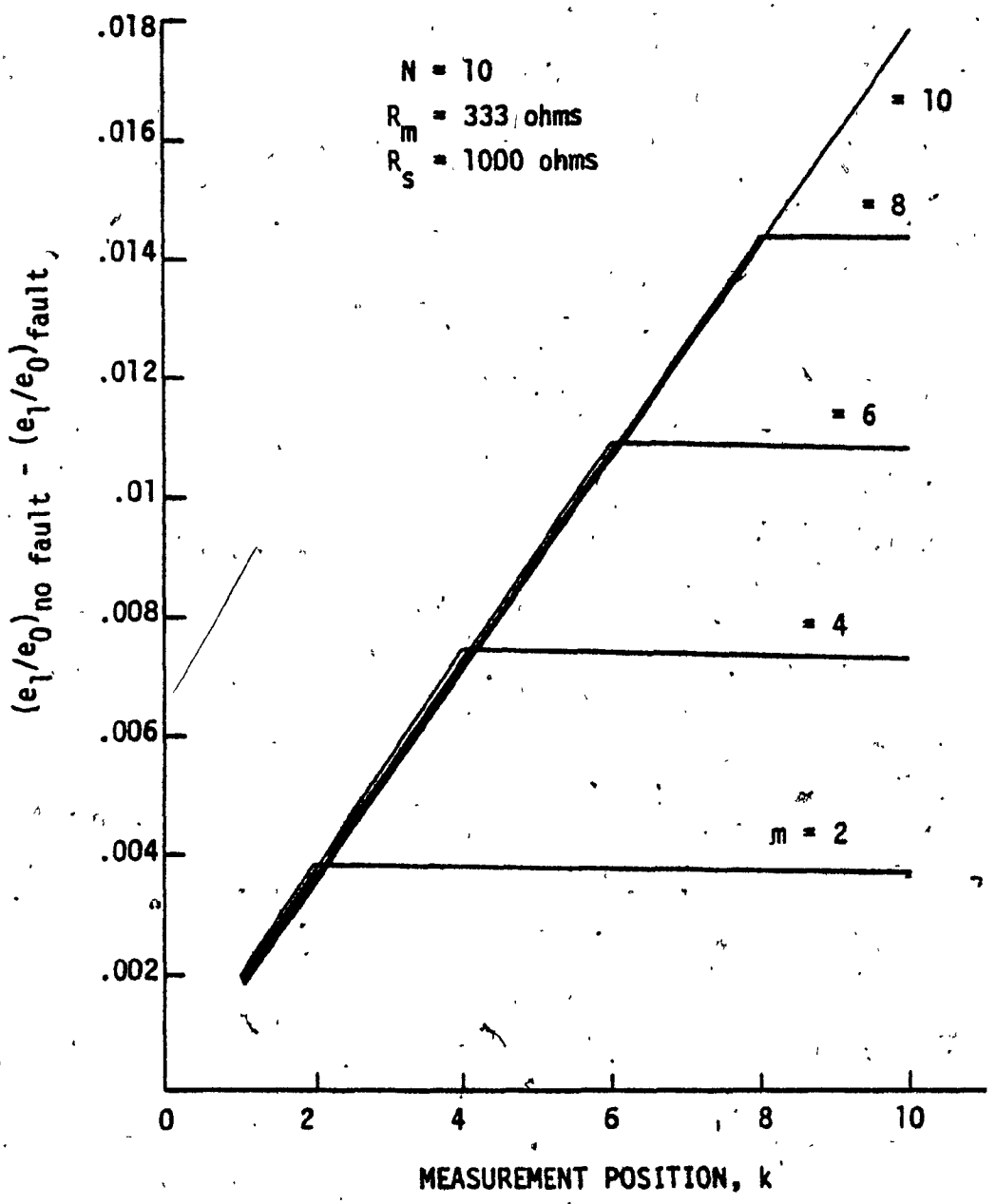

Figure 14. Simulated results of the difference method when applied to linear ladder network for N = 10 and R_m = 333 ohms

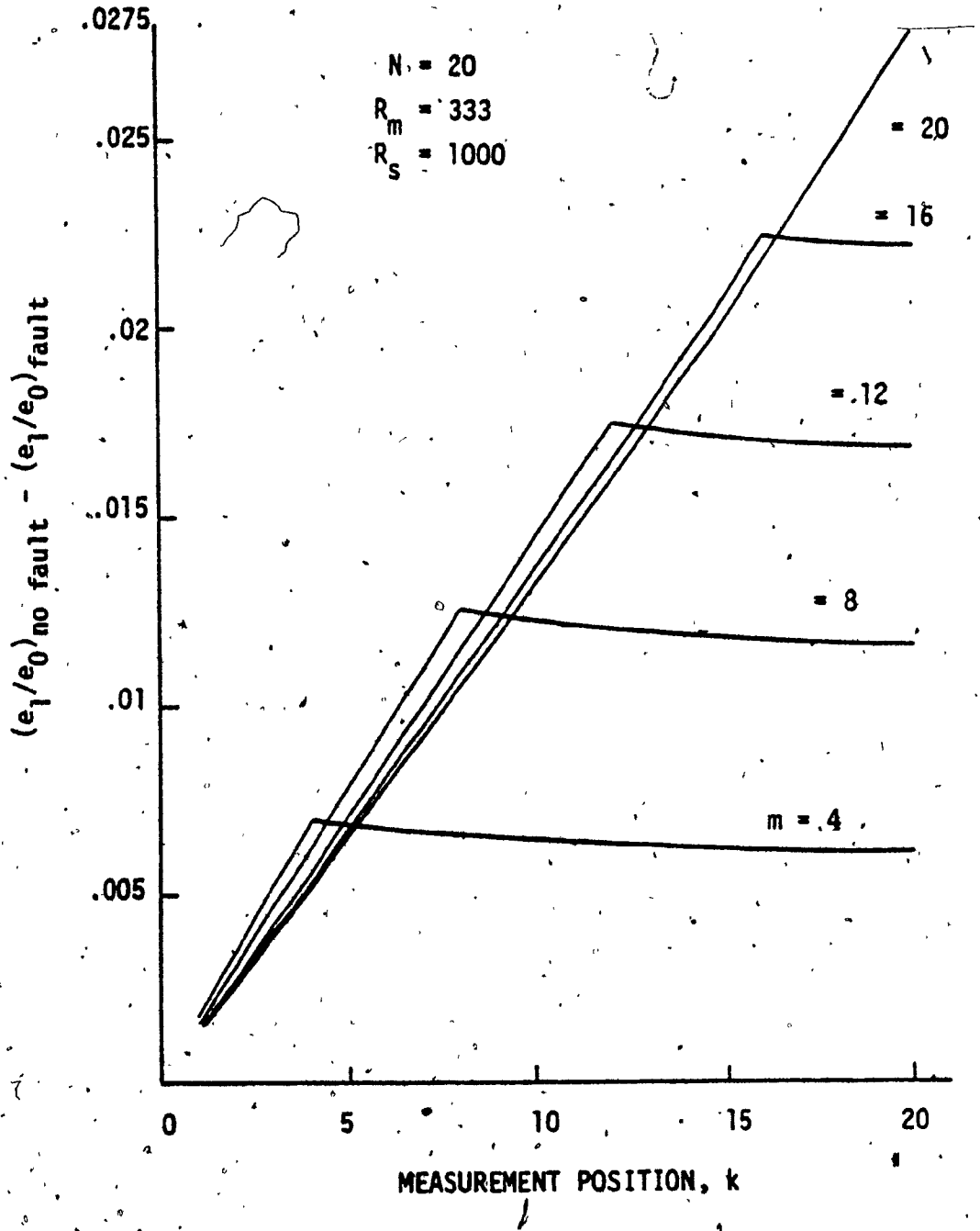

Figure 15. Simulated results of the difference method when applied to linear ladder network for N = 20 and R_m = 333 ohms

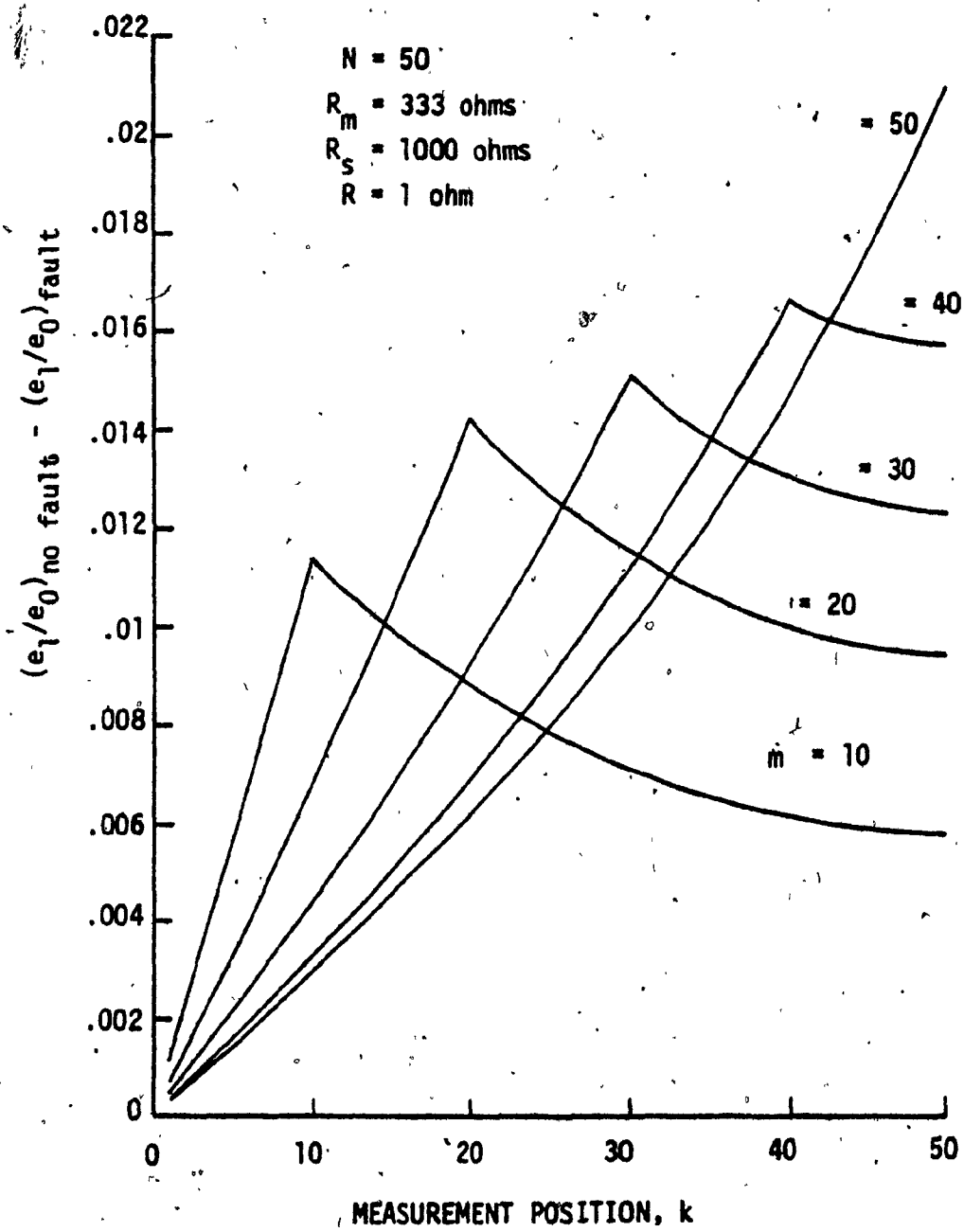

Figure 16. Simulated results of the difference method when applied to linear ladder network for N = 50 and R = 333 ohms

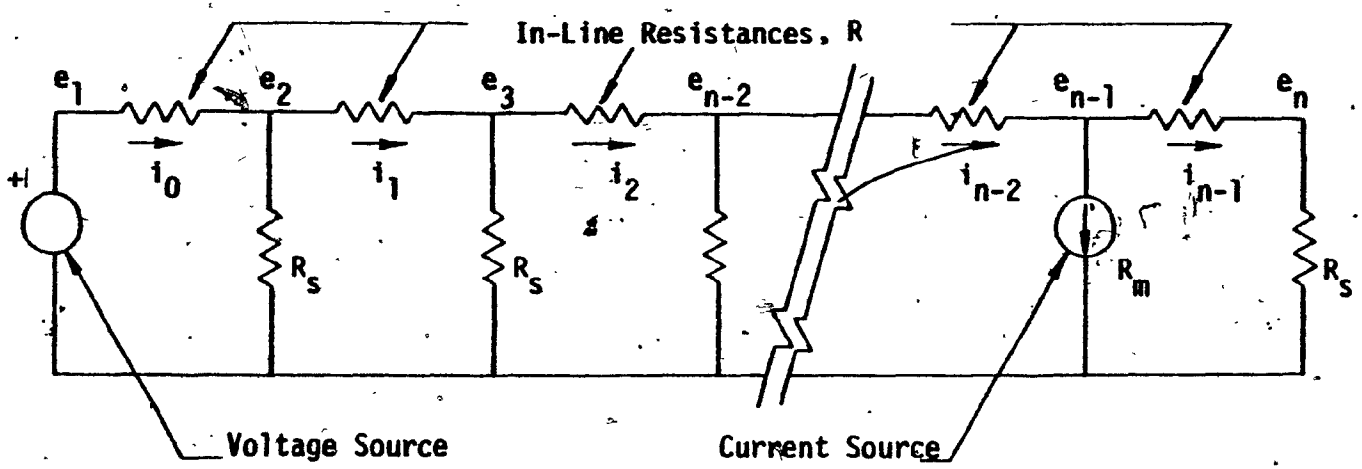

Figure 17. Linear model of the brakepipe for the ratio method

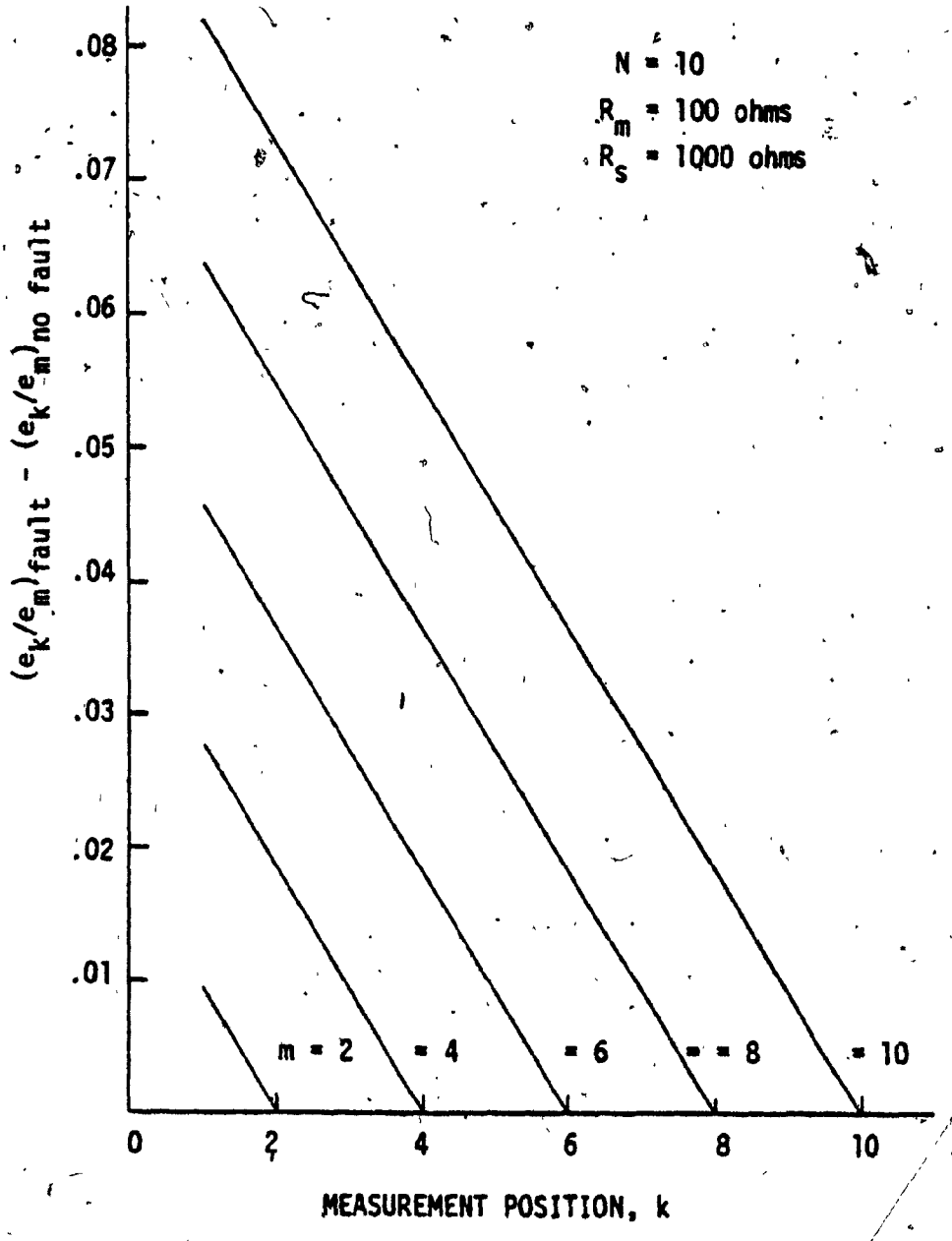

Figure 18. Simulated results on the computer when Ratio method is applied to the linear ladder network for N = 10 and R_m = 100 ohms

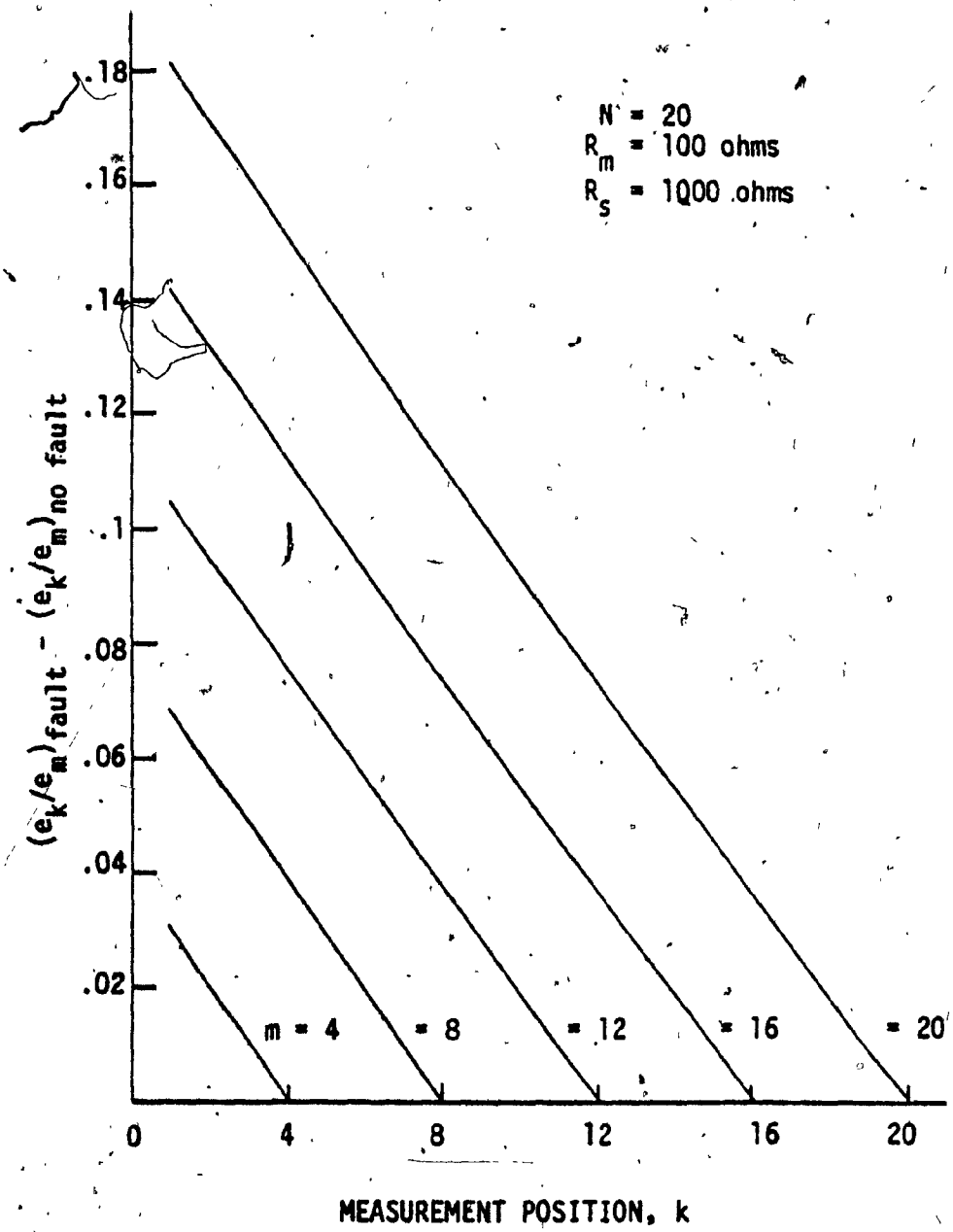

Figure 19. Simulated results on the computer when Ratio method is applied to the linear ladder network for N = 10 and R_m = 100 ohms

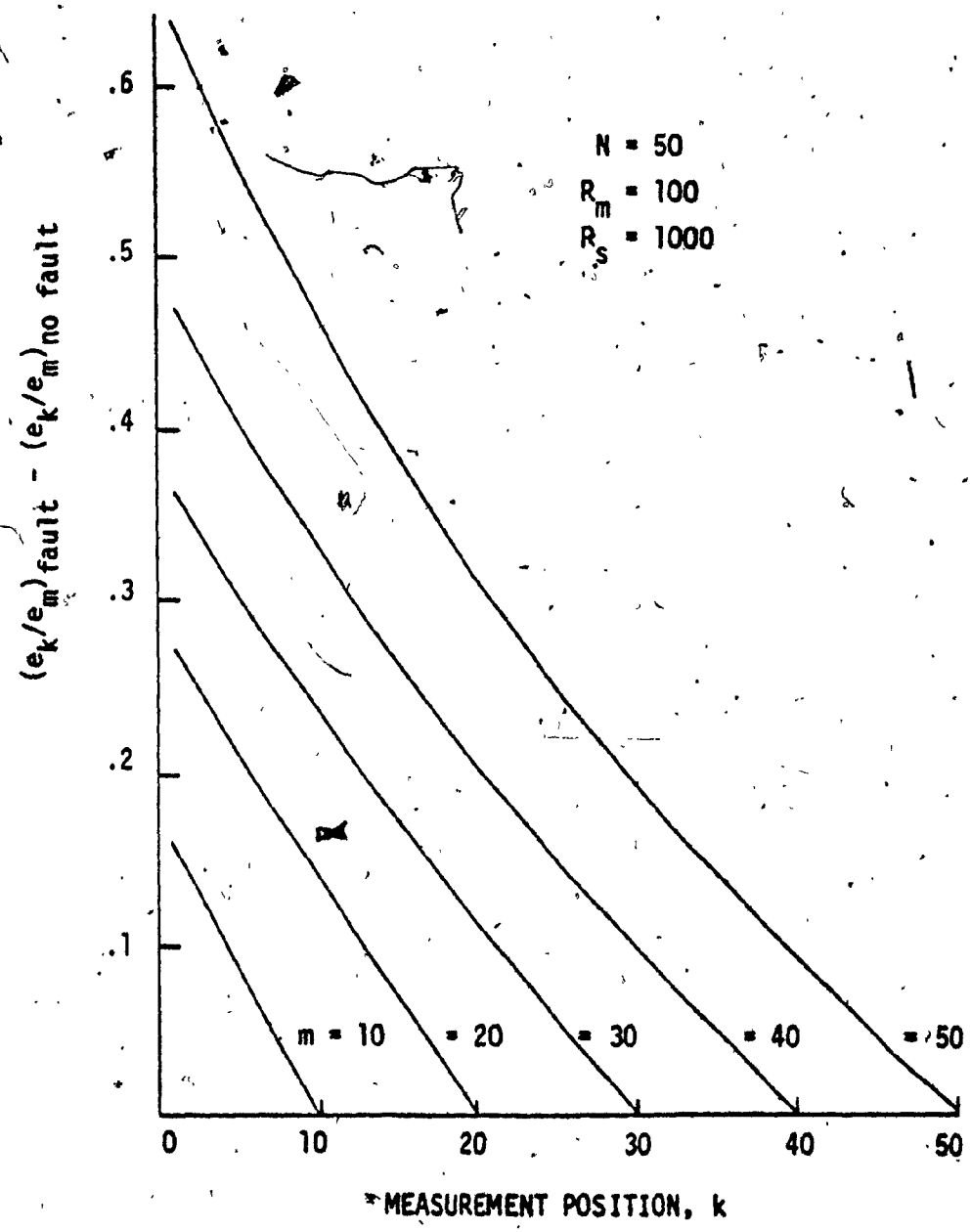

Figure 20. Simulated results on the computer when Ratio method is applied to the linear ladder network for N = 50 and R_m = 100 ohms

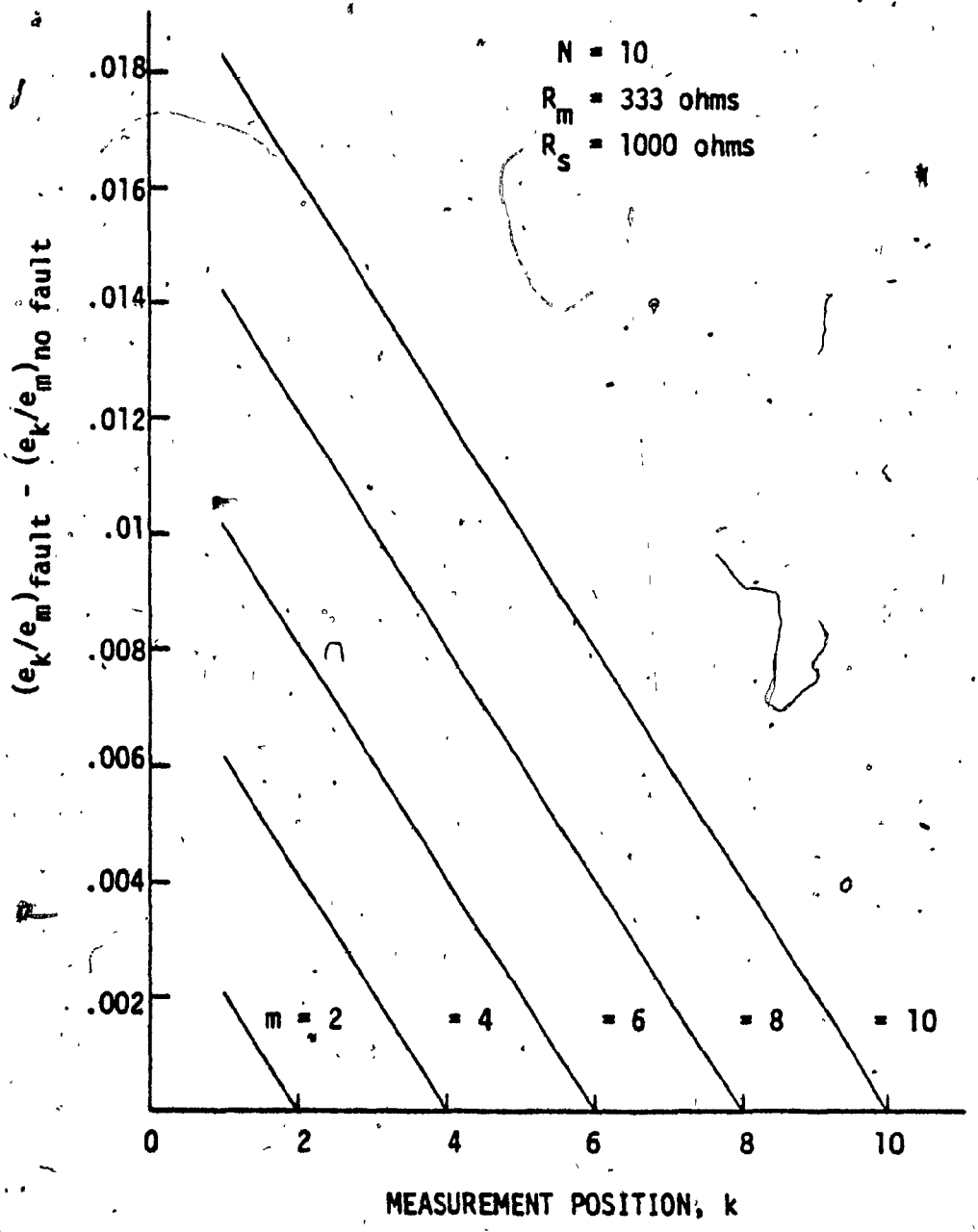

Figure 21. Simulated results on the computer when Ratio method is applied to the linear ladder network for N = 10 and R_m = 333 ohms.

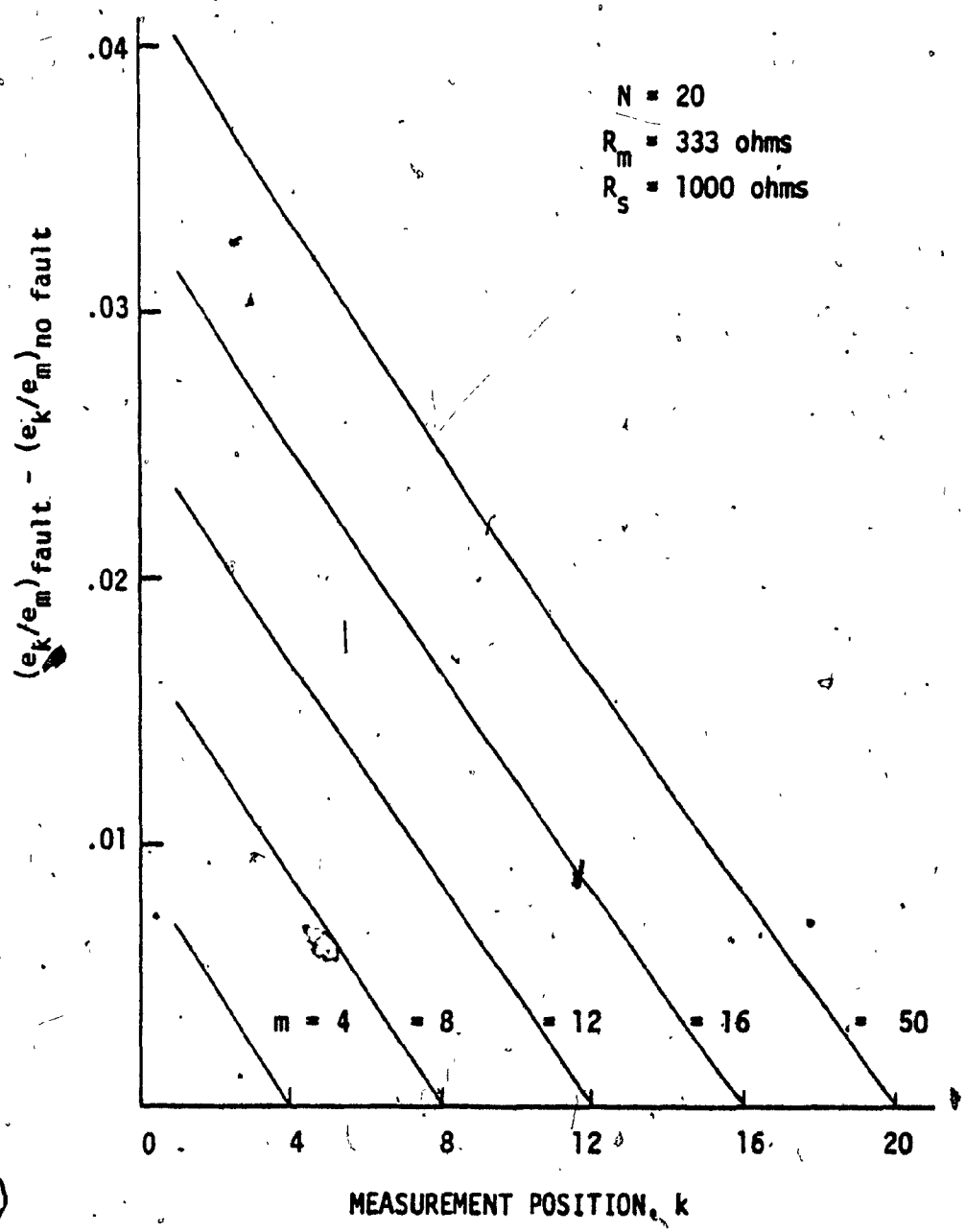

Figure 22. Simulated results on the computer when Ratio method is applied to the linear ladder network for N = 50 and R_m = 333 ohms

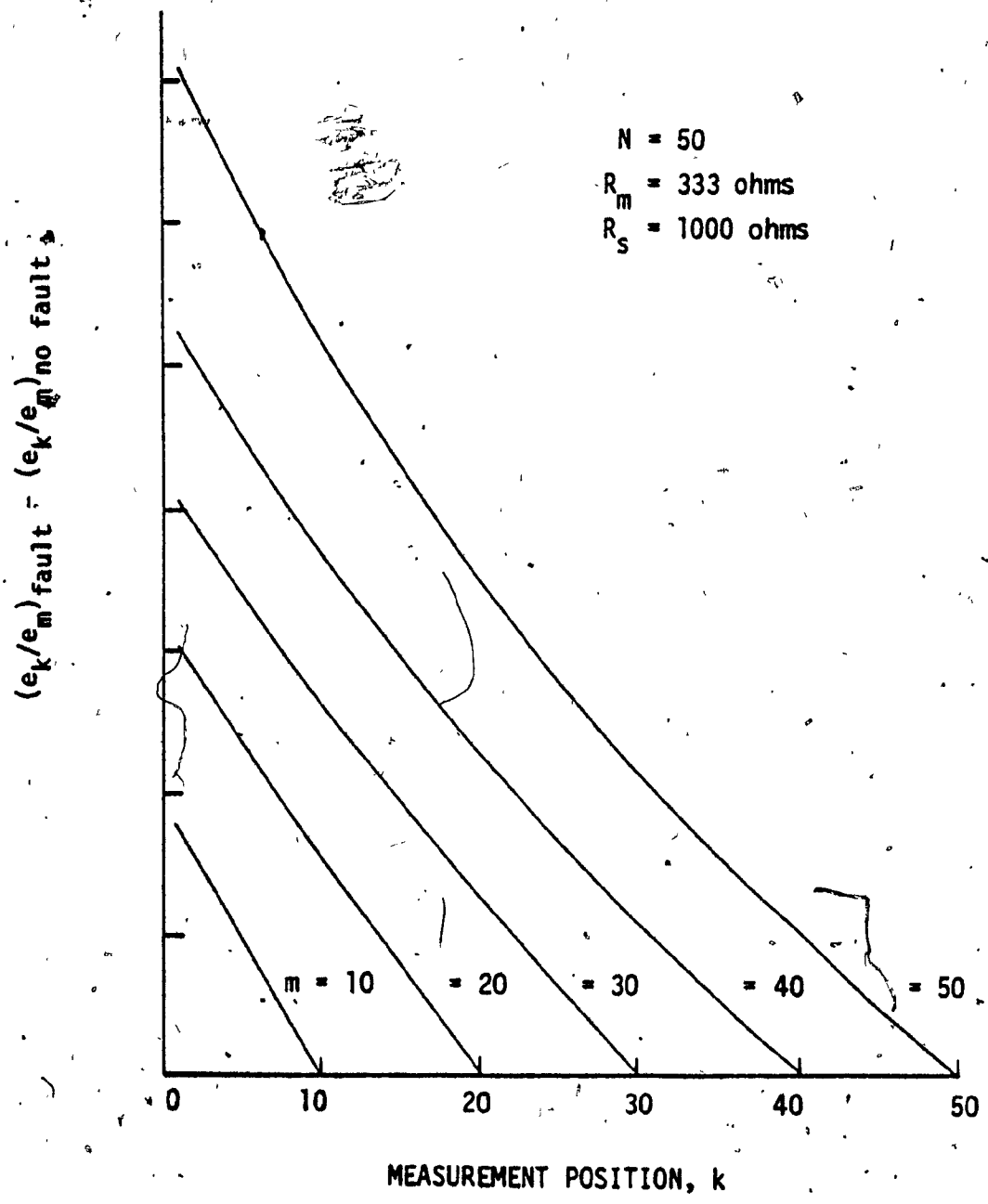

Figure 23. Simulated results on the computer when Ratio method is pplied to the linear ladder network for N = 50 and R_m = 333 ohms

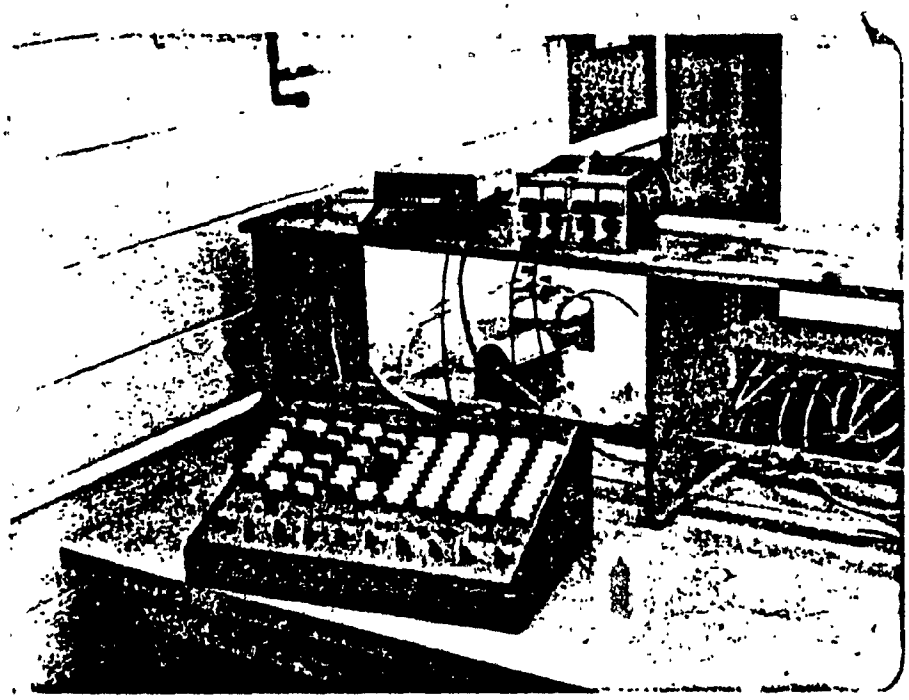

Figure 24. Electrical ladder network model

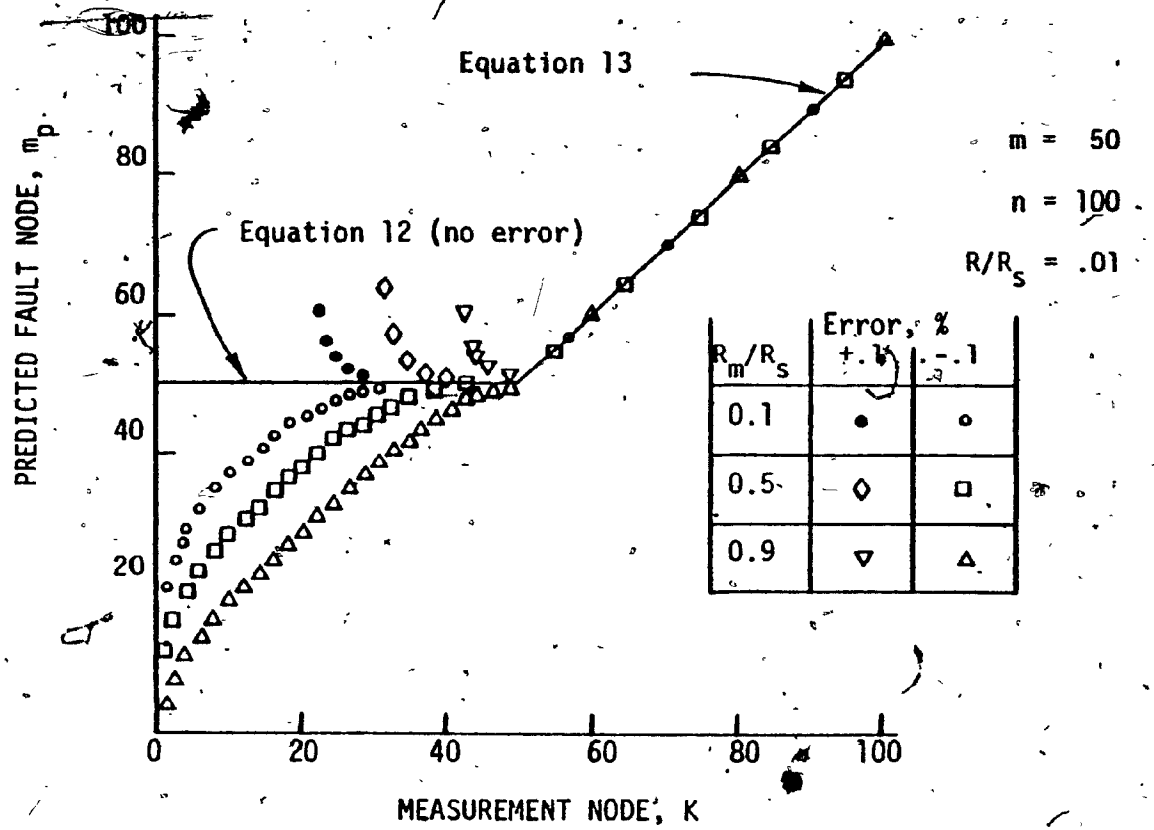

Figure 25. Comparison of Theoretical Fault Prediction and Computer Solution With Simulated Error

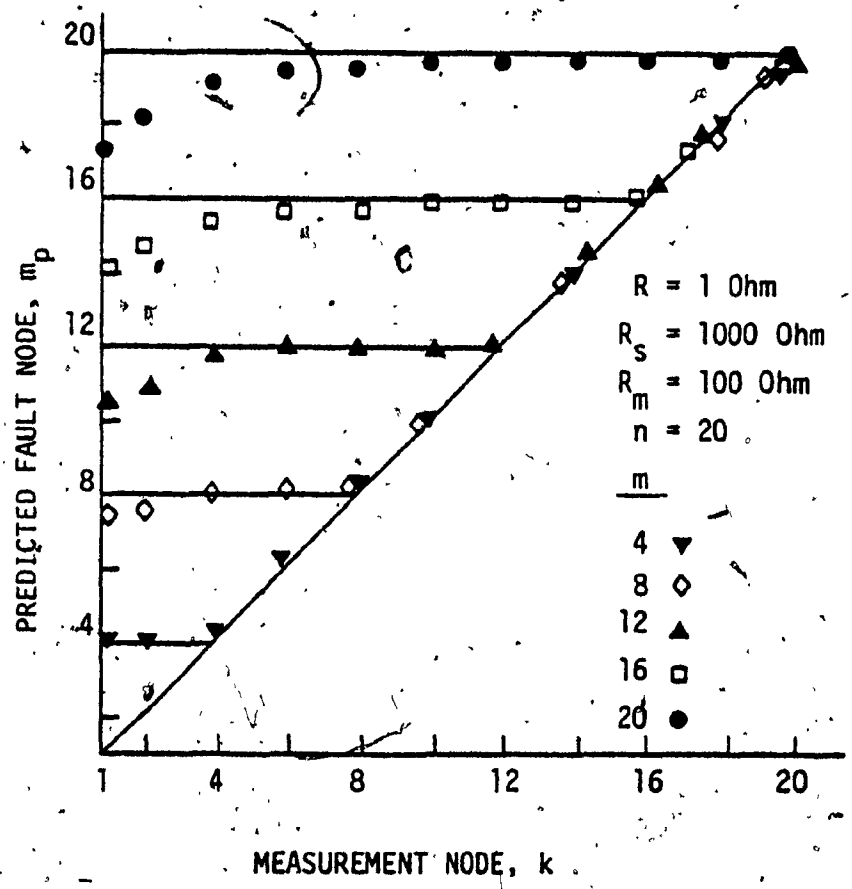

Figure 26. Comparison of Theoretical fault prediction and Electrical model (n = 20, R_m = 100 ohm)

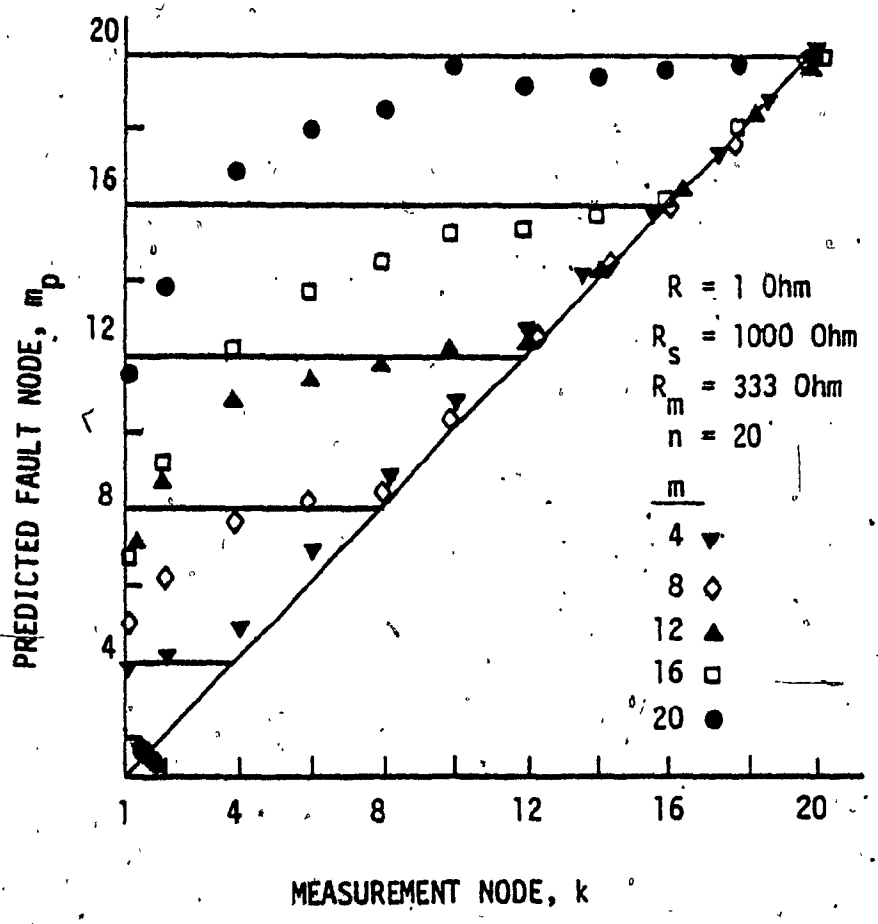

Figure 27. Comparison of theoretical fault prediction and Electrical model (n = 20, R_m = 333 ohm)

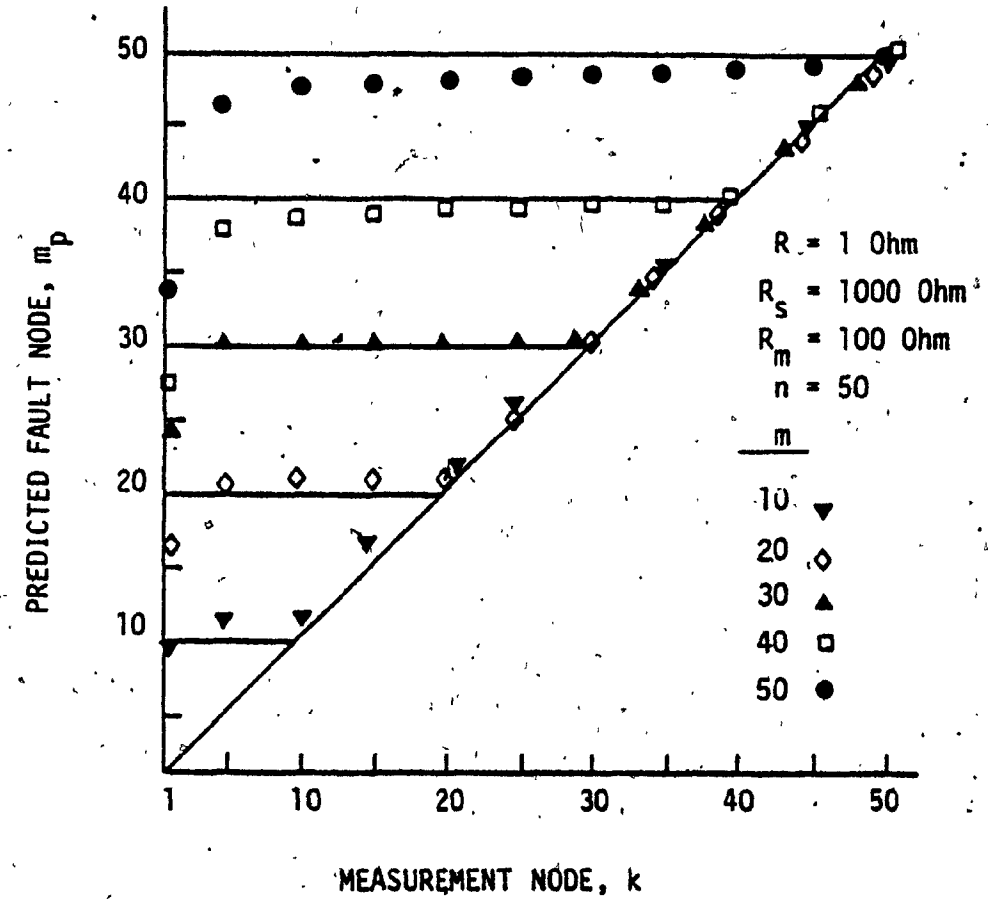

Figure 28. Comparison of Theoretical fault prediction and Electrical model (n = 50, R_m = 100 ohm)

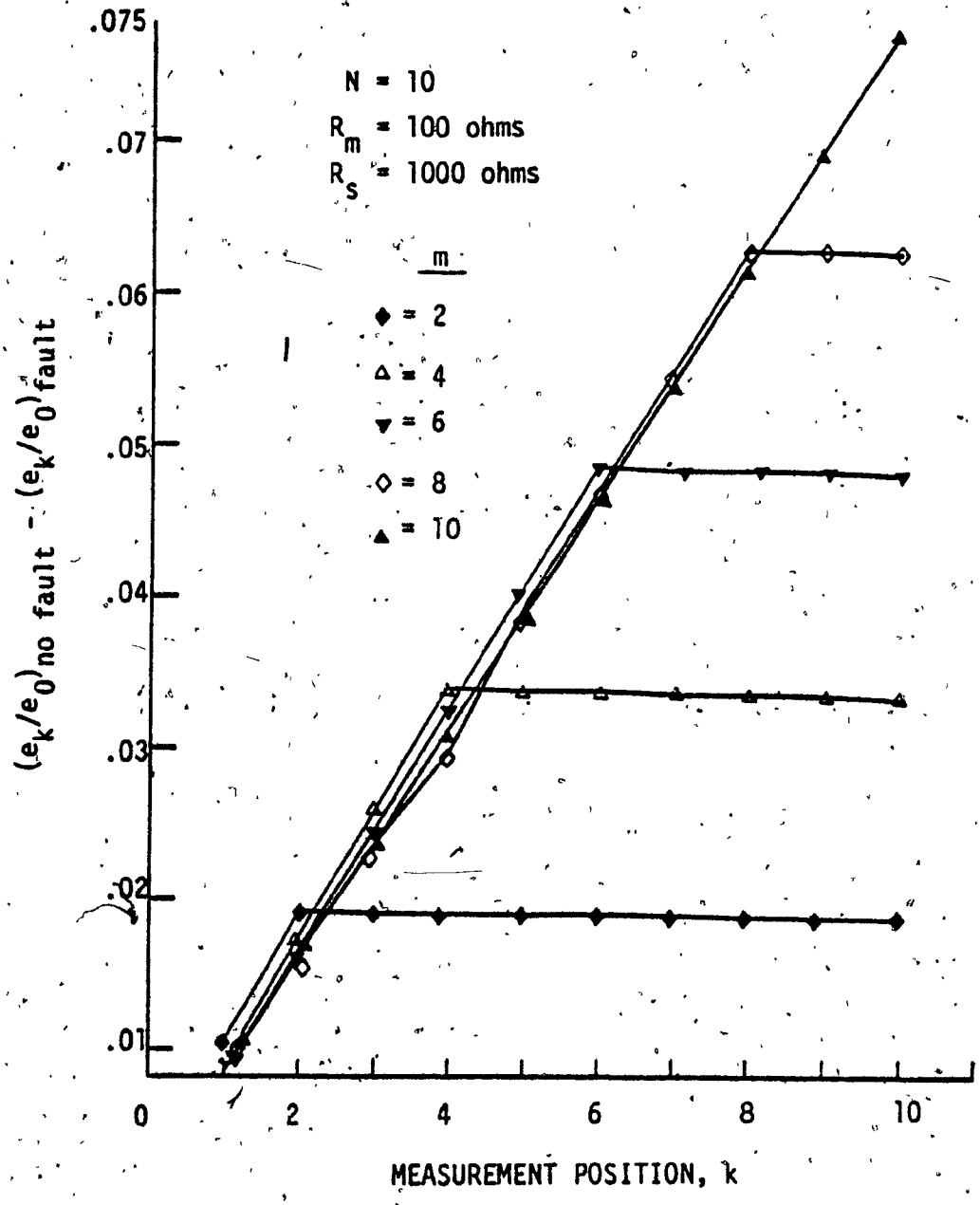

Figure 29. Experimental fault prediction by the Difference method when applied to linear brakepipe model (n = 10, R_m = 100 ohms)

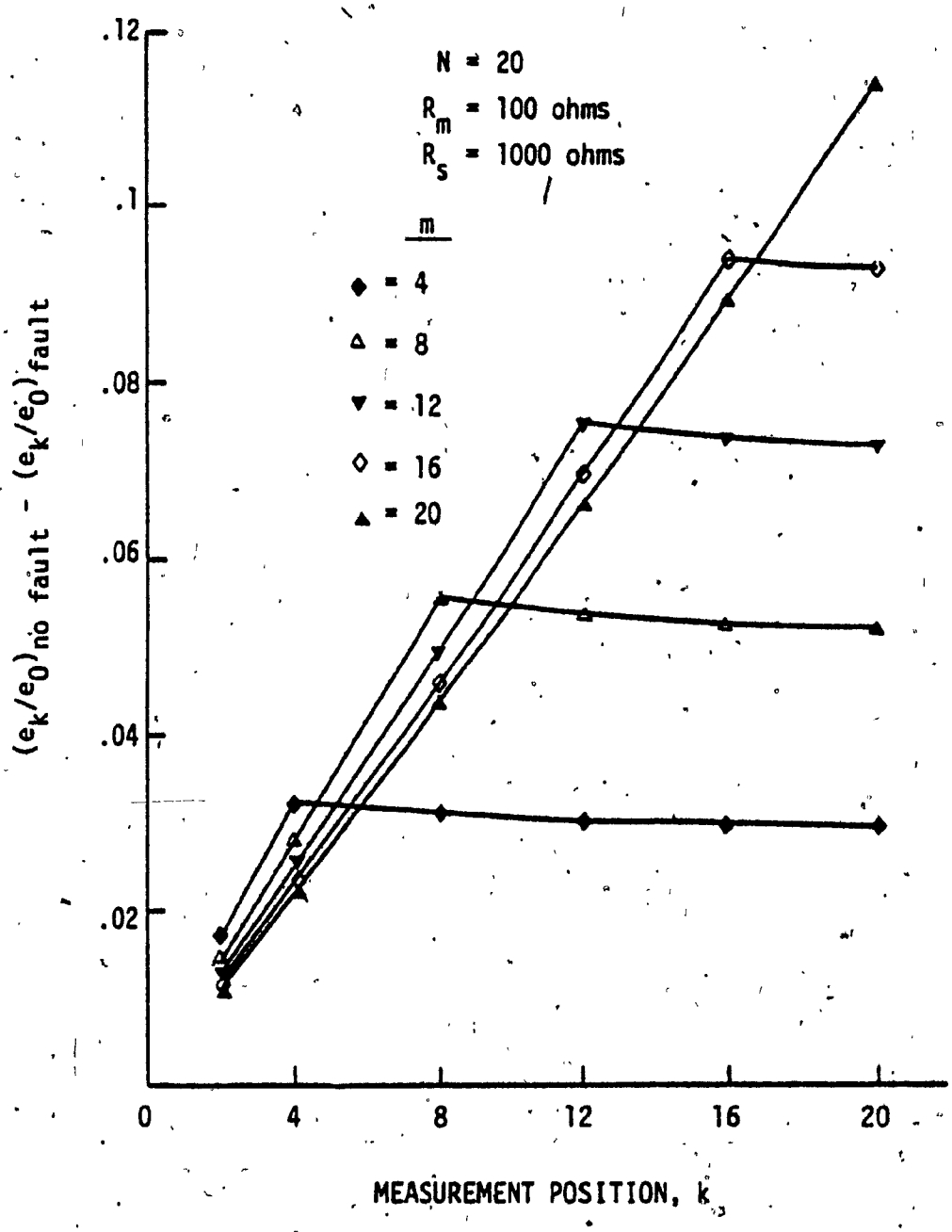

Figure 30. Experimental fault prediction by the Difference method when applied to linear brakepipe model (N = 20, R_m = 100 ohms)

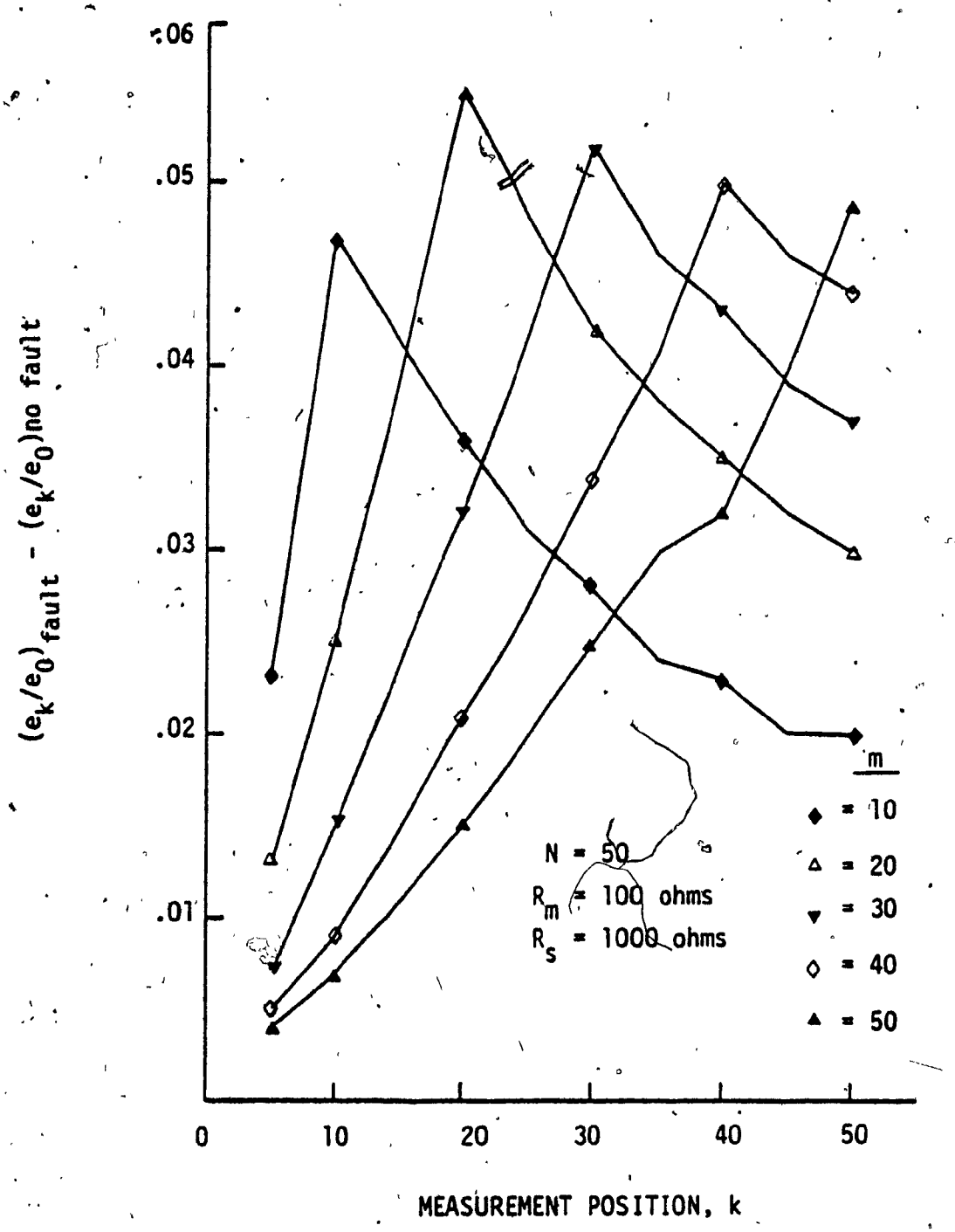

Figure 31. Experimental fault prediction by the Difference method when applied to linear brakepipe model (N = 50, R_m = 100 ohms)

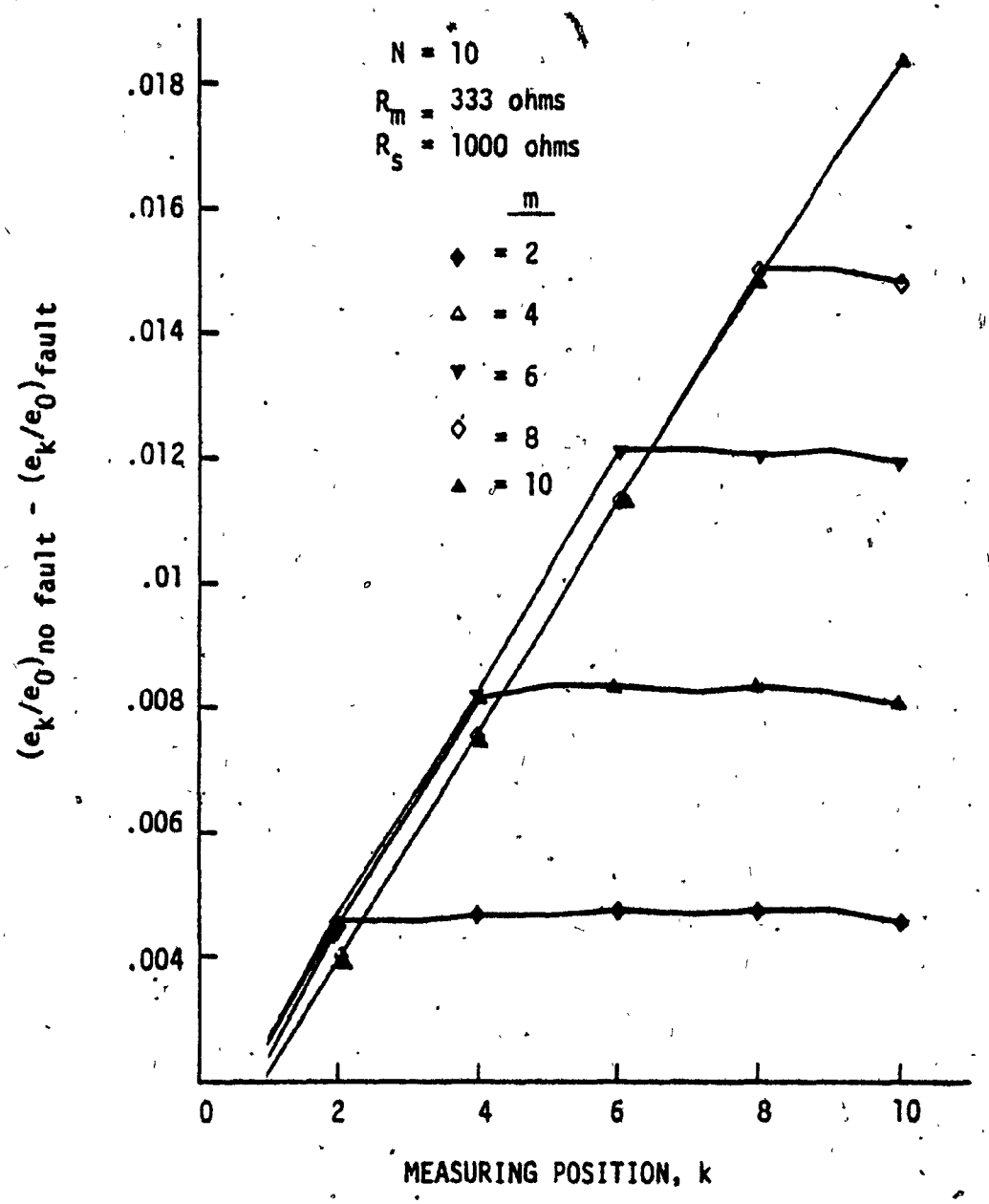

Figure 32. Experimental fault prediction by the Difference method when applied to linear brakepipe model (N = 10, R_m = 333 ohms)

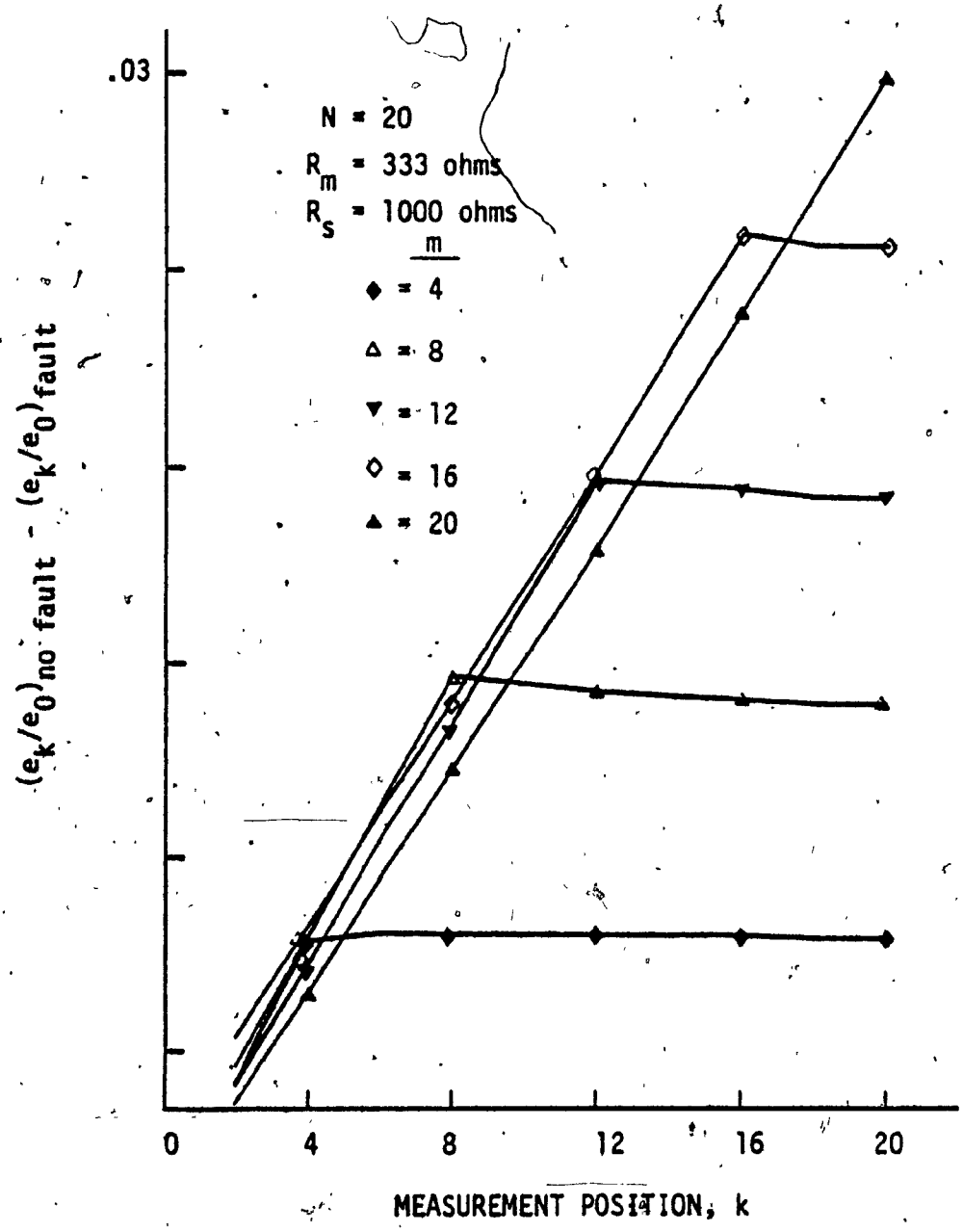

Figure 33.. Experimental fault prediction by the Difference method when applied to linear brakepipe model (N = 20, R_m = 333 ohms)

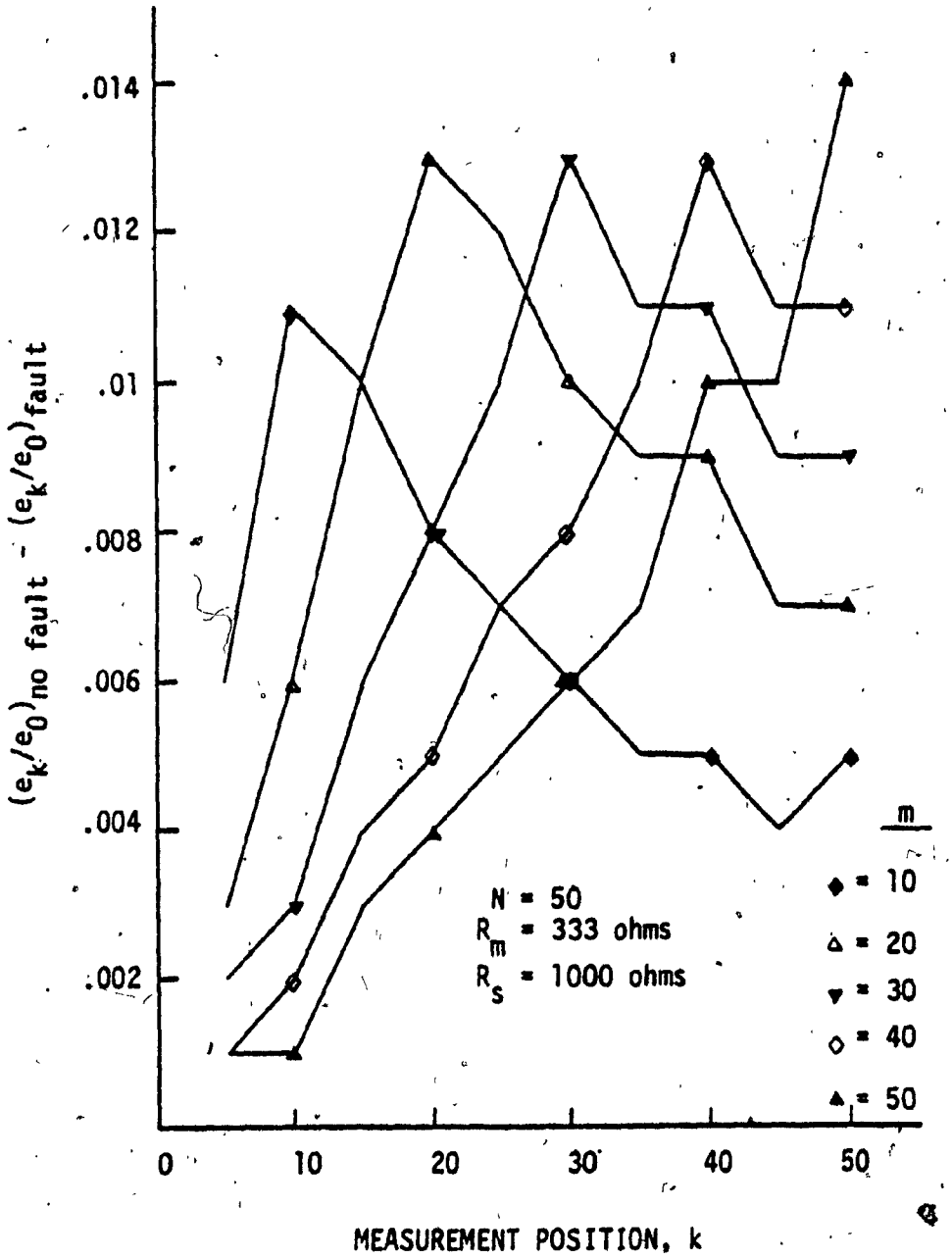

Figure 34. Experimental fault prediction by the Difference model when applied to linear brakepipe model (N = 50, R_m = 333 ohms)

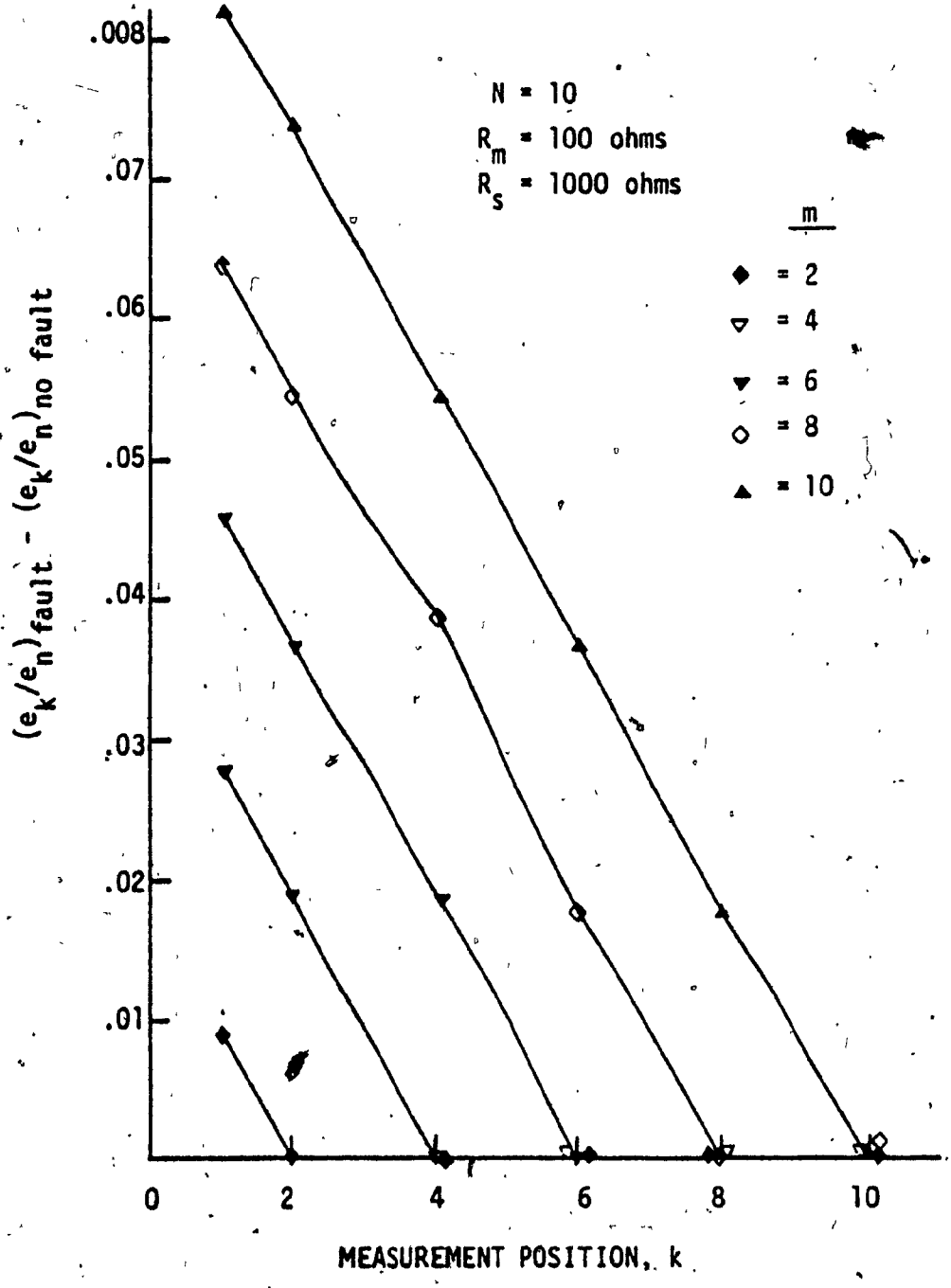

Figure 35. Experimental fault prediction by the Ratio method when applied to linear brakepipe model (N = 10, R_m = 333 ohms)

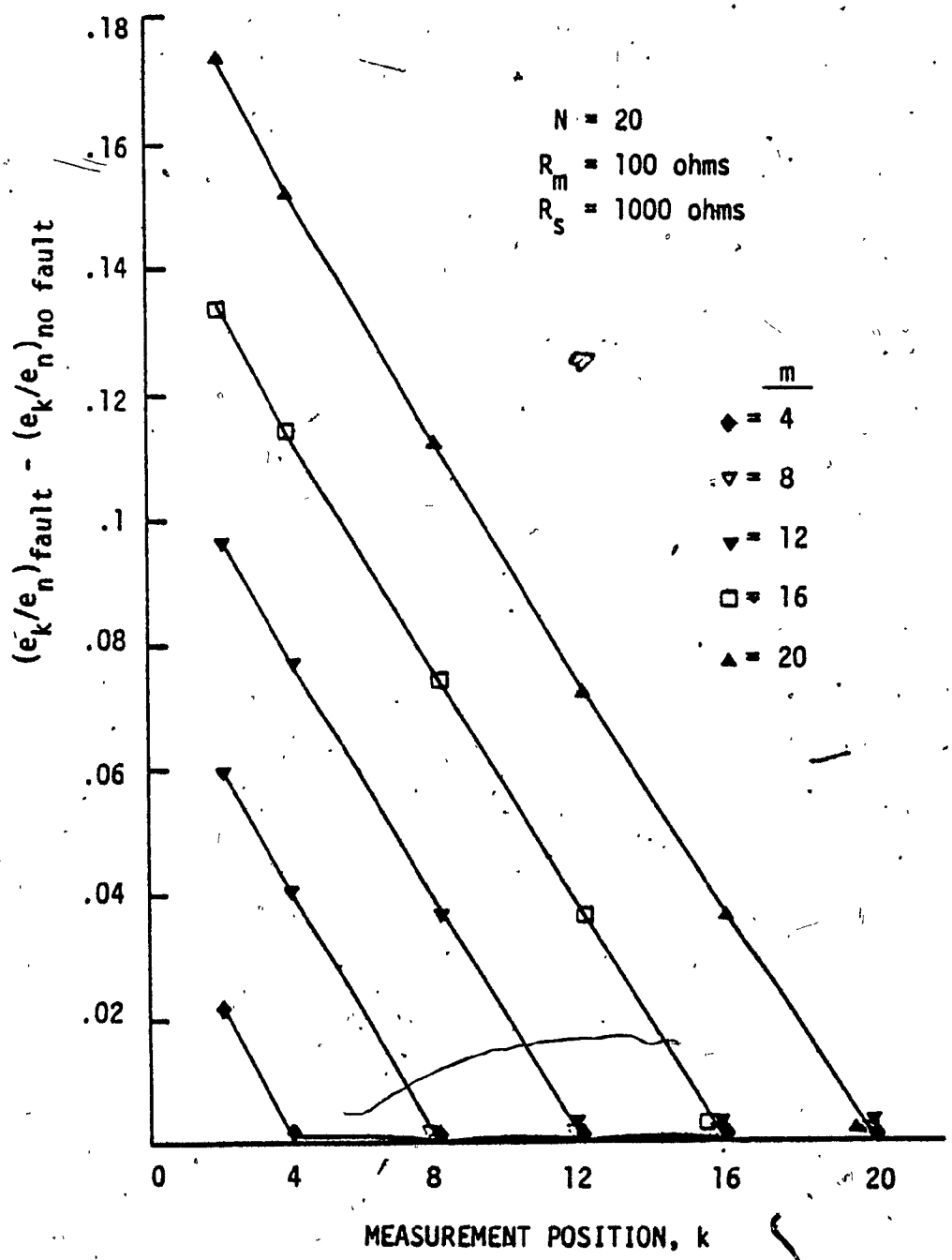

Figure 36. Experimental fault prediction by the Ratio method when applied to linear brakepipe model (N = 20, R_m = 100 ohms)

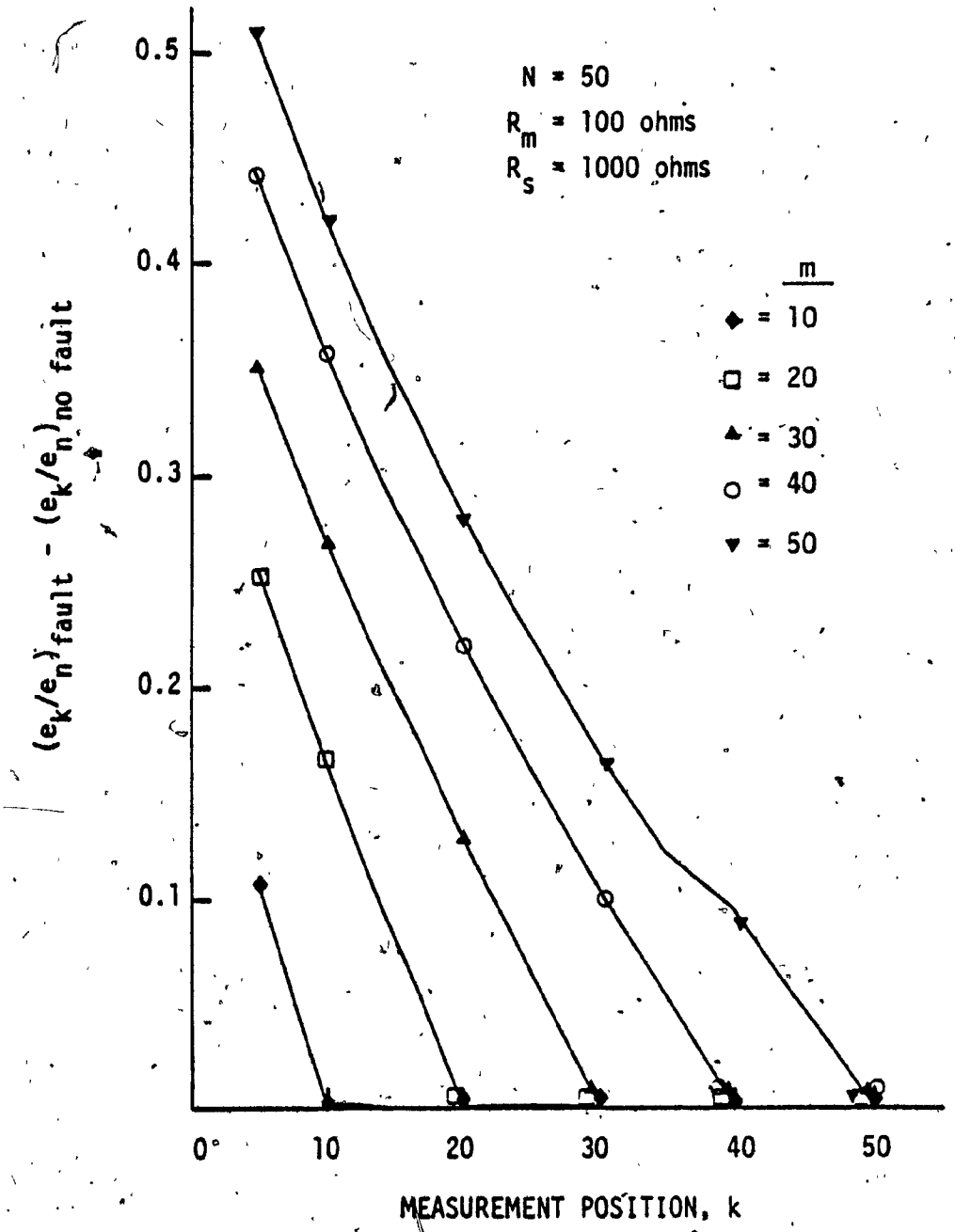

Figure 37. Experimental fault prediction by the Ratio method when applied to linear brakepipe model (N = 50, R_m = 100 ohms)

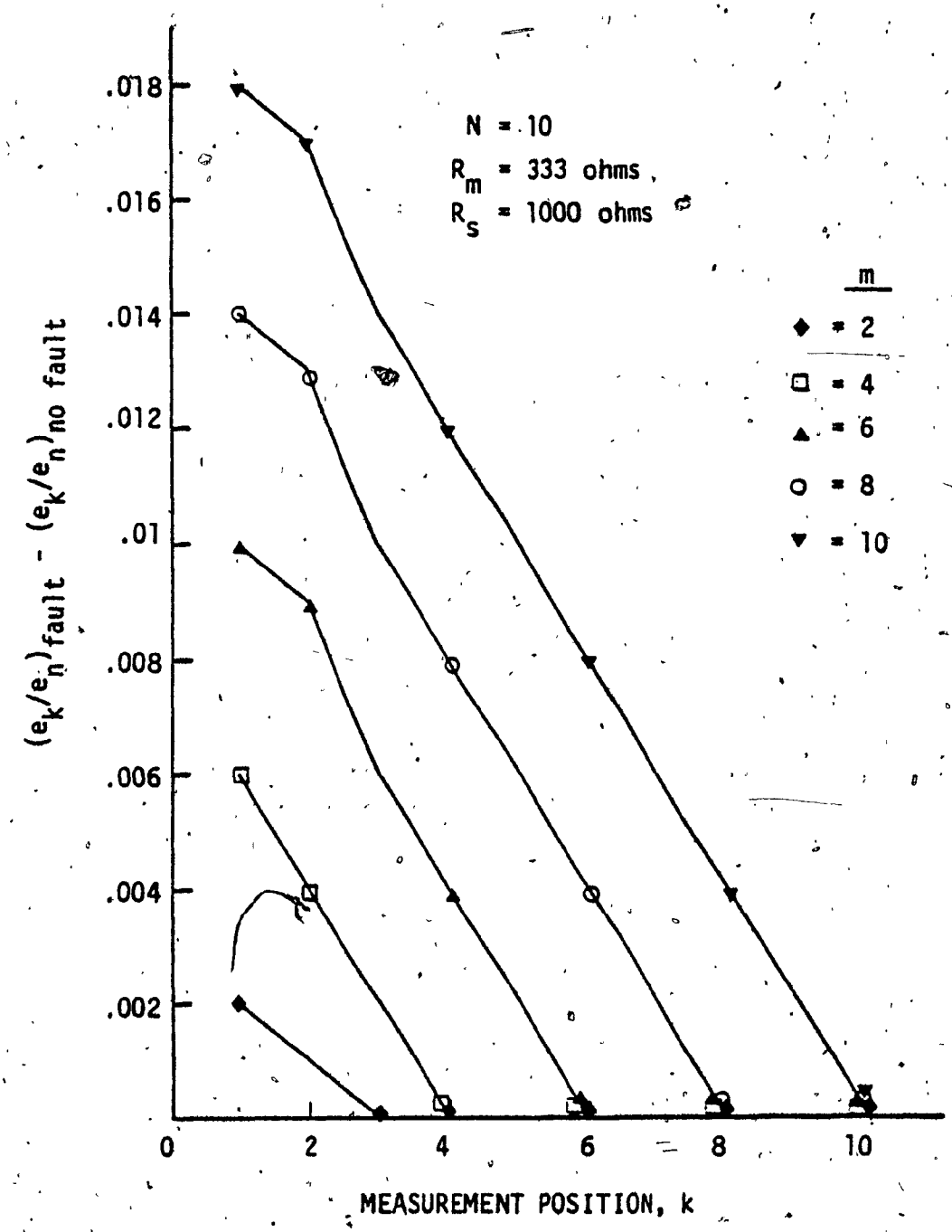

Figure 38. Experimental fault prediction by the Ratio method when applied to linear brakepipe model (N = 10, R_m = 333 ohms)

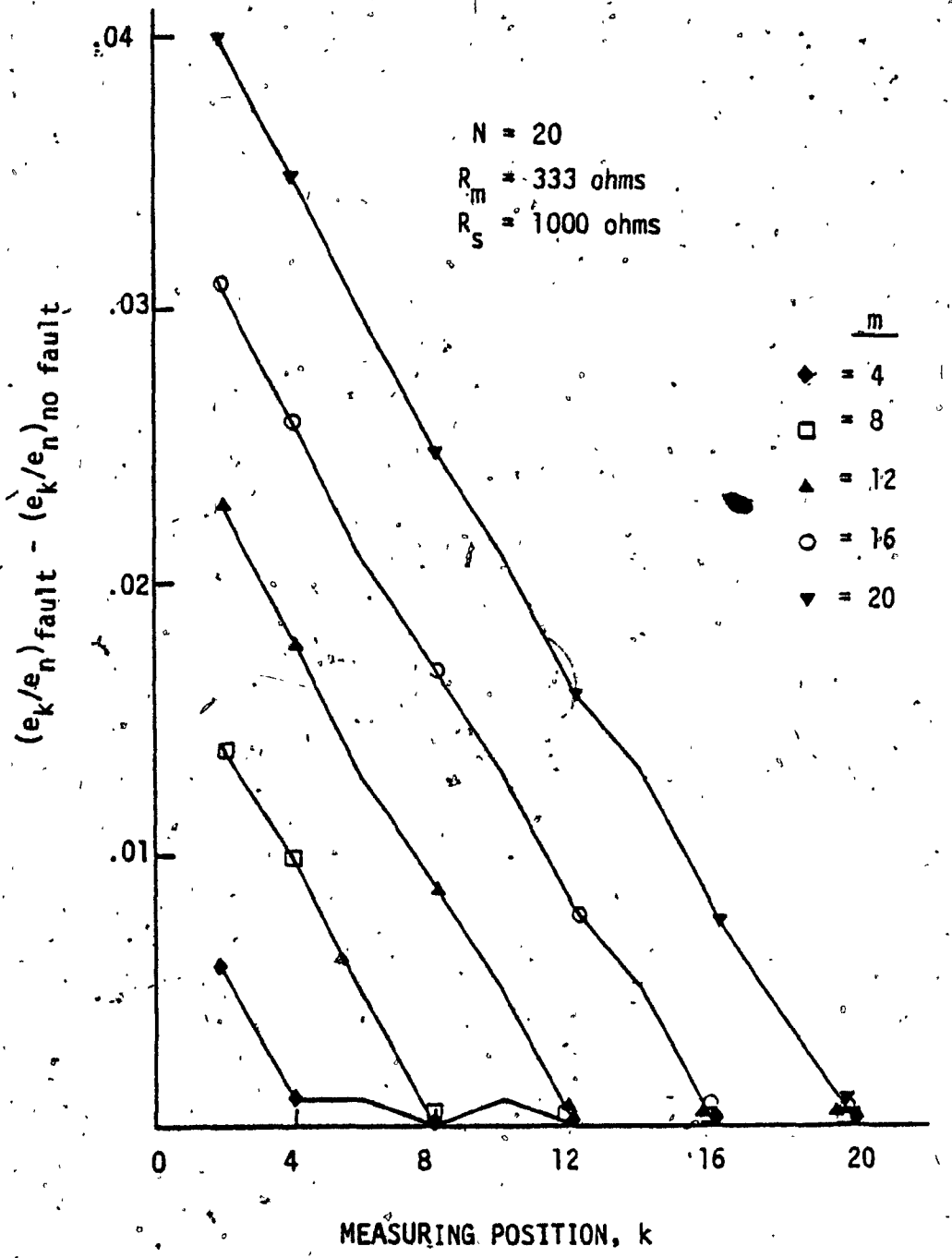

Figure 39. Experimental fault prediction by the Ratio method when applied to linear brakepipe model (N = 20, R_m = 333 ohms)

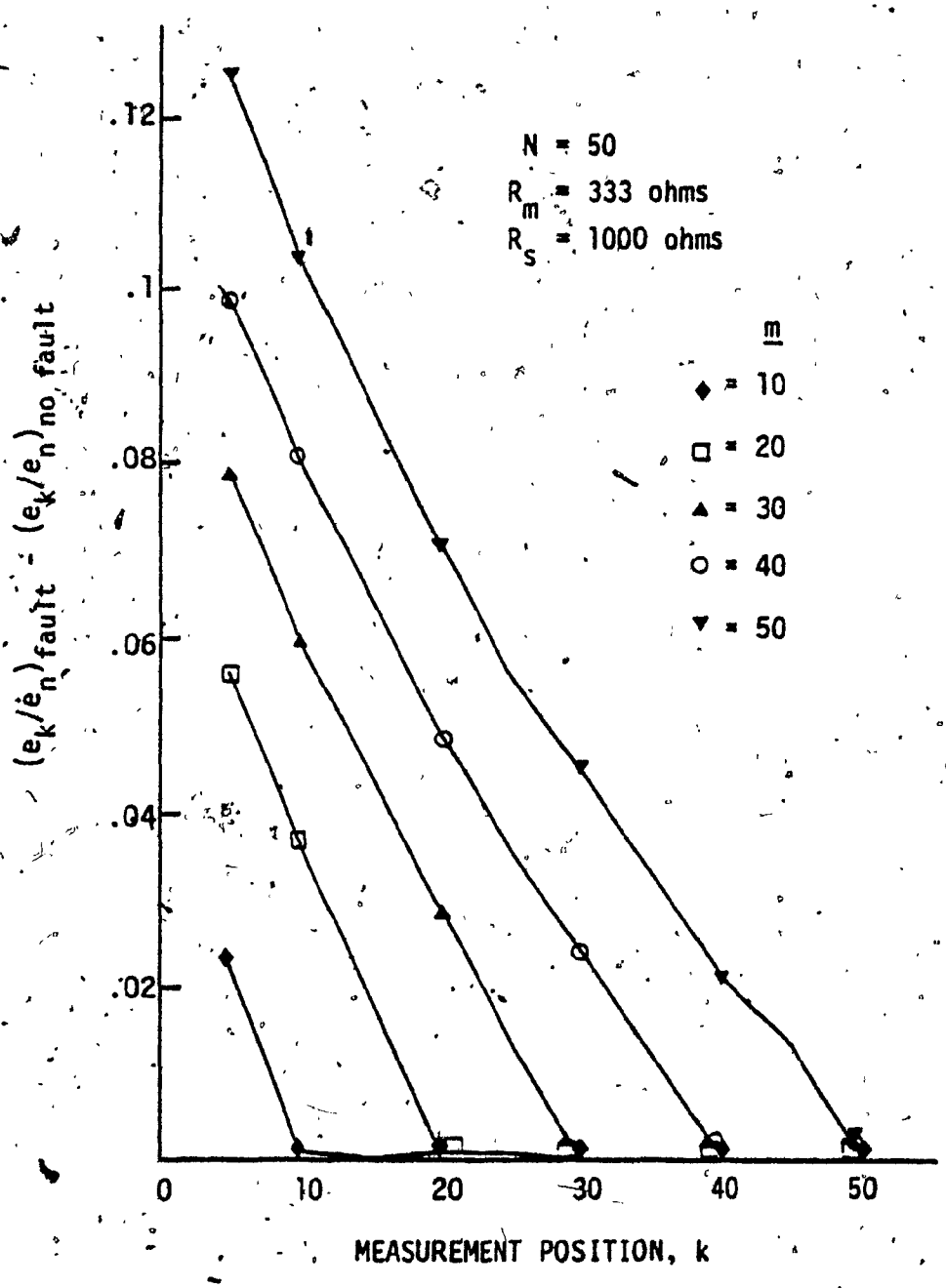

Figure 40. Experimental fault prediction by the Ratio method when applied to linear brakepipe model (N = 20, R_m = 333 ohms)

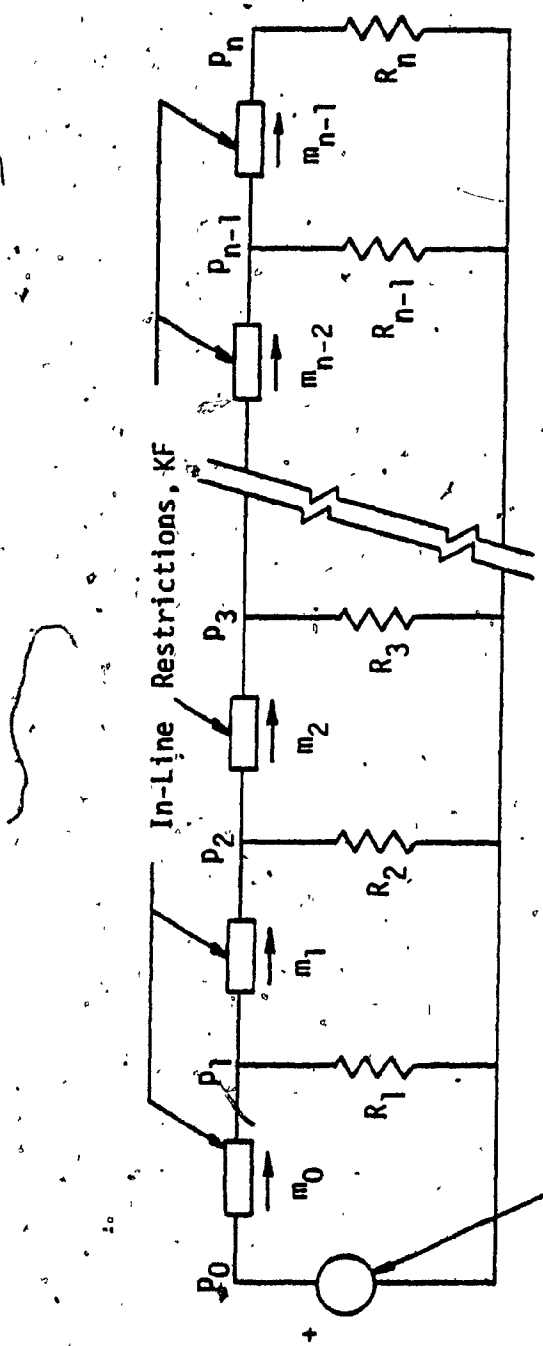

Figure 41. Nonlinear ladder network model for brakepipe leakage

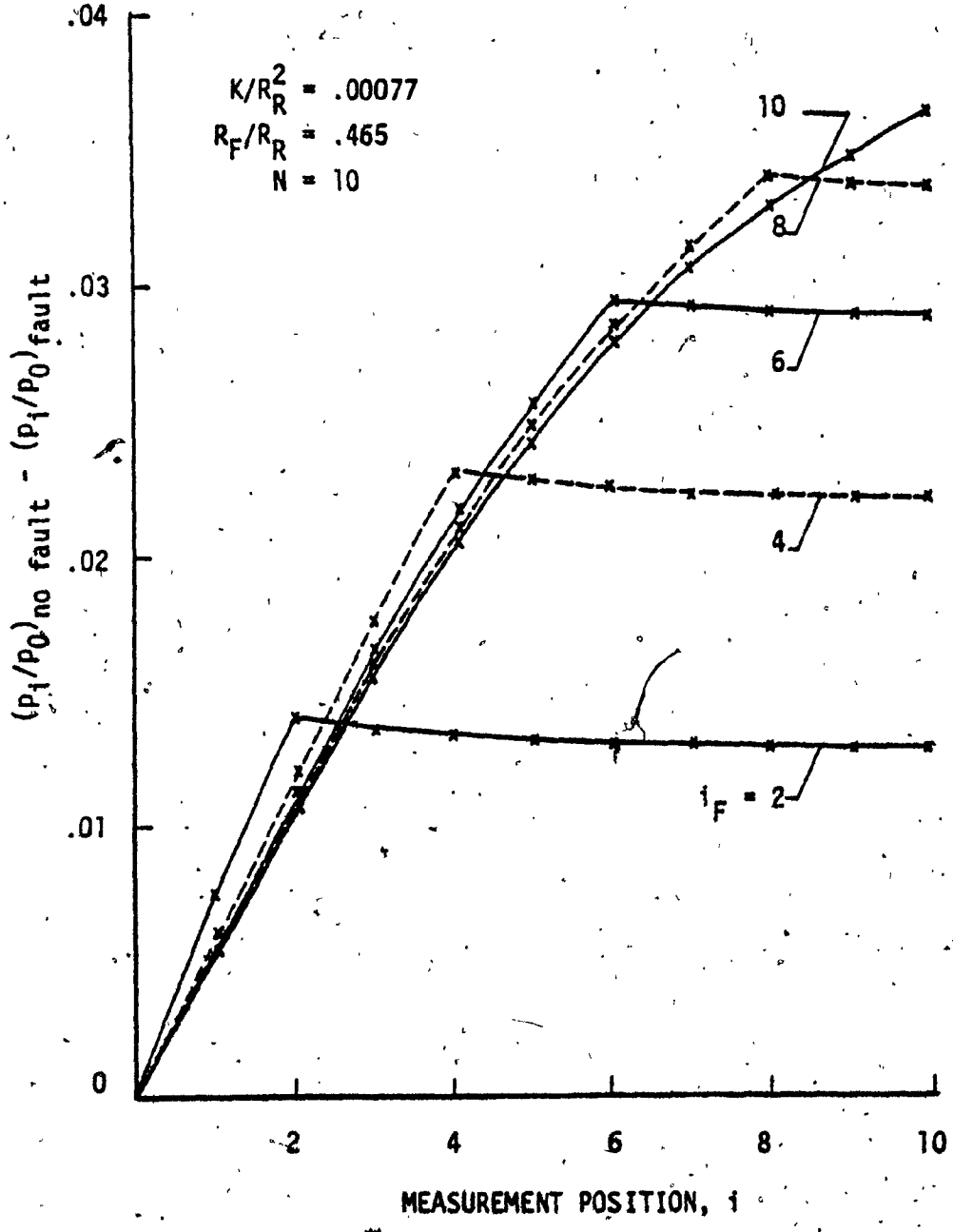

Figure 42. Simulated results of the Difference method when applied to Nonlinear brakepipe model (N = 10, R_F/R_R = 0.465)

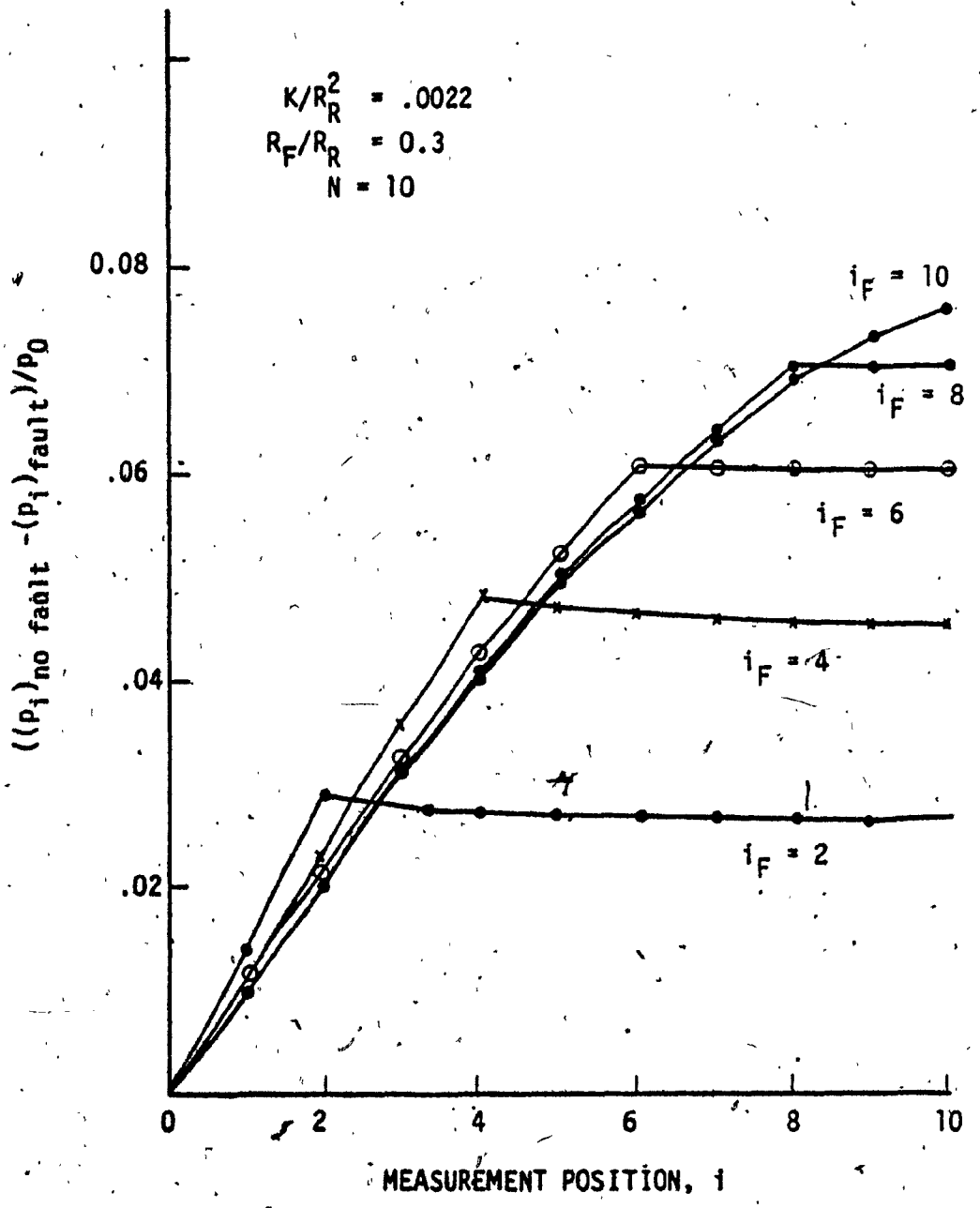

Figure 43. Simulated results of the Difference method when applied to Nonlinear brakepipe model (N = 10, R_F/R_R = 0.3)

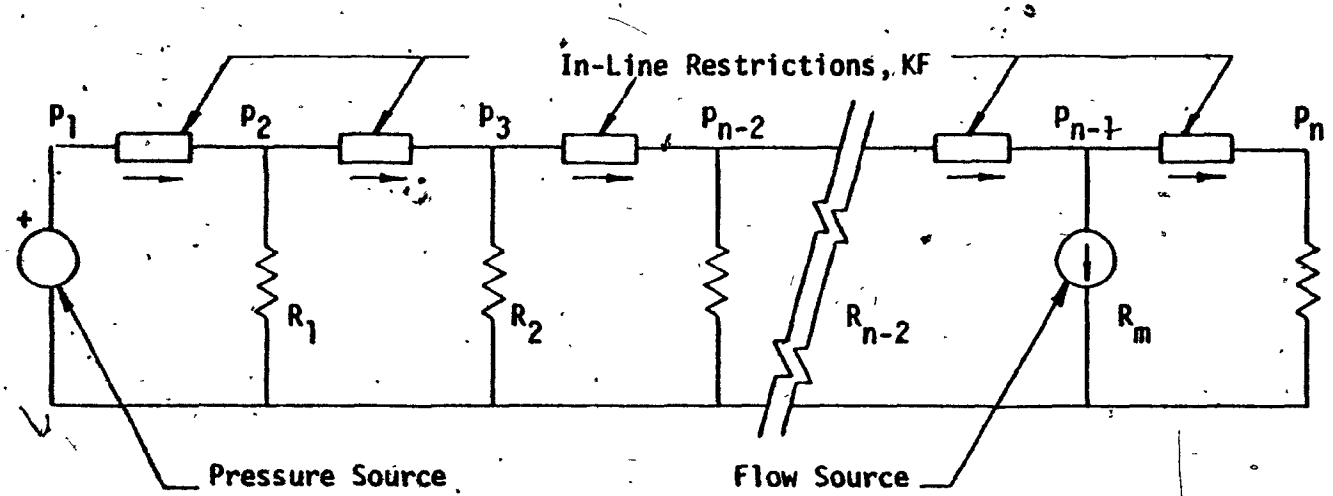

Figure 44. Modified model for the Ratio method

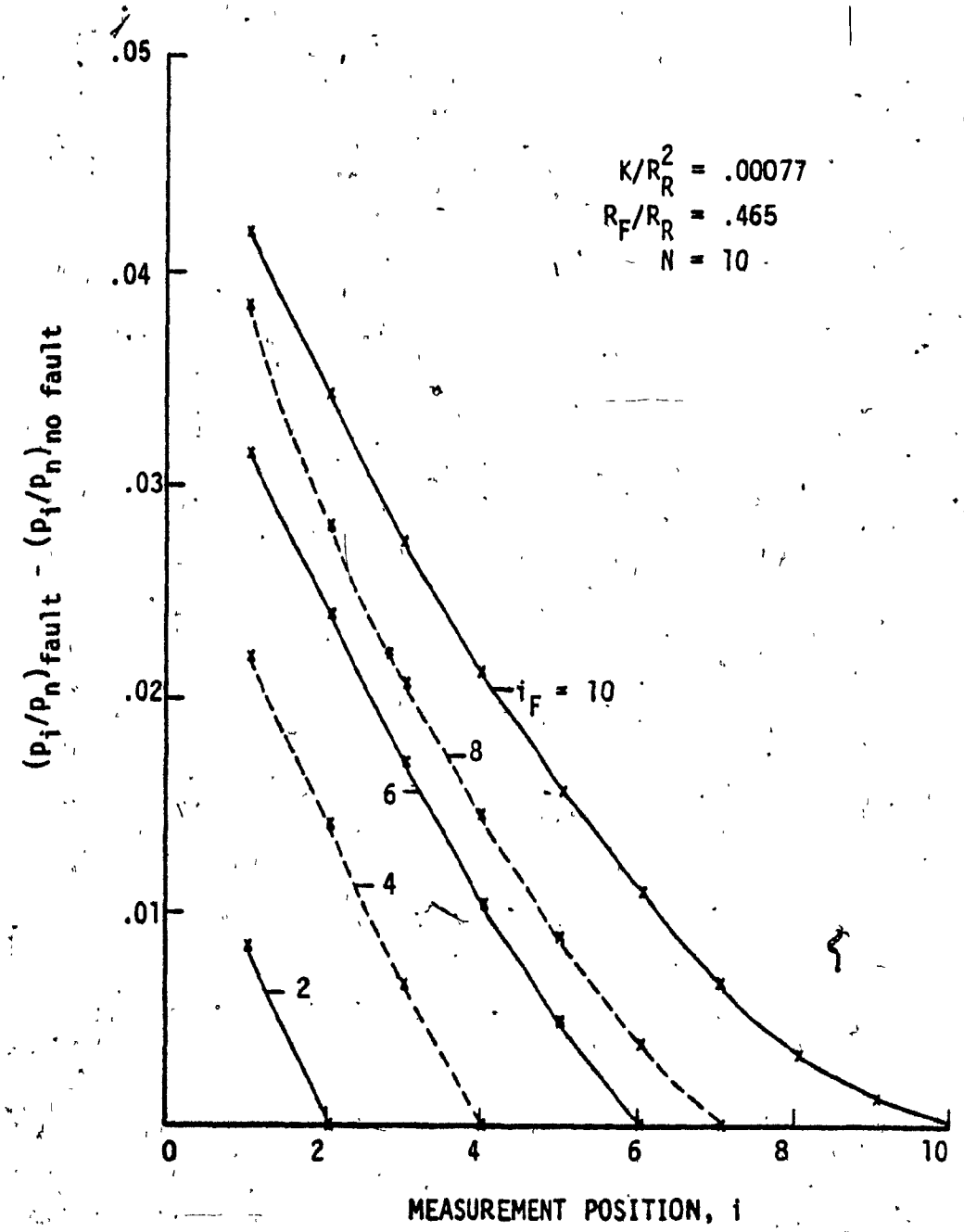

Figure 45. Simulated results of the Ratio method when applied to Nonlinear brakepipe model (N = 10, R_F/R_R = 0.465).

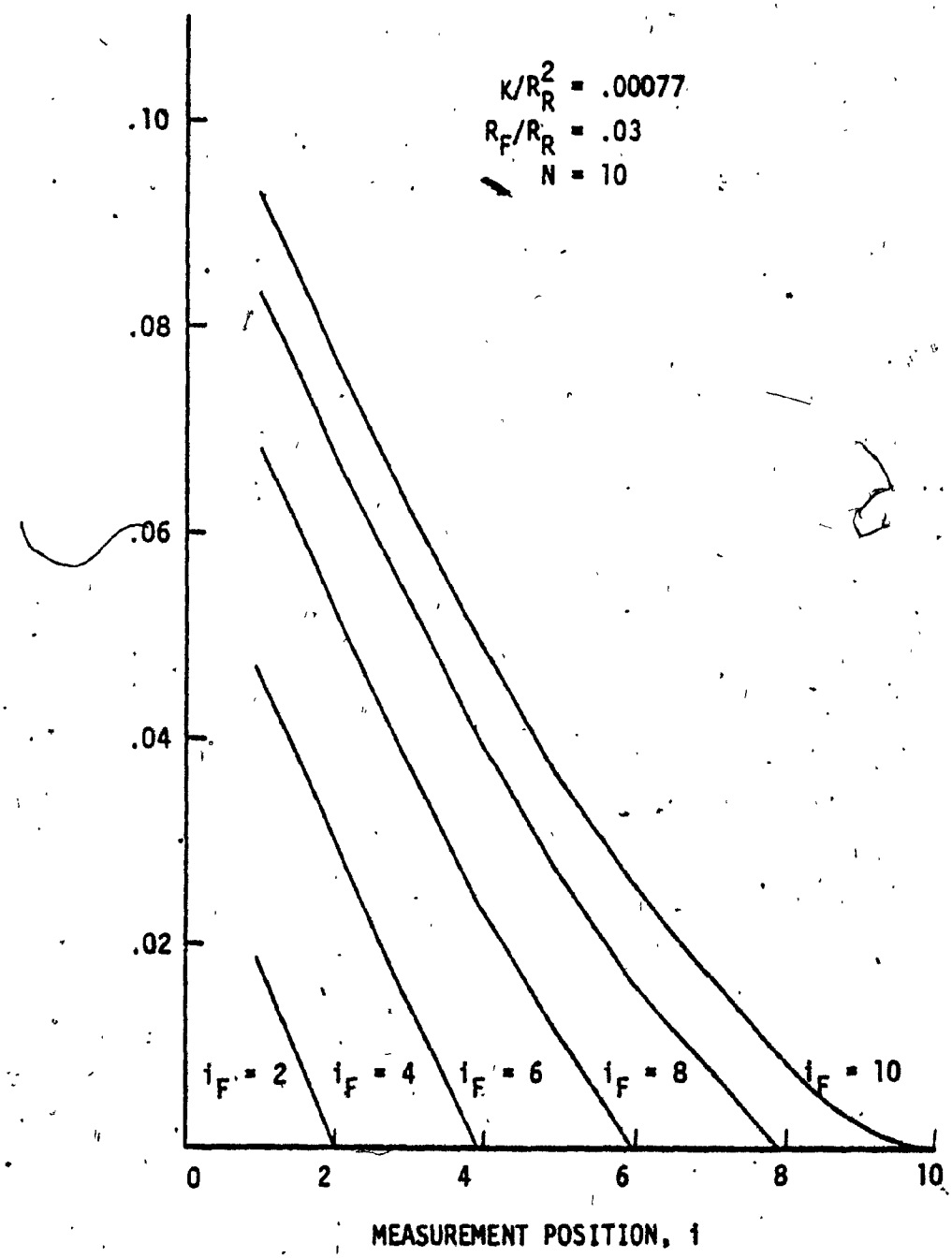

Figure 46. Simulated results of the Ratio method when applied to Non-linear brakepipe model (N = 10, R_F/R_R = 0.3)

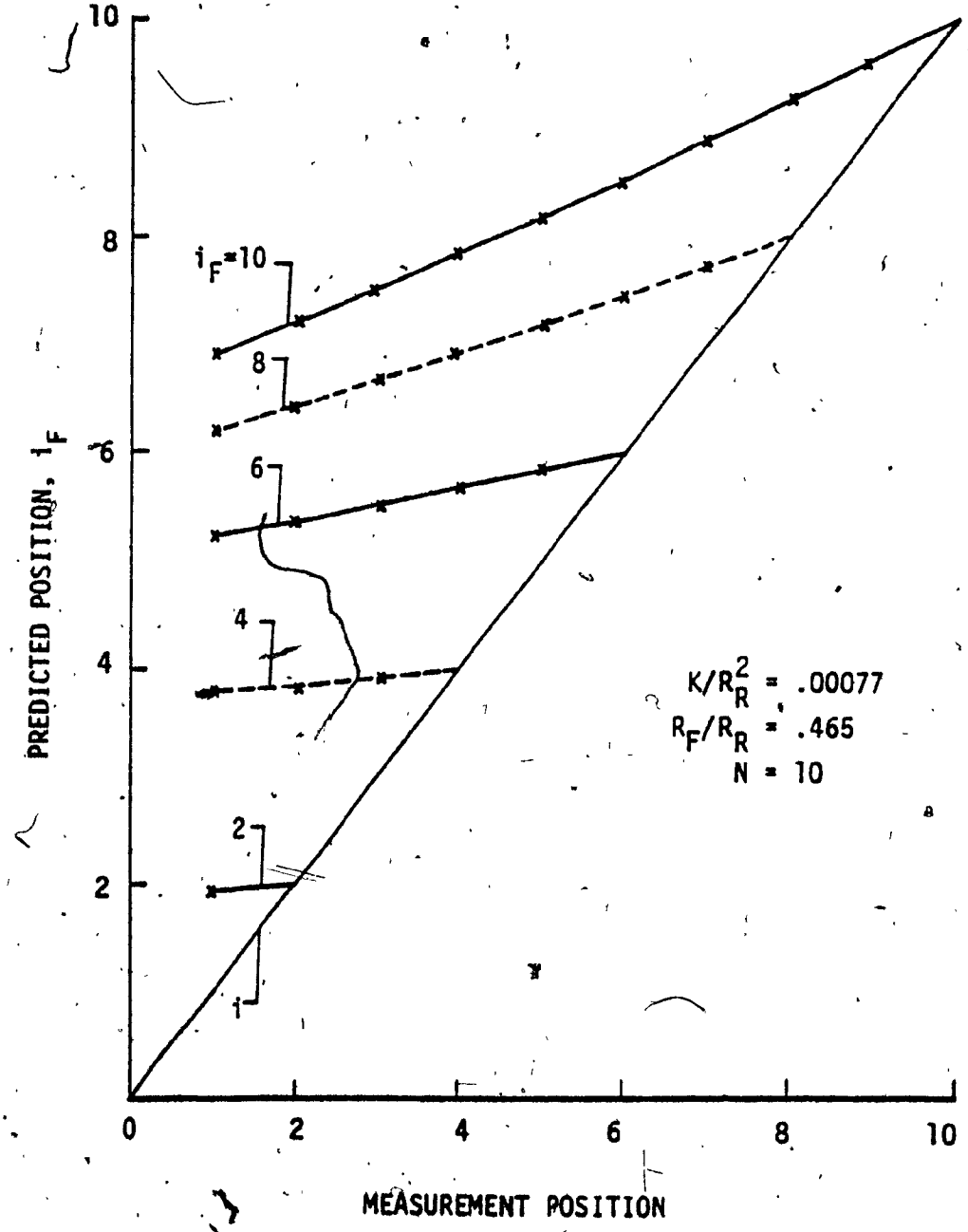

Figure 47. Simulated results of the Transformation method when applied to Nonlinear brakepipe model (N = 10, R_F/R_R = 0.465)

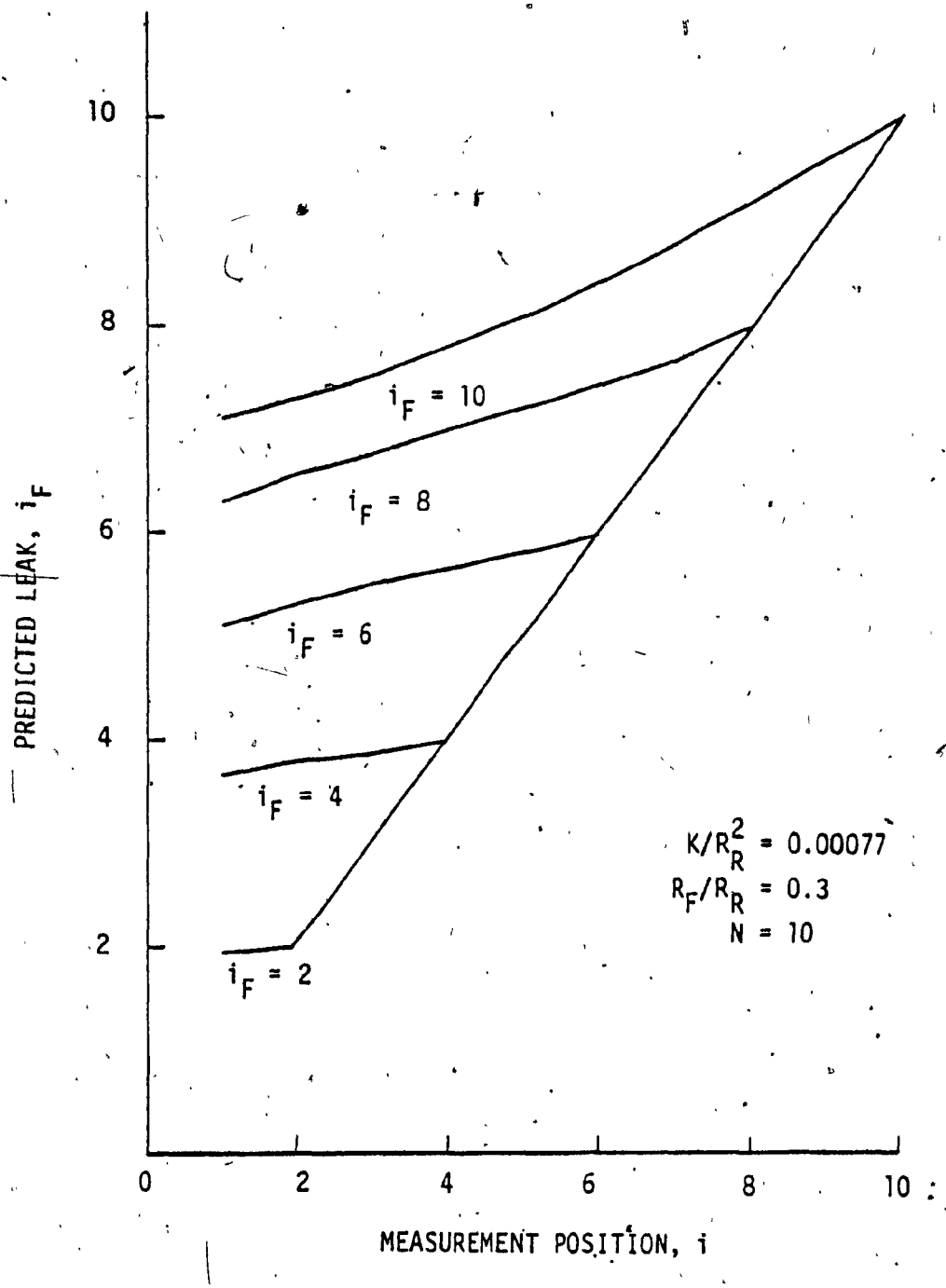

Figure 48. Simulated results of the Transformation method when applied to Nonlinear brakepipe model (N = 10, R_F/R_R = 0.3)

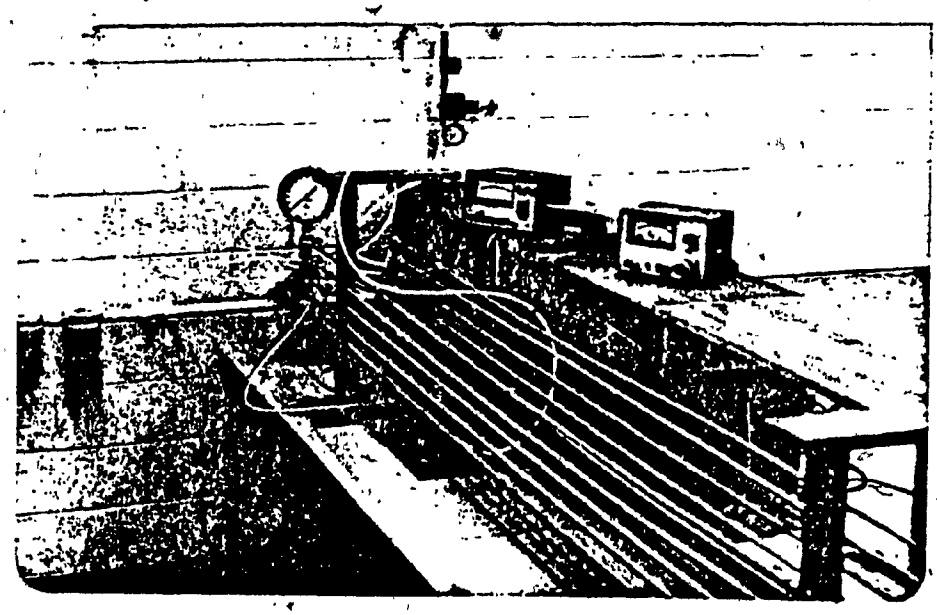

Figure 49. Picture of the scaled-down brakepipe model along with measuring equipment

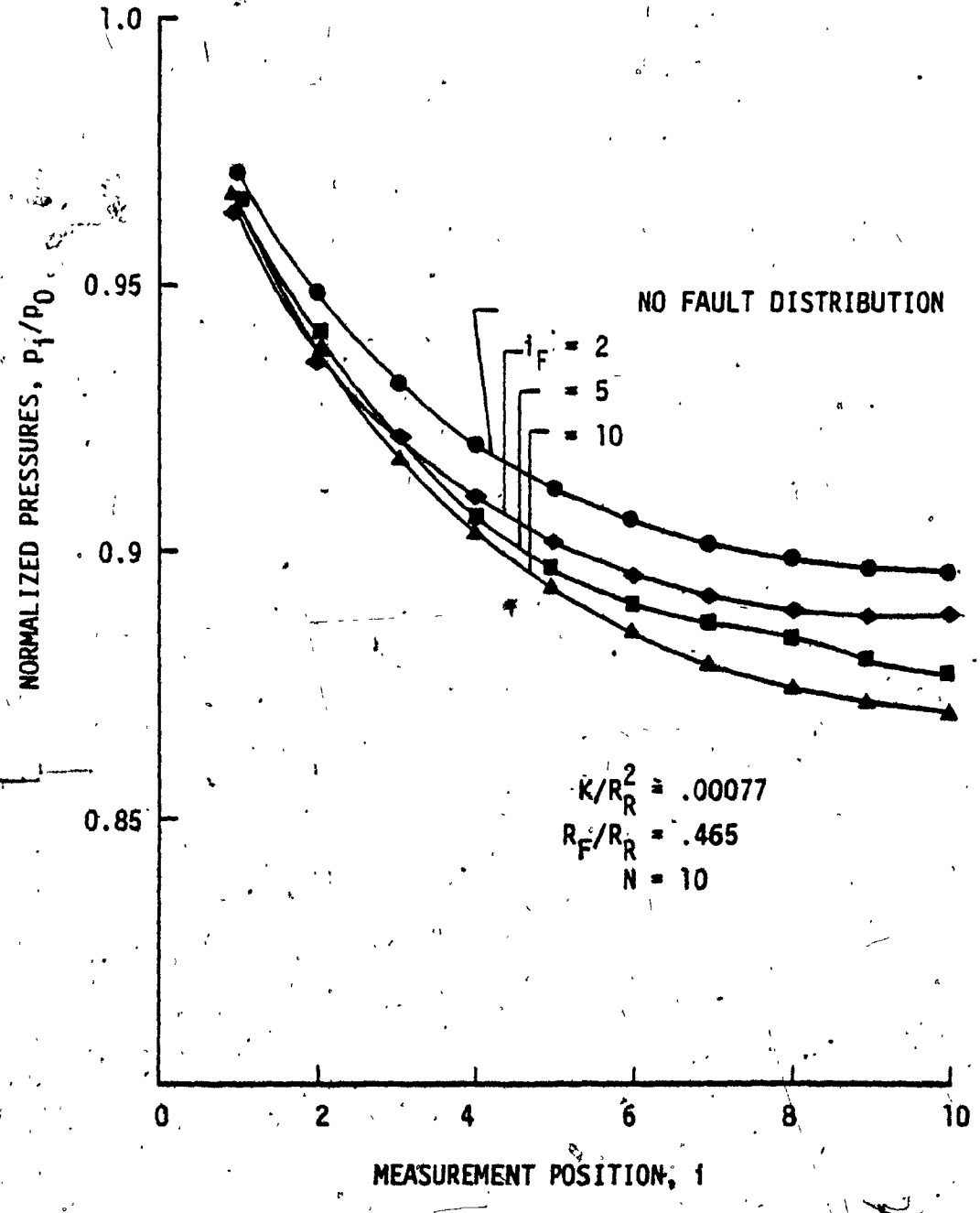

Figure 50. Experimental pressure distribution in the scale model of the brakepipe with R_F/R_R = 0.465

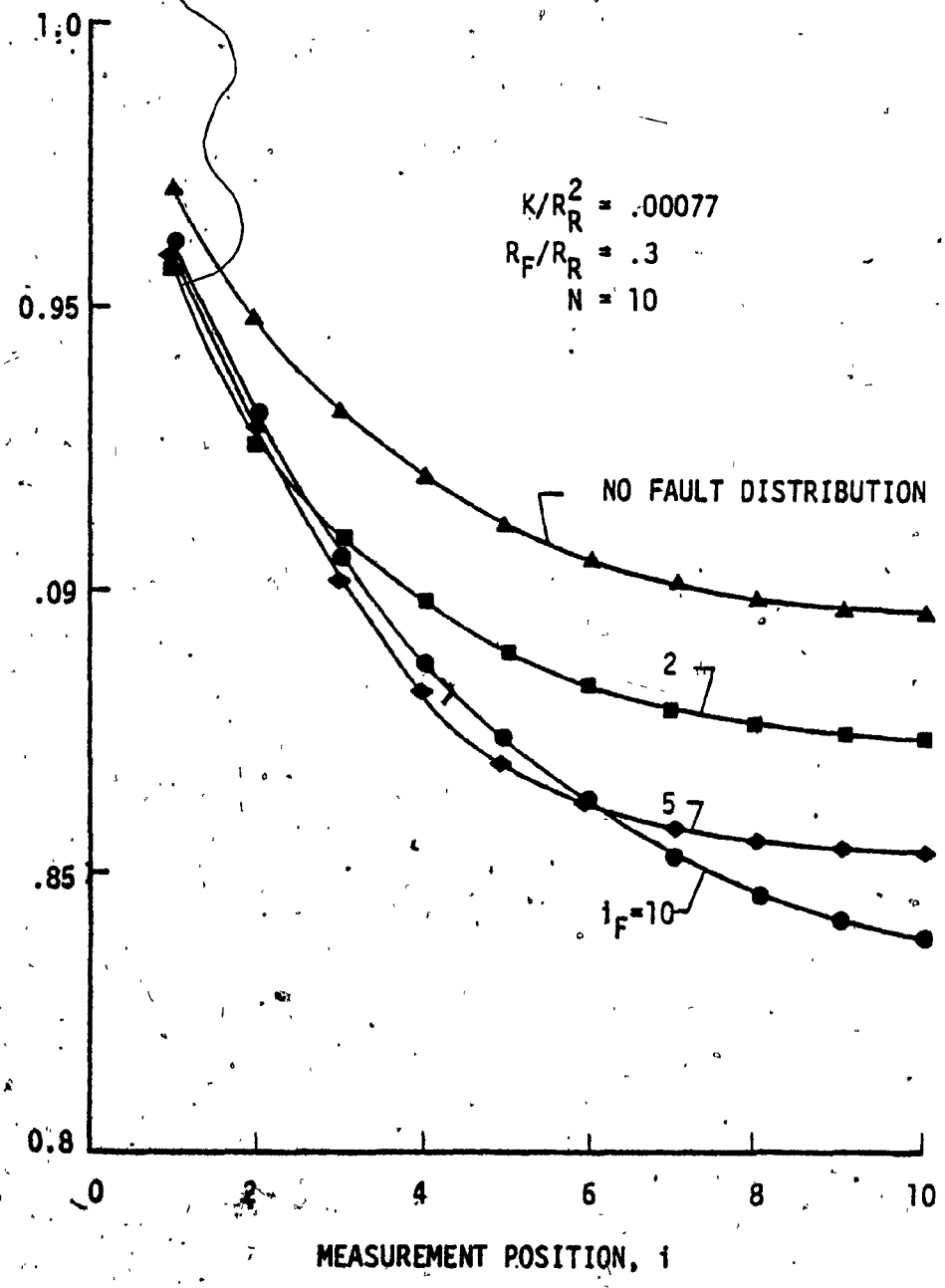

Figure 51. Experimental pressure distribution in the scale model of the brakepipe with R_F/R_R = 0.3

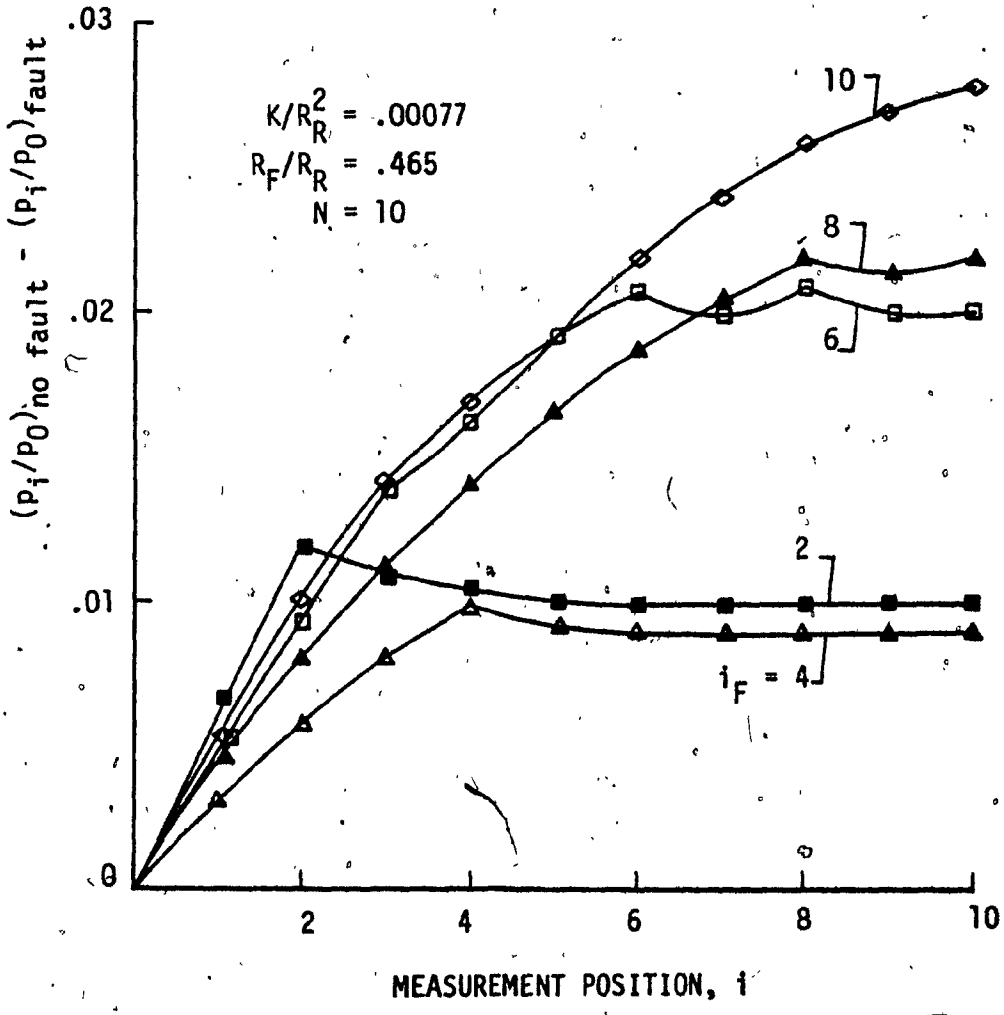

Figure 52. Experimental fault prediction by the Difference method with $R_F/R_R = 0.465$

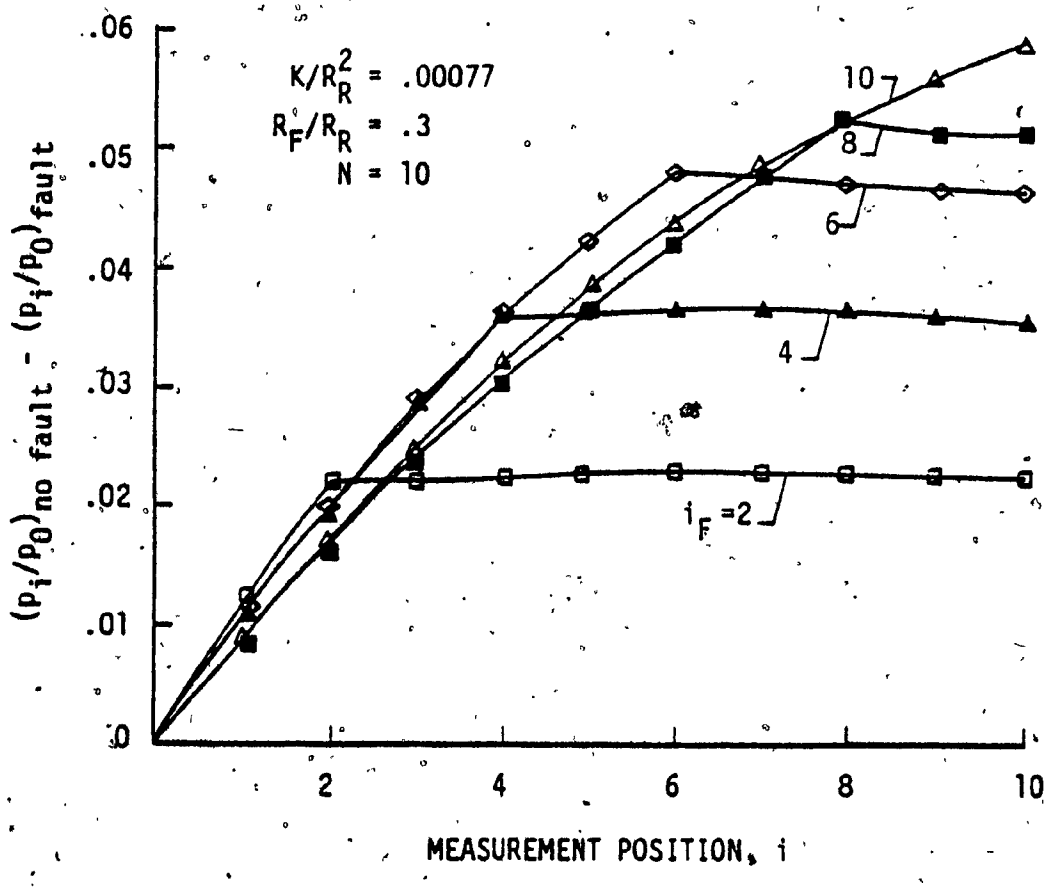

Figure 53. Experimental fault prediction by the Difference method with R_F/R_R = 0.3

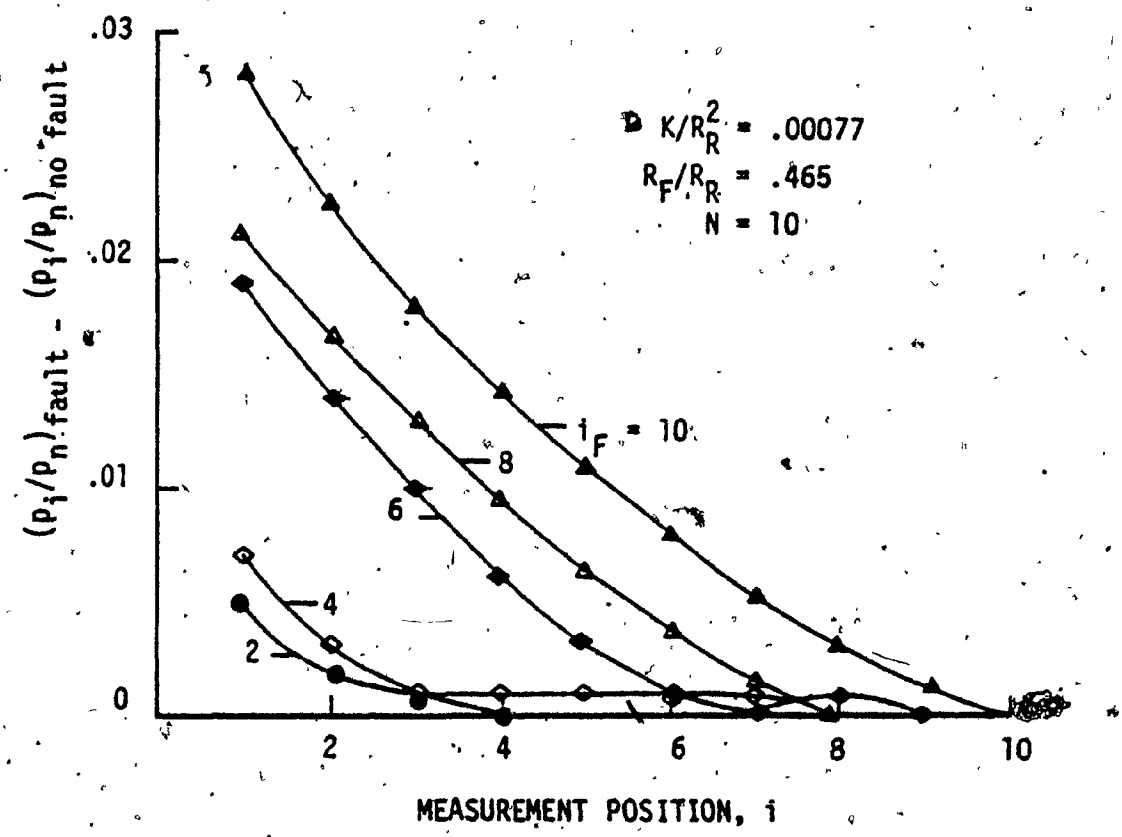

Figure 54. Experimental fault prediction by the Ratio method with R_F/R_R = 0.465.

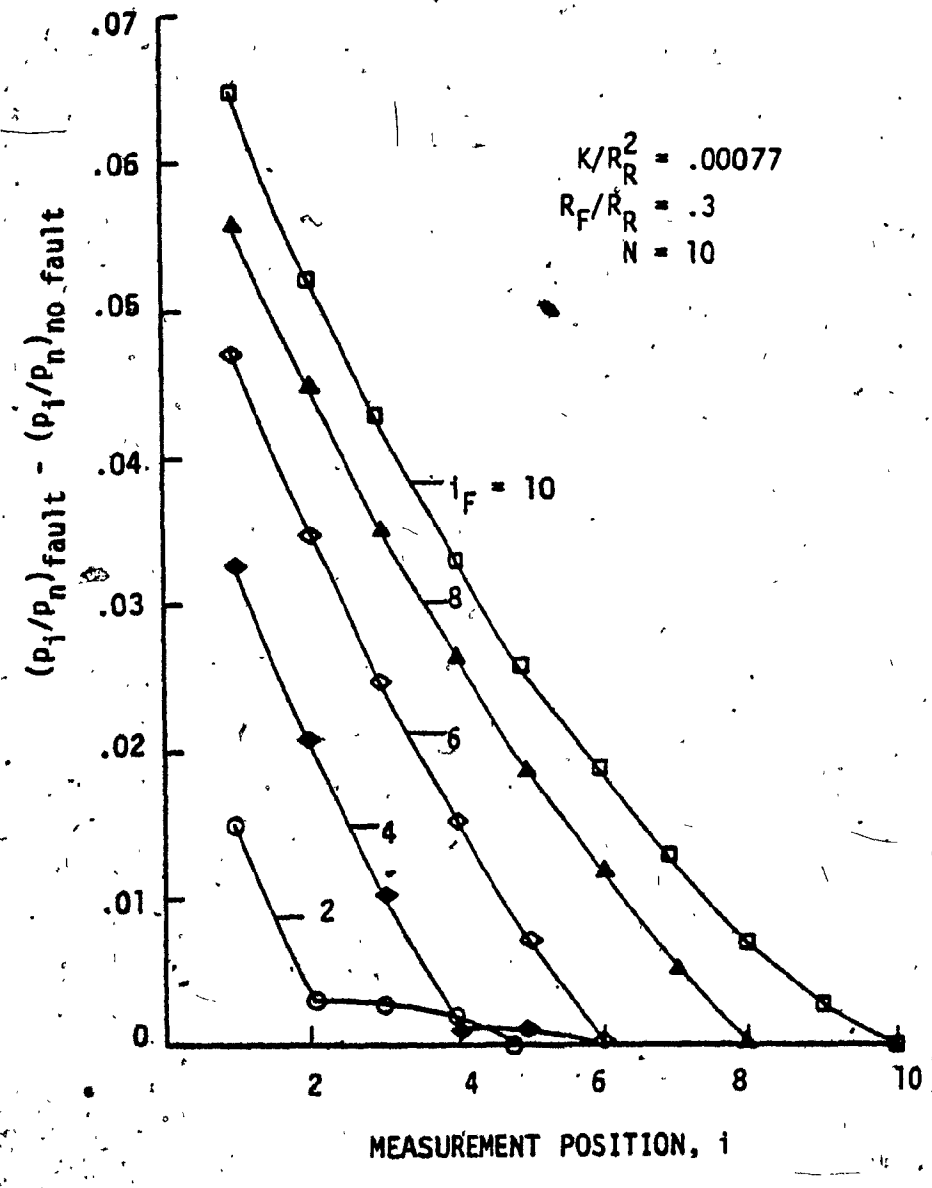

Figure 55. Experimental fault prediction by the Ratio method with $R_F/R_R = 0.3$

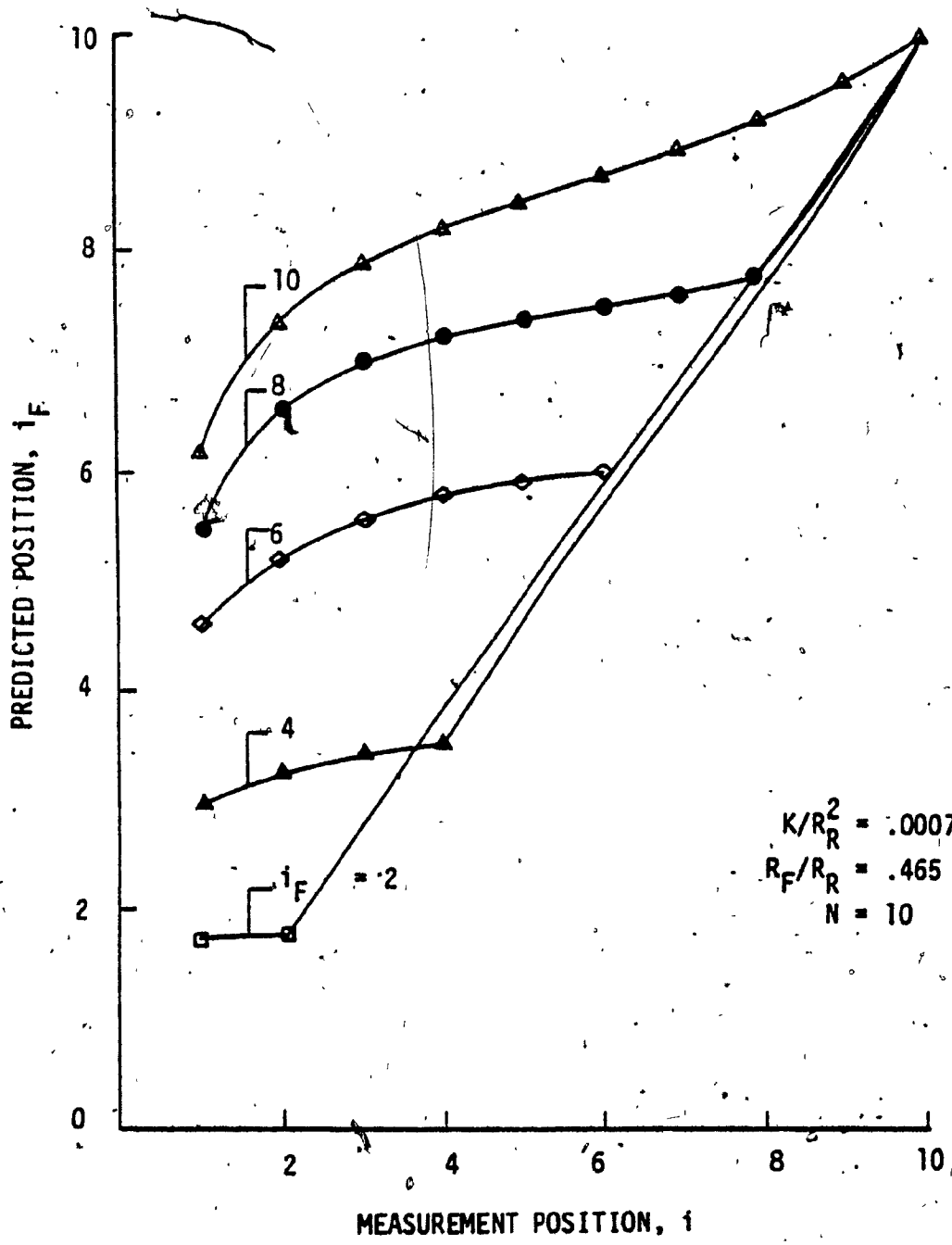

Figure 56. Experimental fault prediction by the Transformation method with R_F/R_R = 0.465

```
C     ****************************************************************
C     **RATIO METHOD FOR THE ELECTRICAL MODEL ***
C     ****************************************************************
      PROGRAM LINDIFF(INPUT,OUTPUT)
C     ****************************************************************
C     **N IS THE NUMBER OF SECTIONS, R IS THE INLINE RESISTANCE
C     RL IS THE SHUNT RESISTANCE, RF IS THE FAULT, PO IS THE
C     SOURCE , P IS PRESSURE OR VOLTAGE, PD IS THE NORMALIZED
C     PRESSURE, DELTP IS THE DIFFERENCE IN THE NORMALIZEDPRESSURES
C     AND LEAK AND GREAT ARE DUMMY VARIABLES.
C     ****************************************************************
      DIMENSION P(10),Q(10),DELTP(10),PD(10),QD(10),PRA(10),PRDIF(10)
C     ****************************************************************
C      *** DATA***
C       ************************************************************
      N=10
      R=1.
      RL=1000.
      RD=RL
      PO=10.
C     ****************************************************************
      PRINT 25,RL
 25   FORMAT(15X,*NO FAULT DISTRIBUTION*,5X,*RL=RD=*,F7.2,//)
      ND=1
C     ****************************************************************
C      ** INVOKING THE SUBROUTINE THAT GENERATES THE NO FAULT
C      **  PRESSURE DISTRIBUTION
C     ****************************************************************
      CALL PRESURE(R,RL,RD,N,ND,P,Q)
      DO 35 KL=1,N
      PD(KL)=P(KL)/P(N)
      QD(KL)=Q(KL)
      PRINT 100,KL,KL,PD(KL)
 100  FORMAT(20X,I3,5X,*P(*,I3,*)/P(N)=*,F10.7)
 35   CONTINUE
C     ****************************************************************
C     **  READING THE SIZE OF THE FAULT**
C      ***************************************************************
      DO 45 LO=1,N
       READ*,RD
       PRINT 200,RD,RL
 200  FORMAT(10X,/,* THE SIZE OF THE FAULT IS =*,F6.2,2X,*OHMS*,2X
     +,*AND THE REST ARE=*,F8.3,1X,*OHMS*)
      DO 1 ND=1,N
      PRINT 400,ND
 400  FORMAT(/,5X,*THE FAULT IS IN POSITION...*,I3,/)
C     ****************************************************************
C     *** GENERATING FAULT PRESSURE DISTRIBUTION AND CALCULATING THE
C     **DIFFERENCE BETWEEN NO FAULT AND FAULT PRESSURES
C      ***************************************************************
      CALL PRESURE(R,RL,RD,N,ND,P,Q)
      DO 55 LU=1,N
      PRA(LU)=P(LU)/P(N)
      PRDIF(LU)=ABS(PRA(LU)-PD(LU))
 55   CONTINUE
C     ****************************************************************
C     *** PROGRAM FOR FORMATTING THE OUTPUT
C       ************************************************************
      DO 23 JZ=1,N
      LF=N-JZ+1
      IF(PRDIF(LF) .GT. 1.E-12) GO TO 90
 23   CONTINUE .
      JG=1
      GO TO 34
```

```
90    IF(LF .EQ. 1) GO TO 41
      JO=LF+1
      GO TO 34
41    JO=LF+1
34    DO 52 JO=1,N
      IF(JO .EQ.5) GO TO 80
      PRINT600,JO,PRA(JO),JO,PRDIF(JO)
600   FORMAT(2X,'P(',I3,')/P(N)=',1X,F10.8,2X,'DELTP(',I3,')/P(N)='
     +,F10.8)
      GO TO 52
80    PRINT 700,JO,PRA(JO),JO,PRDIF(JO),JO
700   FORMAT(2X,'P(',I3,')/P(N)=',1X,F10.8,2X,'DELTP(',I3,
     +')/P(N)=',F10.8,2X,'THE PREDICTED FAULT POSITION IS..',I3)
52    CONTINUE
1       CONTINUE
 45    CONTINUE
      STOP
      END
```

```
C     ****************************************************************
C     **RATIO METHOD APPLIED PNEUMATIC MODEL OF THE BRAKEPIPE**
C     ****************************************************************
      PROGRAM RATIO(INPUT,OUTPUT)
      REAL K
      DIMENSION P(20),B(20),R(20),PR(20),PRA(20),PN(20),PRDIF(20)
      PRINT 28
 28   FORMAT(*1*)
C     ****************************************************************
C     DATA='K' IS THE IN-LINE RESISTANCE.'DIARR' IS THE SIZE OF THE
C     REFERENCE LEAK.'DIARD' IS THE DIAMETER OF THE LEAK.'RR' IS THE
C     RESISTANCE OF THE REFERENCE LEAK.'RD' IS THE RESISTANCE OF THE
C     DIFFERENT LEAK.'BD' IS DIMENSIONLESS QUANTITY.
C     ****************************************************************
      N=10
      K=2.21E+13
      DIARR=0.5715
       RR=1.68E+08
      DIARD=0.838
      RD=7.849E+07
      BD=K/(RR*RR)
C     ****************************************************************
C     INTIALIZING THE INDICES
C     ****************************************************************
      JR=0
      NP=0
      IM=0
C     ****************************************************************
C     INITIALIZING THE LEAKS TO HAVE EQUAL RESISTANCES
C     ****************************************************************
 44   DO 25 JM=1,N
 25    R(JM)=RR
      JR=JR+1
       IF(JR.EQ. 1) GO TO 55
       IL=N-JR+2
      R(IL)=RD
C     ****************************************************************
C     CALLING SUBROUTINE WHICH GENERATES B'S
C     ****************************************************************
 55   CALL PRESGEN(BD,RR,N,R,B)
      NP=NP+1
       IF(NP.NE.1) GO TO 48
       PRINT 333
 333   FORMAT(15X,*ALL LEAKS ARE EQUAL*,//)
C     ****************************************************************
C     CALCULATING THE PRESSURE RATIOS FOR UNIFORM DISTRIBUTION
C     ****************************************************************
       CALL PRERAT(B,N,P,PN)
       PRINT 201,DIARD,DIARR
 201   FORMAT(//,10X,*THE SIZE OF THE FAULT IS =*,F7.3,*MM*,2X,
     +*THE REST ARE OF DIAMETER =*,F7.3,*MM*,//)
      GO TO 321
 48    PRINT 444,IL
 444   FORMAT(//,12X,*THE LEAK POSITION IS..*,I3)
C     ****************************************************************
      CALL PRRATIO(B,P,N,PR,PN,PRA,PRDIF)
C      ****************************************************************
       DO 23 JZ=1,N
       LF=N-JZ+1
       IF(PRDIF(LF) .GT. 1.E-12) GO TO 4
 23    CONTINUE
       JZ=1
       GO TO 34
  4    IF(LF .EQ. 1) GO TO 41
```

```
      JO=LF+1
      GO TO 34
 41   JO=LF+1
 34    DO 52 JO=1,N
       IF(JO .EQ. 5) GO TO 80
       PRINT 222,JO,B(JO),JO,PR(JO),JO,PRA(JO),PRDIF(JO)
 222   FORMAT(2X,*B(*,I2,*)=*,F10.8,2X,*P(*,I2,*)/P0=*,F10.8,2X,
     +*P(*,I2,*)/P(N)=*,3X,F10.8,4X,*DELTP/P(N)=*,1X,F10.8)
       GO TO 52
 80   PRINT 224,JO,B(JO),JO,PR(JO),JO,PRA(JO),PRDIF(JO),JO
 224   FORMAT(2X,*B(*,I2,*)=*,F10.8,2X,*P(*,I2,*)/P0=*,F10.8,2X,
     +*P(*,I2,*)/P(N)=*,3X,F10.8,4X,*DELTP/P(N)=*,1X,F10.8,
     +2X,*THE PREDICTED FAULT POSITION IS...*,I2)
 52    CONTINUE
 321   IM=IM+1
      JV=N+1
       IF(IM.NE. JV) GO TO 44
       STOP
       END
      SUBROUTINE PRESGEN(BD,RR,N,R,B)
C     ************************************************************
C     **THIS SUBPROGRAM GENERATES THE "B"S**
C     ************************************************************
       DIMENSION R(20),B(20)
       B(N)=SQRT(1.+BD*RR*RR/(R(N)*R(N)))
       MM=N-1
       DO 2 J=1,MM
       LL=N-J
       SUM=RR/R(LL)
       PROD=1.0
       DO 3 K=1,J
       PROD=PROD/B(LL+K)
       SUM=SUM+PROD*RR/R(LL+K)
 3     CONTINUE
       B(LL)=SQRT(1.+BD*SUM*SUM)
 2     CONTINUE
       RETURN
       END
       SUBROUTINE PRERAT(B,N,PN)
C     ************************************************************
C     **THIS SUBPROGRAM GENERATES THE RATIO OF PRESSURES P(I)/P0
C     ************************************************************
       DIMENSION B(20),P(20),PN(20)
       PRO=1.
       DO 8 M=1,N
       PRO=PRO/B(M)
       P(M)=PRO
 8     CONTINUE
       DO 66 JK=1,N
       PN(JK)=P(JK)/P(N)
       PRINT 10,JK,B(JK),JK,P(JK),JK,PN(JK)
 10    FORMAT(2X,*B(*,I2,*)*,3X,F10.8,2X,*P(*,I2,*)/P0=*,2X,F10.8,
     +2X,*P(*,I2,*)/P(N)=*,2X,F10.8)
 66    CONTINUE
       RETURN
       END
       SUBROUTINE PRRATIO(B,P,N,PR,PN,PRA,PRDIF)
C     ************************************************************
C     *THIS SUBPROGRAM CALCULATES THE DIFFERENCE IN NORMALIZED
C     PRESSURES**
C     ************************************************************
       DIMENSION B(20),PR(20),PRDIF(20),P(20),PRA(20),PN(20)
       PRESUR=1.0
       DO 27 LB=1,N
       PRESUR=PRESUR/B(LB)
       PR(LB)=PRESUR
```

```
27    CONTINUE
      DO 70 IJ=1,N
      PRA(IJ)=PR(IJ)/PR(N)
70    CONTINUE
      DO 14 JA=1,N,
      PRDIF(JA)=ABS(PN(JA)-PRA(JA))
14     CONTINUE
      RETURN
      END
```

```
C     ****************************************************************
C     **TRANSFORMATION METHOD APPLIED TO PNEUMATIC MODEL **
C     ****************************************************************
      PROGRAM TRANNET(INPUT,OUTPUT)
      REAL K,N1,ND
      DIMENSION P(20),B(20),R(20),PSQ(20),EQI(20)
      PRINT 20
 20   FORMAT(1X)
C     ****************************************************************
C     DATA='K' IS THE IN-LINE RESISTANCE.'DIARR' IS THE SIZE OF THE
C     REFERENCE LEAK.'DIARD' IS THE DIAMETER OF THE LEAK.'RR' IS THE
C     RESISTANCE OF THE REFERENCE LEAK.'RD' IS THE RESISTANCE OF THE
C      DIFFERENT LEAK.'BD' IS DIMENSIONLESS QUANTITY..
C     ****************************************************************
      N=10
      K=2.21E+13
      DIARR=0.5715
       RR=1.68E+08
      DIARD=0.838
      RD=7.849E+07
      BD=K/(RR*RR)
C     ****************************************************************
C      CALLING SUBPROGRAM WHICH CALCULATES THE EQUIVALENT LINEAR .
C     VALUES (N) FOR THE CORRESPONDING NONLINEAR VALUES
C     ****************************************************************
      CALL EQTRAN(N,K,RR,RD,BD,T,EQI)
C     ****************************************************************
      DO 25 JN=1,N
 25   R(JN)=RR
C     ****************************************************************
C     CALLING SUBROUTINE WHICH GENERATES B'S
C     ****************************************************************
 55   CALL PRESGEN(BD,RR,N,R,B)
C     ****************************************************************
C     CALCULATING THE PRESSURE RATIOS FOR UNIFORM DISTRIBUTION
C     ****************************************************************
      CALL PRERAT(B,N,P,PSQ)
      DO 43 LB=1,N
      DO 56 JN=1,N
 56   R(JN)=RR
      KB=N-LB+1
      R(KB)=RD
C     ****************************************************************
      CALL PRESGEN(BD,RR,N,R,B)
      CALL PRERAT(B,N,P,PSQ)
C     ****************************************************************
      PRINT 456
 456  FORMAT(//,3X,'NONLINEAR N#',2X,'EQUIVALENT#',2X,'PREDICTED FAULT#',
     +/,23X,'LINEAR N#',2X,'POSITION IN LINEAR N#',/,54('-'))
C     ****************************************************************
C      THIS PART OF THE PROGRAM CALCULATES THE FAULT POSITION IN LINEAR
C     TERMS. THEY HAVE TO BE RETRANSFORMED TO EQUIVALENT NONLINEAR
C       VALUES BYU INTERPOLATION.
C      ****************************************************************
      DO 700 KL=1,N
      R(KL)=PSQ(KL)
      RR=PSQ(N)
      AR=T*EQI(KL)
      ARR=((T*EQI(N))+(Y/2.))
      B1=(R(KL)-SINH(AR)+COSH(AR))*COSH(T/2.)
      B2=(R(KL)+SINH(AR)-COSH(AR))*COSH(T/2.)
      C1=RR*SINH(AR)*(SINH(ARR)+COSH(ARR))
      C2=RR*SINH(AR)*(SINH(ARR)-COSH(ARR))
      D1=(B1+C1)/(B2+C2)
```

```
      KD=N-1
      DO 7 KZ=1,KD
      CC=AASPSQ(N-KZ)
      DO=ALOG(CC+SQRT(CC*CC-1.))
      EQI(N-KZ)=(ARG-DO)/DD
    7 CONTINUE
      EQI(N)=H1
      RETURN
      END
```

```
      ND=1./(2.*T)*ALOG(D1)
C      ***************************************************************
      PRINT 804, KL,EQI(KL),ND,KB
 804  FORMAT(/,10X,I3,7X,F10.6,7X,F10.6,7X,I3)
 700    CONTINUE
 43    CONTINUE
      STOP
      END
      SUBROUTINE PRESGEN(BD,RR,N,R,B)
C     ************************************************************
C     **THIS SUBPROGRAM GENERATES THE 'B'S**
C     ************************************************************
      DIMENSION R(20),B(20)
      B(N)=SQRT(1.+BD*RR*RR/(R(N)*R(N)))
      MM=NN-1
      DO 2 J=1,MM
      LL=N-J
      SUM=RR/R(LL)
      PROD=1.0
      DO 3 K=1,J
      PROD=PROD/B(LL+K)
      SUM=SUM+PROD*RR/R(LL+K)
 3    CONTINUE
      B(LL)=SQRT(1.+BD*SUM*SUM)
 2    CONTINUE
      RETURN
      END
      SUBROUTINE PRERAT(B,N,P,PSQ)
C     ************************************************************
C     **THIS SUBPROGRAM GENERATES THE RATIO OF PRESSURES P(I)/P0
C     ************************************************************
      DIMENSION B(20),P(20),PSQ(20)
      PRO=1.
      DO 8 M=1,N
      PRO=PRO/B(M)
      P(M)=PRO
      PSQ(M)=P(M)*P(M)
 8    CONTINUE
      RETURN
      END
      SUBROUTINE EQTRAN(N,R,RR,RD,BD,T,EQI)
      DIMENSION P(20),R(20),B(20),EQI(20),PSQ(20)
      REAL K,N1
      ARG1=(2.+BD)/2.
      T=ALOG(ARG1+SQRT(ARG1*ARG1-1.))
      DO 25 JM=1,N
      R(JM)=RR
 25   CONTINUE
      CALL PRESGEN(BD,RR,N,P,B)
      CALL EQUIVA(N,BD,PSQ,EQI)
      DO 250 KKJ=1,N
      EQI(KKJ)=EQI(KKJ)
 250    CONTINUE
      RETURN
      END
      SUBROUTINE EQUIVA(N,BD,PSQ,EQI)
      DIMENSION PSQ(20),EQI(20)
      REAL N1
      U=(2.+BD)/2.
      BB=ALOG(U+SQRT(U*U-1.))
      XX=COSH(BB/2.)
      YY=XX/PSQ(N)
      ZZ=ALOG(YY+SQRT(YY*YY-1.))
      N1=(ZZ-BB/2.)/BB
      ARG=(BB*N1+BB/2.)
      AA=COSH(ARG)
```